Fiber-type Specific Differences in Glucose Uptake and Abundance of Key Metabolic Proteins in Single Fibers from Rat Skeletal Muscle

by

James Gordon MacKrell

A dissertation submitted in partial fulfillment
of the requirements for the degree of
Doctor of Philosophy
(Molecular and Integrative Physiology)
in The University of Michigan
2013

Doctoral Committee:

Professor Gregory D. Cartee, Chair
Professor Martin G. Myers
Associate Professor Susan Brooks-Herzog
Assistant Professor Patrick J. Hu

Dedicated to my beautiful wife Leah and my family

ACKNOWLEDGEMENTS

Reaching this final step of graduate school could not have been achieved without the support and guidance of various people along the way. I owe a great deal of gratitude to my advisor, Dr. Greg Cartee. When I initially rotated through his lab, I noticed a special passion for science which excited me. I joined Greg's Muscle Biology Lab as a young, naïve graduate student and truly appreciate his patience and direction in those early years. I am thankful for his involvement in all facets of the lab and grateful for his selfless effort which helped mold me into a better scientist. His systematic and meticulous approach is something that I will take with me and practice as I continue my journey. I cannot express enough thanks for all of the assistance and mentorship he has provided during my time in the lab.

Thank you to my committee members, Dr. Martin Myers, Dr. Susan Brooks, and Dr. Patrick Hu. Your scientific guidance with my research projects and professional guidance as I pursued post-graduate positions provided me the valuable knowledge allowing me to reach this goal.

My years spent at Michigan were truly enjoyable thanks in large part to my extended family that is the Department of Molecular and Integrative Physiology. I am grateful to all my MIP friends who joined in the various events that made MIP feel like family; from Pub nights, to faculty-student softball games, to weekly seminars and lunches. Thank you to the graduate student chair who recruited me, Dr. Fred Karsch,

who was very influential during my early years at Michigan. I owe great thanks to Dr. Ormond MacDougald, who replaced Fred as the graduate student chair. Ormond has been a great mentor and was also key in helping me to obtain my position at Eli Lilly, introducing me to my next advisor, Dr. Gary Krishnan. The family atmosphere of MIP has continued under Scott Pletcher's leadership and I value his help over the years. That sense of family is also due in large part to the Departmental Chairs; Dr. John Williams, and more recently Dr. Bishr Omary, have always been completely supportive of the MIP graduate students and I thank them both. Physiology would not run as smooth as it does without the tireless effort of Michele Boggs, so thank you very much Michele. She has been an essential member of the MIP family, personally helping me to coordinate various social events, while also helping me to stay organized with deadlines and administrative components involved with graduate school. I am very proud and excited to become a graduate of MIP.

The guys of the Muscle Biology lab have also been instrumental in my success and enjoyment here at Michigan and I am very appreciative of "Kinesiology's finest." I enjoyed our time together inside the lab, and outside of lab at golf outings and happy hours. To Dr. Ed Arias, thank you for always offering up your "T.O.E", it got me out of several binds in the lab and one day I hope to reach your level of experience. Thanks to Dr. Naveen Sharma for helping to keep things in perspective, even when lab got to stressful. Thanks to Carlos Castorena for all his help in the lab and on the golf course, and his patience as I taught him the single fiber method. Immense thanks to the former lab members who have also been influential in helping me to reach this point; Dr. Donel Sequea, Dr. George Schweitzer, and Dr. Katsu Funai.

To all my friends at Michigan, I thank you for the amazing times we had over the years. I am especially thankful for the "Mugclub" crew, meeting nearly every Monday night over a beer and snacks. We began meeting to simply watch football and share stories of weekend events, but it evolved into us complaining (or sometimes celebrating) about our labs and projects as we progressed though graduate school, which evolved into shared excitement over marriages, kids, and careers as we progressed further into life.

To my family, I thank you for your patience and support. You often wandered when I would graduate and get a "real job." But in truth you were always there for me, supporting all of my decisions and actions. I cannot begin to repay my parents for the sacrifices they have made over my lifetime, allowing me to be in the position I am today. From day one when we went apartment hunting in Ann Arbor, to the numerous trips to visit me and take me grocery shopping or out to dinner, my mom has been there for me, putting my needs ahead of hers. I thank her for teaching me her secrets in the kitchen; not only do I think it made me more equipped in the lab, but it also helped me land my wife Leah (with help from Gramma Elsie and her "sauce" recipe). I thank my dad for my passion to discover and quest for knowledge. Since some of my first childhood memories of him reading through medical journals in his attic office, I have continually strived to mimic his work ethic. His hard work has allowed me to pursue my dreams. Thank you to my brother, Andy, and sister, Ali, for keeping me humble and "normal". Spending days on end in the lab can become dull and make you lose sense of what is really meaningful. I cherish the times we get to spend together over holidays, weddings, or just short conversations where I can revert back to just being an older brother and appreciate everything we have.

January 14 happened to be the only day the committee could meet for the defense of my oral dissertation. This was also Pappi Linarelli's birthday and I know that he was looking down smiling as I presented my work. With the dedication of this dissertation to my family, I hold a special place for my late grandfathers, Pappi (Ralph "Sonny" Linarelli) and Grandpa (Jim) MacKrell. Pappi Linarelli loved to have conversations with anyone, regardless of status or interests (when I was around he was always trying to find me a pretty girlfriend, and although he never met Leah, I know he would be very impressed!). What Pappi didn't teach me, Gramma Elsie (Linarelli) stepped in with her "lectures" and filled me in on the nitty-gritty of life. I am also so thankful for all of her cards over the years with money to "buy a steak with" and our phone conversations of stories about Koppel and her dog Bella that were always a nice break after a long day of science. Grandpa MacKrell was an architect and engineer; I know the time spent in his basement workshop helped shaped my interest in the intricate details of things. As an integral member of the church, Grandpa MacKrell did, and my wonderful Grandma MacKrell still does, provide a strong spiritual presence in my life.

Finally, thank you to my beautiful, supportive, and loving wife. You have faithfully been there for me every day since we met. While I was going through prelim's you kept me at ease even though we had just started dating. Through the joys and struggles of everyday lab life, to the stress and excitement of graduating, your patience with my work life and attitude were often saint-like. There have been days, and probably weeks, where I spent more time looking into the eyes of my microscope than your eyes. But you were always there and have been my rock through it all. I know with you next to my side everything will be fine and am so excited to start the next chapter with you!

TABLE OF CONTENTS

LIST OF FIGURES

FIGURE

ABSTRACT

Skeletal muscle is the major tissue for insulin-mediated glucose disposal. Each skeletal muscle is composed of hundreds to thousands of individual fibers. Because of the marked cellular diversity among fibers, it is advantageous to understand muscle function at the single fiber level. This thesis aimed to provide insights on skeletal muscle fiber type heterogeneity, concentrating on single fibers from the rat epitrochlearis muscle. Research from this thesis developed and validated techniques for simultaneous assessment in a single fiber of: glucose uptake (GU), fiber type (by myosin heavy chain isoform expression), fiber volume, and abundance of multiple proteins (by immunoblotting). GU capacity differed by both fiber type and stimulus: 1) IIA fibers consistently had the greatest insulin-stimulated GU capacity (IIA>IIB, IIX, IIB/X) across a wide range of the lifespan (2-, 5-, 9-, and 25-months-old) and 2) IIB fibers had the greatest AICAR-stimulated GU capacity. The primary insulin-responsive glucose transporter (GLUT4) was most abundant in IIA fibers, supporting the idea that insulin-stimulated GU capacity is, in part, a function of the number of GLUT4 transporters present. To better understand insulin resistance, GU was measured by single fibers from obese Zucker (OZ) versus lean Zucker (LZ) rats, and there was significant insulin resistance (44-58%) for each fiber type. Lower levels of IκB-β in OZ fibers supported the idea for greater inflammation and NFκB activation contributing to the insulin resistance. In vivo electroporation of an ectopic gene was successful, allowing

visualization of fluorescent protein (DsRed) expression in single fibers without altering GU. Strong evidence was provided to support the combination of single fiber analysis with genetic manipulation to study the role that a gene-of-interest has on fiber type-specific GU capacity. Overall, results from this dissertation provided the first data showing conclusive evidence for fiber type-specific GU differences within a skeletal muscle. The extensive characterization of single fibers in this thesis provides unique insights for understanding muscle biology. The novel methods and knowledge from this work, combined with continued investigation of single fibers, offer the opportunity to advance our understanding of pathophysiological conditions, providing options for improved therapeutic targets to treat metabolic disorders.

CHAPTER I

INTRODUCTION

Skeletal muscle plays a critical role regulating whole body glucose metabolism, acting as the major tissue for insulin-mediated disposal of blood glucose (1). However, skeletal muscle is a complex tissue composed of hundreds to thousands of muscle fibers with substantial heterogeneity among the fibers. The individual muscle fibers contain different isoforms of myosin heavy chain (MHC), which is used as the gold standard for fiber typing (e.g., types I, IIA, IIB, and IIX) (2-6).

Glucose uptake is not uniform across all skeletal muscles in the body (7). This variation for in vivo glucose uptake may involve the influence of various factors, including the microvascular perfusion and muscle contractile activity in different muscles (7, 8). However, even when muscles are studied ex vivo to minimize the direct effects of these factors, significant muscle-dependent differences for insulin-stimulated glucose uptake rates remain (9). A barrier to fully understanding muscle glucose uptake at the cellular level has been the absence of a method to measure glucose uptake by single fibers of known fiber type from mammalian skeletal muscle. The primary aim of this dissertation was to provide a method and gather evidence to gain a better understanding of single fiber glucose uptake capacity, MHC isoform expression, fiber volume, and abundance of key proteins.

Study 1: A Novel Method to Measure Glucose Uptake and Myosin Heavy Chain Isoform Expression of Single Fibers from Rat Skeletal Muscle

While evidence suggested that glucose uptake was different from one type of muscle fiber to the other, no methods were available for measuring glucose uptake by single fibers of known fiber type from mammalian muscle. This study's primary objective was to develop a method to measure glucose uptake and MHC isoform expression in single fibers from rat skeletal muscle. In addition, defects in whole body glucose metabolism have been linked to a variety of health issues and disease states, including insulin resistance, type 2 diabetes (T2D), and cardiovascular disease (10-12). Insulin resistance, a below normal biological effect of normal insulin doses, is a primary feature of T2D and central defect in the metabolic syndrome (10). Because of its large mass and high expression of GLUT4 (the insulin-regulated glucose transporter), skeletal muscle is the major tissue for insulin-mediated blood glucose disposal, accounting for 70-85% of insulin-stimulated glucose clearance during a hyperinsulinemic clamp in humans (1). Increasing skeletal muscle glucose uptake (GU) is crucial for improving whole body insulin resistance. Therefore, a secondary objective of this study was to assess insulin resistance in single fibers from obese versus lean Zucker rats to gain a better understanding of the role each fiber type plays in this disease state.

Study 2: Fiber Type-Specific Differences in Glucose Uptake by Single Fibers from Skeletal Muscles of 9- and 25-Month-Old Rats

Many of the most prevalent and devastating age-related diseases in humans (including hypertension, coronary heart disease, stroke, some forms of cancer, and type 2 diabetes) have been linked to insulin resistance (13). Whole body glucose disposal during a euglycemic-hyperinsulinemic clamp has been reported to be moderately (~15-35%) lower for old rats (20-25 months old) compared to adult rats (6-10 month old) (14, 15). In addition, age-related insulin resistance does not appear to be uniform in all skeletal muscles (16). However, it is uncertain if the variable extent of age-related insulin resistance is solely attributable to differences in fiber type composition or if there may be a contribution of other differences between the particular skeletal muscles that have been studied. The primary purpose of this study was to assess the feasibility of applying a novel approach to measure glucose uptake capacity, MHC isoform expression, fiber volume, and abundance of key proteins in single fibers from adult (9-month) and old (25-month) rat epitrochlearis muscles. The overall goal of the study was to advance the currently limited understanding of the relationship between fiber type, and age-associated insulin resistance in skeletal muscle by studying muscle glucose uptake of adult and old rats for the first time at the level of the single fiber.

Study 3: Effects of Electroporation and Expression of DsRed on Glucose Uptake, Fiber Size and Protein Abundance in Rat Skeletal Muscle Single Fibers.

In vivo electroporation (IVE) of genetic material is a commonly used method for ectopic gene expression in skeletal muscle (17, 18). Because of the crucial role skeletal muscle plays in glucoregulation, the glucose uptake capacity of this tissue is widely studied, while the effect that a specific genetic modification has on skeletal muscle

glucose uptake is an area of focus. The primary purpose of Study 3 was to apply the novel method studying single fibers (developed in Study 1) to muscles that had undergone IVE of a plasmid containing the gene for a DsRed reporter protein. Ultimately, this study aimed to gain novel insight on glucose uptake capacity, MHC isoform expression, fiber volume, and abundance of key proteins (GLUT4 and COXIV) in rat epitrochlearis single fibers that express a fluorescent reporter gene (DsRed) following delivery by IVE. The overall goal was to provide validation for future studies combining single fiber analysis with the IVE approach for genetic manipulation.

References

1. DeFronzo RA. Lilly lecture 1987. The triumvirate: beta-cell, muscle, liver. A collusion responsible for NIDDM. Diabetes. 1988;37(6):667-87.
2. Pandorf CE, Caiozzo VJ, Haddad F, Baldwin KM. A rationale for SDS-PAGE of MHC isoforms as a gold standard for determining contractile phenotype. J Appl Physiol. 2010;108(1):222-2; author reply 6.
3. Bigard AX, Sanchez H, Birot O, Serrurier B. Myosin heavy chain composition of skeletal muscles in young rats growing under hypobaric hypoxia conditions. J Appl Physiol. 2000;88(2):479-86.
4. Schiaffino S, Reggiani C. Molecular diversity of myofibrillar proteins: gene regulation and functional significance. Physiological reviews. 1996;76(2):371-423.
5. Schiaffino S, Reggiani C. Myosin isoforms in mammalian skeletal muscle. J Appl Physiol. 1994;77(2):493-501.
6. Thomason DB, Baldwin KM, Herrick RE. Myosin isozyme distribution in rodent hindlimb skeletal muscle. J Appl Physiol. 1986;60(6):1923-31.
7. James DE, Jenkins AB, Kraegen EW. Heterogeneity of insulin action in individual muscles in vivo: euglycemic clamp studies in rats. The American journal of physiology. 1985;248(5 Pt 1):E567-74.
8. Clerk LH, Smith ME, Rattigan S, Clark MG. Nonnutritive flow impairs uptake of fatty acid by white muscles of the perfused rat hindlimb. Am J Physiol Endocrinol Metab. 2003;284(3):E611-7.
9. Henriksen EJ, Bourey RE, Rodnick KJ, Koranyi L, Permutt MA, Holloszy JO. Glucose transporter protein content and glucose transport capacity in rat skeletal muscles. The American journal of physiology. 1990;259(4 Pt 1):E593-8.
10. Ginsberg HN. Insulin resistance and cardiovascular disease. J Clin Invest. 2000;106(4):453-8. PMCID: 380256.
11. Savage DB, Petersen KF, Shulman GI. Mechanisms of insulin resistance in humans and possible links with inflammation. Hypertension. 2005;45(5):828-33.

12. Ariza MA, Vimalananda VG, Rosenzweig JL. The economic consequences of diabetes and cardiovascular disease in the United States. Rev Endocr Metab Disord. 2010;11(1):1-10.
13. Facchini FS, Hua N, Abbasi F, Reaven GM. Insulin resistance as a predictor of age-related diseases. J Clin Endocrinol Metab. 2001;86(8):3574-8.
14. Catalano KJ, Bergman RN, Ader M. Increased susceptibility to insulin resistance associated with abdominal obesity in aging rats. Obes Res. 2005;13(1):11-20.
15. Nishimura H, Kuzuya H, Okamoto M, Yoshimasa Y, Yamada K, Ida T, et al. Change of insulin action with aging in conscious rats determined by euglycemic clamp. The American journal of physiology. 1988;254(1 Pt 1):E92-8.
16. Sharma N, Arias EB, Sajan MP, MacKrell JG, Bhat AD, Farese RV, et al. Insulin resistance for glucose uptake and Akt2 phosphorylation in the soleus, but not epitrochlearis, muscles of old vs. adult rats. J Appl Physiol. 2010;108(6):1631-40. PMCID: 2886681.
17. Aihara H, Miyazaki J. Gene transfer into muscle by electroporation in vivo. Nat Biotechnol. 1998;16(9):867-70.
18. Mir LM, Bureau MF, Gehl J, Rangara R, Rouy D, Caillaud JM, et al. High-efficiency gene transfer into skeletal muscle mediated by electric pulses. Proceedings of the National Academy of Sciences of the United States of America. 1999;96(8):4262-7.

CHAPTER II

REVIEW OF LITERATURE

Skeletal Muscle Physiology

Skeletal muscles make up 30-40% of the body's mass in mammals including humans and rodents (1). Skeletal muscles have multiple and diverse functional and metabolic characteristics, with principal roles including movement, stability, communication, control of body openings, thermogenesis, and the maintenance of glucose homeostasis. Individual, elongated, multinucleated cells, called fibers, form the basic cellular unit of skeletal muscle tissue, while other cell types are present to provide structure (fibroblasts), nutrient supply (vascular/endothelial tissue, neutrophils, erythrocytes), and enervation (nerve cells). Each muscle fiber includes smaller units of filaments, organized into myofibrils. These myofibrils are the basic unit of all skeletal muscle cells and create the distinctive striated pattern. Within each myofibril are regularly arranged thick and thin filaments arranged in units termed sarcomeres. The space between overlapping thick and thin filaments is connected by cross-bridges. Globular heads within the myosin molecule (thick filament) extend out to form the cross-bridges in what ultimately is the mechanism for muscle contraction termed the cross-bridge cycle. The number of myofibrils arranged in parallel determines the force

generating capacity of the fiber, while the speed at which contraction of a fiber can occur is controlled by the adenosine triphosphatase (ATPase) activity of the myosin molecule (2-4).

Skeletal Muscle and Basal Metabolic Rate

Contraction of skeletal muscle is essential for movement [e.g., walking using a variety of leg, trunk, core, and limb muscles (5, 6)], stability [e.g., postural muscles such as the soleus (7)], control of body openings [e.g., jaw muscles (8)], and adaptive thermogenesis [e.g., shivering (9)]. This contraction process requires energy production in the muscle. Basal metabolic rate (BMR) reflects the lowest energy required at rest in postabsorptive, thermoneutral conditions to perform basic cell functions (e.g., maintaining cell potentials, driving the heart and circulation, synthetic and housekeeping functions, and maintenance of body temperature) (10). In the basal state, skeletal muscle accounts for ~20-30% of BMR (11). Depending on the intensity, duration and type of muscle contraction, variable increases in the amount of energy expended (i.e., metabolic rate) require additional intake of oxygen along with the metabolism of energy substrates, from macronutrients, [i.e., carbohydrates, fats, and proteins (12)].

Skeletal Muscle Fuel Selection and Energy Metabolism

Skeletal muscle is dynamic in its energy metabolism and substrate utilization. Breakdown of adenosine triphosphate (ATP) and subsequent release of free energy provides the direct energy source for skeletal muscle. At rest under fasting conditions, the muscle predominantly uses fatty acids as its fuel to regenerate ATP via beta

oxidation, the Krebs Cycle and the electron transport chain. A number of other biochemical processes are also responsible for maintaining a constant supply of ATP: 1) phosphocreatine pathway 2) oxidative phosphorylation; and 3) glycolysis (glucose breakdown) (13). The macronutrient fuel mix used to maintain ATP is variable depending on the tissue. The ability to use multiple macronutrients as fuel sources renders muscle an important component in modulating whole body fuel selection and homeostasis. Depending on conditions, metabolic breakdown of glucose (or stored glucose in the form of glycogen) can occur either anaerobically or aerobically in the muscle. Anaerobic glycolysis supplies energy during brief, high-intensity activity. Aerobic glycolysis is the primary process for glucose metabolism in the muscle under resting fed conditions, and thus significant for energy production as well as whole body glucose homeostasis (14). As a metabolically flexible tissue, skeletal muscle metabolism is a product of its functional needs as well as its physiological makeup, i.e., the distribution of different fiber types throughout a particular muscle.

Distinction of Skeletal Muscle Fiber Type

Skeletal muscle's functional capacity is influenced by its fiber type composition, with each muscle being a mix of several fiber types (15, 16). The initial approach for distinguishing fiber type was based on color (red vs. white) as well as the speed of contraction (fast vs. slow) (3, 17). This ultimately progressed to different classification systems currently used today. Myosin ATPase staining is a commonly used method to identify fiber type. Myosin ATPase (mATPase) is the enzyme located on the globular head of myosin molecules within the sarcomere. The mATPase hydrolysis rates for fast

fibers are 2-3 times greater than those of slow fibers (18). However, the staining of mATPase does not directly measure activity, rather fiber types are identified based on the staining intensities because of differences in pH sensitivity (15, 19). This method has been used for identification of type I, IIA, IIB, and IIX fibers, but because the delineations are based on qualitative analysis, fiber type designation can be variable (3). Another method often used to identify fiber type involves biochemical classification which combines mATPase staining information with qualitative histochemistry for particular enzymes that reflect metabolic properties of the fiber (16). Fibers are grouped as type I or type II via histochemical mATPase, and the enzymes measured reflect metabolic pathways that are either aerobic/oxidative or anaerobic/glycolytic (19). This ultimately provides for fibers to be classified as slow-twitch oxidative (SO), fast-twitch oxidative – glycolytic (FOG), or fast-twitch glycolytic (FG). However, there is a high level of subjectivity involved in this fiber typing method (3). The gold standard for classifying fiber types has been the identification of different myosin heavy chain isoforms (20). Immunohistochemical analysis using anti-myosin antibodies, or by SDS-PAGE separation with visualization using Coomassie or silver staining, allows for the MHC isoform(s) expressed in muscle, or a fiber, to be reproducibly determined (20). In skeletal muscle of adult rats, four isoforms are expressed, MHC I, MHC IIA, MHC IIB, and MHC IIX (21-24). Since a single fiber can contain more than one MHC isoform, this method proves useful in delineating these hybrid fibers (e.g. co-expression of IIB and IIX within a fiber) (25). Hybrid fibers can be abundant in rat muscle (26, 27), and may reflect fiber type conversion, thus blurring the unambiguous distinction of muscle fiber type (26, 27). Furthermore, the objective, quantitative identification of MHC isoforms

allows for precise determination of all MHC isoforms in a given muscle or fiber, and has been proven sensitive to subtle or marked differences between muscles of different fiber-types (28-30).

Importance of Skeletal Muscle Glucose Transport

Insulin resistance is defined as a subnormal biologic response to normal insulin concentrations. Skeletal muscle insulin resistance is an essential and perhaps primary defect in the progression to Type 2 diabetes mellitus (T2DM) (31-34). T2DM affects approximately 6% of the adult population in Western society and accounts for 90-95% of all diabetes cases in the United States. This disease represents an enormous economic burden, costing $174 billion per year, with those costs expected to rise as 11.2% of the population over 20 years of age are expected to be diagnosed with the disease by 2030 (35-37). In addition, insulin resistance and hyperinsulinemia (both important features of T2DM) have been linked to prevalent pathologies in the US including atherosclerosis, hypertension, cardiovascular disease, some cancers, and cognitive disorders (38-40).

Insulin resistance can manifest itself for a multitude of reasons including genetic factors, obesity complications, diet, physical inactivity, inflammation, endocrine disorders and aging. Skeletal muscle is a major site of insulin resistance and candidate target for therapeutic intervention (41). Because of its large mass and high expression of GLUT4 (the insulin-regulated glucose transporter (42, 43)), skeletal muscle accounts for a significant percentage of insulin-stimulated blood glucose clearance; accounting for ~70-85% in a study using a hyperinsulinemic-euglycemic clamp in humans (44). As a rate limiting step in muscle glucose metabolism (45), glucose transport into skeletal

muscle is primarily stimulated by insulin and exercise (46, 47). In the case of insulin resistance, a decline in insulin-stimulated glucose uptake results in increased circulating glucose unless the pancreatic beta cells adequately compensate by increased insulin secretion. In time, overworked beta-cells can fail, ultimately leading to the pathology of T2DM (34). Obtaining a clearer understanding of the glucose transport process by muscle is important in the context of identifying strategies to oppose insulin resistance and T2DM.

Effect of Insulin on Skeletal Muscle Glucose Transport

GLUT4 Glucose Transporter

Because glucose is a polar molecule, its movement through biological membranes and into cells requires specific transport proteins. A family of facilitated glucose transporters, GLUTs, provides facilitated diffusion of glucose into cells. GLUT4 serves as the primary glucose transporter for adipose tissue and skeletal muscle in insulin-stimulated conditions (48, 49). GLUT4 is also crucial for insulin-independent activation of glucose transport stimulated by exercise /contraction (50, 51). In basal conditions, GLUT4 is mostly localized intracellularly within GLUT4 storage vesicles (GSVs). GLUT4 translocation to the cell surface occurs with through insulin dependent- and independent-signaling pathways, ultimately resulting in increased glucose transport.

Insulin Signaling Pathway Leading to GLUT4 Translocation

To enhance glucose uptake into muscle, insulin promotes the translocation of GLUT4 glucose transporters to the cell surface (52-54). Insulin binding to its receptor

causes a conformational change resulting in the autophosphorylation of tyrosine residues, thus triggering the insulin-signaling pathway (55, 56). Briefly, with this activation, tyrosine phosphorylation of insulin receptor substrate proteins (IRS1 and IRS2 (57, 58)), and recruitment/activation of PI3K (a lipid kinase) occurs. This results in the generation of phosphatidylinositol (3,4,5)-triphosphate (PIP3; a lipid product of PI3K) (59-61). A key downstream effector of insulin-stimulated glucose uptake, the serine/threonine kinase Akt (also known as protein kinase B, PKB) (62-65), is recruited to the plasma membrane and binds PIP3. Activation of Akt is achieved via phosphorylation on its Thr308 site (via PDK1) (66) and on it Ser473 site (possibly via mTORC2) (67). Once active, Akt phosphorylates multiple proteins containing consensus sequences for Ser/Thr Akt phosphorylation, including AS160 (Akt substrate of 160kDa; also known as TBC1D4) (68, 69). TBC1D1 also contains several conserved motifs found within AS160 (namely the GTPase activating protein, GAP, domain and two Akt phosphomotifs) and is phosphorylated by Akt in response to insulin (70, 71). The Rab-GAP activity of AS160 and/or TBC1D1 promotes GTP hydrolysis of interacting Rab protein(s) with the GSV, thus more inactive (GDP-bound) Rabs are present retaining GLUT4 intracellularly. The phosphorylation of AS160 and/or TBC1D1 on specific Akt motifs results in their inactivation and in conjunction, a reduction in their GAP activity (70, 72-74) resulting in the release of GLUT4 from intracellular compartments and translocation to the cell surface, ultimately providing for increased glucose uptake (42, 43, 75).

Insulin-stimulated GLUT4 Translocation and Glucose Uptake in Muscles

The abundance of GLUT4 protein appears to be one of the major determinants of the skeletal muscle cell's glucose uptake capacity in response to insulin. Various studies have investigated the connection between GLUT4 abundance and insulin-stimulated glucose uptake utilizing transgenic mouse models (76-78). Under euglycemic hyperinsulinemic clamp conditions, Ren et al. showed that a mouse model overexpressing GLUT4 in a tissue specific manner displayed increased basal and insulin-stimulated whole body glucose disposal. These results suggested the importance of GLUT4, as muscle glucose transport appeared to be a rate-limiting step for whole body glucose disposal (77). In addition, Dr. Maureen Charron's group has studied muscle-specific overexpression of GLUT4 using transgenic mouse models (79, 80). GLUT4 protein expression was increased 3-4 fold in glycolytic muscles (i.e., gastrocnemius and EDL). In this model, a 2.5-fold increase in whole body insulin-stimulated glucose utilization was observed (80). Thus, with a greater amount of the glucose transporter present in the muscle, there was a greater capacity for insulin-stimulated glucose uptake. Cleasby et al. aimed to acutely manipulate GLUT4 expression in rat skeletal muscle; GLUT4 protein expression in the tibialis anterior muscle was reduced using in vivo electroporation (IVE) to induce intracellular expression of GLUT4 short hairpin RNAs (shRNAs). The decrease in GLUT4 expression was associated with attenuated clearance of glucose tracer, confirming that the relative abundance of GLUT4 in the muscle is a key determinant for glucose uptake by the muscle (81). These in vivo studies manipulating skeletal muscle GLUT4 expression provide important evidence for the transport capacity of GLUT4 as well as its rate-limiting role in muscle metabolism.

Muscle Specific Difference in GLUT4 and Insulin-stimulated Glucose Uptake

Skeletal muscles display differential expression of GLUT4 as evidenced by Castorena et al. who assessed GLUT4 abundance in 12 different muscles (or muscle portions) of varying fiber types and found a 2.5-fold range among the different muscles (28). A number of studies have provided evidence that the fiber type makeup of a muscle plays an important role on maximally effective insulin stimulated glucose uptake (82-84). John Holloszy's group aimed to better understand the relationship between glucose transporter protein content and glucose transport capacity in different muscles. Using ex vivo incubated muscles, Henriksen et al. measured GLUT4 abundance and glucose uptake in 4 muscles, the epitrochlearis (fiber type composition is 8% type I, 13% IIA, 51% IIB, 28% IIX), the flexor digitorum brevis (FDB; 7% type I, 92% IIA, 1% IIB,) the soleus (88% type I, 12% IIA, 0% IIB, 0% IIX), and the extensor digitorum longus (EDL; 2% type I, 12% IIA, 57% IIB, 29% IIX). They showed that the rank order of GLUT4 abundance among the muscles was FDB > Soleus > EDL > epitrochlearis (~ 3-fold difference between FDB vs. epitrochlearis). Likewise, ex vivo maximally effective insulin-stimulated glucose uptake differed among the muscles, with the rank-order being soleus > FDB > EDL > epitrochlearis. While there were similar glucose uptake values for the soleus (primarily type I fibers) and FDB (primarily IIA fibers), an approximately 3-fold difference between soleus vs. epitrochlearis existed (49). These studies provided evidence for possible fiber-type differences for insulin-stimulated glucose uptake. Though because only muscle tissue was analyzed, the possibility cannot be ruled out that glucose uptake differences may be related to the muscles themselves, independent of fiber type.

In summary, insulin stimulation of skeletal muscle ultimately leads to increased GLUT4 translocation and subsequent glucose transport into the tissue. Glucose transport capacity is a rate-limiting step in glucose metabolism and is a function of both the number and intrinsic activity of glucose transporter proteins (GLUT4). The various skeletal muscles throughout the body have differential expression GLUT4 and also variable insulin-stimulated glucose uptake capacity. The abundance of GLUT4 varies according to muscle, perhaps in a fiber-type manner. At the tissue level, GLUT4 protein content and glucose transport capacity are closely correlated under maximally effective insulin-stimulated conditions, with muscles that express greater GLUT4 protein levels having greater capacity for maximally effective insulin-stimulated glucose transport. However, whether this relationship is specific to the muscles themselves, or due to differences that are intrinsic to the fiber types per se remains unclear.

Role of AMP-activated Protein Kinase in Insulin-independent Glucose Transport

GLUT4 translocation and subsequent glucose uptake can also occur via a mechanism distinct from the insulin stimulatory pathway. Several lines of evidence illustrate the stimulation of glucose transport via the AMP-activated protein kinase (AMPK) signaling pathway, typically through exercise/contraction, or exposure to 5-amino-1-β-D-ribofuranosyl-imidazole-4-carboxamide (AICAR). AICAR (converted into the AMP analog, ZMP, upon cell-entry) stimulation can increase glucose transport in skeletal muscle (85) and is independent of the insulin-signaling pathway [wortmannin, a PI3K inhibitor, does not inhibit AICAR's stimulation of glucose transport (86)]. In addition, while the effect of AICAR plus contraction is often not additive (86-88), many

studies have reported an increase (or additive effect) in glucose transport when AICAR and insulin-stimulation are combined (86, 88). Similar to insulin-stimulation, AICAR-stimulation has been reported to result in muscle, and possibly fiber-type, specific differences in glucose uptake. Ai et al. incubated epitrochlearis, FDB, and soleus muscles with 2mM AICAR. Glucose uptake in response to the AICAR stimulation increased ~2-fold above basal in the epitrochlearis, ~1.4 in the FDB, and not at all in the soleus (87). In addition, Bergeron et al. investigated glucose uptake ex vivo using the isolated epitrochlearis muscle incubated with AICAR (0.5 mM), insulin (20mU/ml) or a combination of AICAR and insulin. Incubation of muscles with AICAR or insulin resulted in increased 2-DG uptake rates by ~2- and 2.7-fold, respectively, compared with basal rates. Combining AICAR and insulin led to a fully additive effect on muscle glucose transport rate (86). These data provide evidence for distinct signaling pathways which ultimately results in increased glucose uptake by the muscle. For the purpose of understanding the disease state such as type 2 diabetes, insulin-independent glucose uptake has been reported to be unaltered in affected individuals, while insulin dependent glucose uptake is significantly reduced. So a better understanding of the insulin-independent stimulation of (e.g., AICAR) glucose uptake by skeletal muscles may prove useful in developing therapeutic targets.

Importance of Studying Muscle Single Fiber Glucose Uptake

Research Using Myogenic Cells

Muscle cell lines have been the workhorse for many studies investigating insulin signaling, including GLUT4 translocation, and glucose uptake (89-92). David Yaffe's

L6 myogenic line from rat muscle (93) is frequently used as a cellular model for studying insulin-stimulated glucose transport (94), since both L6 myoblasts and fused myotubes have the GLUT4 machinery activated by insulin stimulation (95). The mouse derived C2C12 myogenic cell line (96) is primarily used to study cell differentiation and development (97-99). Primary cell lines isolated from muscle provide a cell model with the closest relationship to actual muscle, though they still exhibit myogenic features and do not remain viable for long periods of time. Nonetheless, a classic study by Amira Klip's group compared insulin-stimulated glucose uptake in fused myotubes of human muscle cells (primary myocytes), myotubes from the rat L6 cell line, and mouse C2C12 muscle cell line. Insulin stimulated glucose uptake was increased to a larger extent (2.37-fold) in L6 cells than in either human (1.58-fold) or C2C12 (1.39-fold) myotubes. The glucose uptake capacity was inhibited by 90% in all cell types by cytochalasin B (a glucose transport inhibitor). This study provided evidence of similarities in glucose uptake capacity among myogenic cell types (100), however aside from the clear physiological differences, fold differences in glucose uptake were lower in the cells than the 4-6 fold increases observed in mature skeletal muscle (46, 101, 102). Many other groups have utilized cell cultures to study the importance of a gene of interest via overexpression or knockdown studies in culture. For example, Robinson et al. provided novel evidence for the role of glucose transporters and phosphorylation events via overexpressing GLUT1 or GLUT4 in L6 myoblasts (103). Thong et al. were able to utilize mutant version of AS160 that was constitutively active (AS160-4P) or constitutively inactive (AS160-RK) in L6 myoblasts to better explain the role of AS160 as a regulator of GLUT4 translocation (104). In addition, cell culture models allow for

valuable experiments including the ability to measure glucose uptake via a real time imaging method (105) and visualization of trafficking events via fluorescent based, single cell assays (106).

Limitation of Myogenic Cells and Importance of Studying Single Fibers from Mature Skeletal Muscle

While myogenic cell studies are clearly valuable, these cell lines lack many important properties of mature skeletal muscle fibers (107). Adult MHC isoforms (I, IIA, IIB, IIX) appear only later in postnatal development, thus fiber type classification is limited to mature muscle fibers, highlighting limitations of cell lines (108). In addition, cultured cell lines are limited in the application of physiologic interventions and condition (e.g., different diets, exercise, aging, etc). Also, the effects of physiological processes involved with exercise and aging cannot be studied in the cultured muscle cell model. The primary function of skeletal muscle (i.e. contraction) cannot be adequately investigated in cell culture models which ultimately limit the ability to utilize this model in understanding physiological properties of muscle. In addition, the array of hormonal influences that mature muscle is exposed to under physiological conditions is difficult to replicate in the cell culture model, highlighting further limitations. For these reasons, there has been a strong motivation for utilizing mature muscle single fibers isolated from skeletal muscle.

Initial work using mature muscle single fibers was performed by Bekoff and Betz in which they described the isolation of single fibers from the FDB muscle, which could then be cultured as muscle cells (109). Rosenblatt et al. went on to utilize this method to

isolate single fibers and advance the understanding of satellite cell attachment and movement from the fibers (110). A significant amount of work has been done in single fibers to better understand force generation and contraction. In single permeabilized muscle fiber experiments, the force per cross-bridge (111), fraction of myosin heads forming cross bridges (112), muscle fiber weakness (113), ATP consumption (114), and force transmission measurements have resulted (115). However, there has been only modest investigation of the metabolic characteristics of single fibers, and surprisingly little in the way of investigating insulin signaling, GLUT4 translocation, and glucose uptake in mature single skeletal muscle fibers.

Research Using Muscle Single Fibers

Research on mature muscle single fibers from skeletal muscle has been performed to a limited extent in studies of metabolism and protein expression. Some of the seminal single fiber studies to investigate metabolism utilized the giant muscle fibers from the large barnacle, *Balanus nubilus*. These barnacles contain muscles made up of large fibers that are over 2 mm thick and several centimeters long (116, 117). Along with studying the neuromuscular physiology, these giant fibers were utilized for sugar transport experiments. Peter Baker and Anthony Carruthers investigated the 3-0-methylglucose transport into the large barnacle muscle fibers which lead to an increased understanding of glucose transport kinetics and control. They found that both insulin and contraction stimulation were able to lead to increased glucose transport in the fibers via a limited number of membrane transport sites (118, 119). This amphibian muscle is composed of several different fiber types (similar to mammalian muscle). Although these initial single

fiber studies did not make an effort to fiber type the samples, the use of these giant muscle fibers was the first published attempt to avoid problems associated with population heterogeneity within a muscle.

While these large barnacle single fiber studies were being performed, David James, Paul Pilch, and others were providing evidence of a specific glucose transporter, GLUT4, that was insulin responsive and would be shown as the primary glucose transporter in adipose and skeletal muscle (120). Evidence showing fiber-type dependent GLUT4 expression in human skeletal muscle biopsy sections were analyzed via immunohistochemical staining; GLUT4 protein was more abundant in slow fibers than fast fibers (121). By pooling fibers of known fiber type isolated from human skeletal muscle, Erik Richter's group confirmed that the GLUT4 abundance was greatest in human muscle fibers expressing MHC type I > IIA > IIX (122). Kong et al. were able to isolate single fibers from the rabbit tibialis anterior muscle and measured GLUT4 abundance via immunoblotting, showing that fiber-type differences varied by a factor of 20 with slow oxidative > fast oxidative glycolytic > fast glycolytic (123). In an attempt to better understand signaling properties in mature muscle single fibers, Lauritzen et al. established a model to allow for the in-vivo visualization of GLUT4 translocation in mature mouse muscle fibers. Utilizing a confocal imaging technique, delineation of the spatial distribution of GFP-tagged GLUT4 translocation in living muscle fibers in situ in anesthetized mice (124) was achieved. After intravenous insulin injection, PI3-kinase activation and subsequently GLUT4 translocation were initiated at the plasma membrane. (125, 126). However, conclusions regarding the specific role of insulin in this model cannot be made due to other hormonal and intrinsic factors that may be involved in vivo.

In addition, this experimental design did not investigate the role of different fiber types. Accordingly, a better understanding of key signaling protein abundance will prove useful in understanding the glucose transport process as well as possible therapeutic targets, with important distinctions between fiber type differences a point of focus.

Recent studies by Håkan Wasterblad's group have investigated glucose uptake by pooled single fibers isolated from the flexor digitorum brevis (FDB) muscle of mice (127). These fibers (termed cells in the study), while physiologically closer to whole muscle, had been cultured for an extended period of time prior to the study's experiments. Their results provide an indication of basal and insulin-stimulated glucose uptake following ~20 hour culture of the cells. Similar to results exhibited when measuring insulin-stimulated glucose uptake by cultured myogenic cells, the FDB cells displayed a response to insulin when using fluorescent 2-DG (2-NBDG) to assess glucose uptake (127). Because this study did not determine the fiber type of the cultured FDB cells, it is uncertain if the cells continued to express adult MHC isoforms, or if the long-term culture of these fibers caused the adult MHC isoform expression to be deregulated in favor of fetal MHC isoforms as others have reported to occur with long-term culture (128). Although this possible reversion of muscle fibers to precursor cell types may have important implications for remodeling of muscle and for "engineered" muscle or other tissues (129), it may prove detrimental when studying muscle fiber glucose uptake. In addition to the morphological changes observed during fiber dedifferentiation in culture, functional changes are also often evident (130, 131). Ultimately, although cultured fiber systems can provide useful data (calcium signaling, satellite cell

physiology, dedifferentiation, etc.), they unfortunately fail to fully mimic the biology of authentic adult muscle fibers.

In summary, the study of cultured myogenic cells has provided important insights into cellular and molecular mechanisms that regulate glucose uptake (132-138). However, because cultured cells fail to replicate many important properties of mature skeletal muscle, the ability to measure glucose uptake by mature single fibers would be extremely useful. Previous studies have raised important questions regarding aspects of fiber type differences from whole muscle analysis, which raises the question of whether differences are intrinsic to the specific muscle, or the fiber type itself. In addition, a relationship between protein expression (e.g., GLUT4 abundance) and fiber-type in mammalian muscle exist in the literature, though to a limited extent. Furthermore, hundreds of publications have elucidated the contractile properties of single fibers from mammalian muscles (see Edman 2010 (139)). In striking contrast, there is currently no knowledge available for measuring glucose uptake by single fibers of known fiber type from mammalian skeletal muscle. Development of such a method would be valuable for future studies designed to improve the understanding of skeletal muscle metabolism.

Effect of Obesity on Skeletal Muscle and Skeletal Muscle Glucose Transport

The prevalence of obesity continues to escalate in the United States, with more than one-third of US adults currently considered obese with a body mass index (BMI) ≥ 30 (140). Although both genetic and environmental factors are involved, the root cause of obesity is an energy imbalance such that more calories are consumed than expended. This energy imbalance leads to storage of excess energy in adipocytes and skeletal

muscle as triglycerides and intramyocellular lipid (141, 142). Obesity-related insulin resistance ultimately develops resulting in the metabolic syndrome (including dyslipidemia, hypertension, type 2 diabetes, cardiovascular disease).

The relationship between skeletal muscle insulin resistance and obesity has received considerable attention. The reduced ability of insulin to stimulate glucose metabolism in skeletal muscle involves defects of insulin signaling and glucose transport (143-145). There have been many rodent models created to study these defects, and several rat models have provided a substantial understanding of obesity's effect on skeletal muscle (146). The obese Zucker rat is one of the most widely used animal models of genetic obesity. There are two types of Zucker rat that have been widely studied, a lean Zucker (LZ) rat denoted as the dominant trait (Fa/Fa) or (Fa/fa), and the obese Zucker (OZ) rat, which possesses a recessive trait (fa/fa) of the leptin receptor, ultimately resulting in hyperphagia and obesity. The OZ model of obesity provides a model where dramatic insulin resistance can be studied to determine the underlying mechanism. Brozinick et al. measured glucose uptake in the perfused hindlimb of OZ and LZ rats. In the basal condition, LZ and OZ rats displayed similar glucose uptake, however LZ rats had an approximate four-fold greater capacity for insulin-stimulated glucose uptake than OZ rats. Measurement of plasma membrane GLUT4 abundance suggested the glucose uptake differences were in part due to impairment in the translocation process of GLUT4. Importantly, contraction-stimulated glucose uptake and GLUT4 translocation were not different between OZ and LZ rats suggesting a specific defect in the insulin-stimulation of GLUT4 translocation and subsequent glucose uptake (147). Sherman et al. further characterized the insulin resistance observed in OZ skeletal

muscle with specific focus on whether insulin resistance was muscle, and possibly fiber type, specific. Utilizing the perfused hindlimb method and focusing on four muscle/muscle portions (soleus, red quadriceps, white quadriceps, and gastrocnemius), the results confirmed previous work indicating muscle insulin resistance in the OZ rat is a result of impairment of the glucose transport process. This impairment was shown to occur at similar magnitude for each skeletal muscle of the study (148). Etgen et al. aimed to better understand the impaired insulin-stimulated glucose transport process in muscle from the OZ rat by measuring ex vivo glucose uptake and cell-surface GLUT4 in isolated muscles allowing for control of vivo factors (e.g., hormonal influence, blood flow, innervation, etc.). In the OZ rat isolated soleus and epitrochlearis muscles with insulin-stimulation, reduced glucose transport and cell-surface GLUT4 was observed compared to the LZ muscles. In contrast, there were no differences in either glucose uptake or cell-surface GLUT4 observed between OZ and LZ rat muscles (with either the soleus or epitrochlearis) when stimulated by ex vivo contraction (149). These results suggested that decreased cell-surface GLUT4 and glucose uptake observed in the OZ muscles under insulin-stimulated conditions was a consequence of a mechanism not affecting contraction-stimulation.

Effect of Aging on Skeletal Muscle and Skeletal Muscle Glucose Transport

Effect of Aging on Skeletal Muscle Glucose Metabolism

Glucose metabolism is altered across the lifespan in both humans (150) and rats (151), with progressive insulin resistance appearing over the lifetime. In rats, a profound age-related reduction in glucose uptake by skeletal comes early in life (2-4 months old)

(152) when studying the perfused hindlimb. The magnitude of further decreases is tempered later in life. Escriva et al. showed that 20-24 month old rats compared to 6-10 month old rats had a moderate degree of age-related insulin resistance during a euglycemic-hyperinsulinemic clamp. When investigating the muscles, there was a significant decrease in glucose uptake by the soleus (primarily type I fibers), but not in the quadriceps femoris (primarily type II fibers) (153), suggesting not all skeletal muscle become insulin resistant with age. Studying the isolated soleus and epitrochlearis (primarily II fibers) muscles from 9 month and 25 month old rats, Sharma et al. observed similar results, with the soleus displaying an age-related decrement in insulin-stimulated glucose uptake, while the epitrochlearis displayed no significant aging effects on insulin-stimulated glucose uptake capacity (154), as supported by other studies (155-158). Importantly, GLUT4 abundance does not significantly differ in adult versus old rats (158, 159).

Although, insulin-stimulated glucose uptake capacity of does not typically diminish between adult (8-13 months old) and old (24-26 months old) rat epitrochlearis muscles, there is evidence suggesting that age-related changes are often unmasked once the system's adaptive capacity is challenged (e.g. exercise or calorie restriction). Cartee et al. evaluated the persistent effects of exercise on skeletal muscle across the life-span of rats. When evaluating insulin-stimulation of the epitrochlearis immediately post-exercise, muscles from the 25 month old rat exhibited less glucose uptake than the 13 month old rat (155). Likewise, when evaluating the effects of calorie restriction on the epitrochlearis from 8, 18, and 23 month old rats, Cartee et al. showed differential glucose uptake capacity with maximally effective insulin stimulation among the age groups (160).

In addition, earlier research using whole muscles found that the primarily type I soleus muscle displayed insulin resistance while the quadriceps and epitrochlearis muscles (primarily type II fibers) remain protected from the age-related insulin resistance. These studies highlight the importance of potential fiber type differences in the aging model, as well as the effect that various interventions may have on specific fiber types. Although the aged muscle under standard conditions often does not deviate from the adult muscle with regards to glucose uptake capacity, studying an intervention (e.g. exercise or calorie restriction) offers a perspective on the effect that aging has under challenged conditions.

Rationale for Research Models Used in this Thesis

Experimental Animals

Rats were used for all experiments in this dissertation research. The metabolic physiology of the rat is closer to humans than in mice, which makes the rat a popular and valuable model to study metabolism (161, 162). There is a large body of literature that describes insulin-stimulated glucose transport in rat skeletal muscle. Research characterizing glucose uptake by rat muscles of different fiber-types includes, but is not limited to: 1) in vivo perfused hindlimb method measuring glucose uptake by hindlimb muscles of varying fiber types, 2) in vitro basal and insulin-stimulated glucose uptake by muscles of varying fiber types, 3) in vitro basal and AICAR-stimulated whole muscle glucose uptake by muscles of varying fiber types. These experiments have contributed to our current understanding of the role that fiber-type may have on glucose uptake capacity, though do not rule out the possibility of the glucose uptake differences being muscle specific rather than fiber type specific. Thus, measuring glucose uptake by a

single fiber of known fiber type would be the most direct approach to understand potential fiber type differences.

Study 1 and Study 3 used male Wistar rats. This albino model of rat has been utilized for nearly a century, and provides a standardized animal for comparison across many studies (163). Study 1 also utilized Lean and Obese Zucker rats. The obese Zucker (OZ) rat possesses a recessive trait (fa/fa) of the leptin receptor, ultimately resulting in hyperphagia. It is a widely used model for metabolic syndrome, characterized by insulin resistance, dyslipidemia, mild glucose intolerance, hyperinsulinemia, and hypertension (164-167). As in obese humans, the cause for insulin resistance in OZ rats is a reduced ability of insulin to stimulate GLUT4 translocation rather than reduced GLUT4 expression by muscle (149). Insulin resistance in the OZ rat muscle (as well as human muscle (168)) is commonly accompanied by defects in insulin signaling steps, including insulin receptor substrate 1 (IRS1)-associated phosphatidylinositol 3-kinase activity (PI3K), Akt phosphorylation (169), and decreased AS160 phosphorylation (170, 171). Moreover, this model displays robust insulin resistance, specifically when measuring glucose uptake. Thus, as the initial model used to investigate insulin resistance in single fibers, the OZ rat provided the projected discernible differences when comparing glucose uptake results to LZ rat.

Study 2 used adult (9 month) and old (25 month) Fisher Brown Norway (FBN) rats. The FBN strain has been well characterized for aging research. The 25 month old rats is roughly comparable to a 60-70 year old human (172) and is representative of the onset of old age in humans. Similar to humans, rats have a modest decline in glucose

disposal from adulthood to old age (~15-35%) (151, 173), while knowledge with regard to the role that different fiber types play in this age-related insulin resistance is lacking.

Rat Epitrochlearis Muscle

The isolated rat epitrochlearis muscle was used in all studies. The epitrochlearis has been widely used to study ex vivo glucose uptake because its flat geometry (21-24 fibers thick) greatly facilitates delivery of O_2 and 2-deoxyglucose by diffusion. In the animal, the epitrochlearis muscle contributes in extension of the forelimb and originates from the tendon of the m. latissimus dorsi and inserts on the medial epicondyle of the humerus (174). Because its fibers run parallel, from tendon-to-tendon, and its collagen content is modest, it is ideal for the collagenase method of fiber isolation. Although the fiber type composition of the epitrochlearis corresponds to the composition of most muscles in the rat (175), a limitation is the low percentage of type I fibers. Nonetheless, the epitrochlearis allows comparison of type IIA fibers (muscles composed largely of type IIA fibers vs. predominantly type I muscles have similar glucose uptake) with type IIB and IIX fibers. These isoforms (IIA, IIB, IIX) represent greater than 90% of the fiber type composition of skeletal muscles in the entire rat hindlimb stressing the importance of studying these fiber types (176, 177). With respect to the models studied, there is evidence to show that the whole epitrochlearis of OZ vs. LZ is very insulin resistant (149). While the whole epitrochlearis muscle of 25 month-old rats does not display aging associated insulin resistance (vs. 9 month old), the possibility of fiber-type specific insulin resistance remains and can be investigated utilizing the single fiber method

(developed in Study1). Finally, the superficial anatomic location of the epitrochlearis in the rat forelimb also makes it easily accessible for in vivo electroporation in Study 3.

In Vitro Glucose Uptake

In all experiments, glucose uptake was evaluated by measurements of ^{3}H-2-deoxy-D-glucose (2DG) uptake. 2DG is a glucose analog that becomes phosphorylated upon entering into the muscle cell, though is not further metabolized, and thus allows the study of glucose uptake independent of glucose metabolism subsequent to hexokinase.

In Vivo Electroporation

In Study 3, in vivo electroporation (IVE) was used as a non-viral method gene delivery for ectopic expression in the rat epitrochlearis muscle. A possible alternative would have been a viral-based method such as adeno-associated virus or retrovirus protocols. While these methods are efficient, there are critical deficiencies including possible immunogenic/toxicity effects and time intensive requirements to produce transgenic animals. Conversely, IVE allows for localized expression in a relatively short time period (7-14 days) and minimizing possible toxicity concerns observed with viral transfection. As a superficially localized muscle, the epitrochlearis provides easy access for injection and electroporation. In addition, the use of a plasmid allows for production of large quantities, low toxicity, and the ability to accommodate expression of large genes or even multiple genes. Evidence exists showing that electroporated plasmid in skeletal muscle is safe and effective (178-181), providing rationale in selecting electroporation for plasmid-based delivery.

References

1. Rolfe DF, Brown GC. Cellular energy utilization and molecular origin of standard metabolic rate in mammals. Physiological reviews. 1997;77(3):731-58.
2. Brooks SV. Current topics for teaching skeletal muscle physiology. Adv Physiol Educ. 2003;27(1-4):171-82.
3. Scott W, Stevens J, Binder-Macleod SA. Human skeletal muscle fiber type classifications. Phys Ther. 2001;81(11):1810-6.
4. Exeter D, Connell DA. Skeletal muscle: functional anatomy and pathophysiology. Semin Musculoskelet Radiol. 2010;14(2):97-105.
5. Saibene F, Minetti AE. Biomechanical and physiological aspects of legged locomotion in humans. Eur J Appl Physiol. 2003;88(4-5):297-316.
6. Zajac FE, Neptune RR, Kautz SA. Biomechanics and muscle coordination of human walking: part II: lessons from dynamical simulations and clinical implications. Gait Posture. 2003;17(1):1-17.
7. Fraix M. Role of the musculoskeletal system and the prevention of falls. J Am Osteopath Assoc. 2012;112(1):17-21.
8. Koolstra JH, van Eijden TM. The jaw open-close movements predicted by biomechanical modelling. Journal of biomechanics. 1997;30(9):943-50.
9. Bell DG, Tikuisis P, Jacobs I. Relative intensity of muscular contraction during shivering. J Appl Physiol. 1992;72(6):2336-42.
10. Weibel ER, Hoppeler H. Exercise-induced maximal metabolic rate scales with muscle aerobic capacity. J Exp Biol. 2005;208(Pt 9):1635-44.
11. Zurlo F, Larson K, Bogardus C, Ravussin E. Skeletal muscle metabolism is a major determinant of resting energy expenditure. J Clin Invest. 1990;86(5):1423-7. PMCID: 296885.
12. Felig P, Wahren J. Fuel homeostasis in exercise. N Engl J Med. 1975;293(21):1078-84.
13. Darras BT, Friedman NR. Metabolic myopathies: a clinical approach; part I. Pediatr Neurol. 2000;22(2):87-97.
14. Tirone TA, Brunicardi FC. Overview of glucose regulation. World J Surg. 2001;25(4):461-7.
15. Staron RS. Human skeletal muscle fiber types: delineation, development, and distribution. Can J Appl Physiol. 1997;22(4):307-27.
16. Pette D, Staron RS. Mammalian skeletal muscle fiber type transitions. Int Rev Cytol. 1997;170:143-223.
17. Greising SM, Gransee HM, Mantilla CB, Sieck GC. Systems biology of skeletal muscle: fiber type as an organizing principle. Wiley Interdiscip Rev Syst Biol Med. 2012;4(5):457-73.
18. Essen B, Jansson E, Henriksson J, Taylor AW, Saltin B. Metabolic characteristics of fibre types in human skeletal muscle. Acta Physiol Scand. 1975;95(2):153-65.
19. Pette D, Peuker H, Staron RS. The impact of biochemical methods for single muscle fibre analysis. Acta Physiol Scand. 1999;166(4):261-77.
20. Pandorf CE, Caiozzo VJ, Haddad F, Baldwin KM. A rationale for SDS-PAGE of MHC isoforms as a gold standard for determining contractile phenotype. J Appl Physiol. 2010;108(1):222-2; author reply 6.

21. Bigard AX, Sanchez H, Birot O, Serrurier B. Myosin heavy chain composition of skeletal muscles in young rats growing under hypobaric hypoxia conditions. J Appl Physiol. 2000;88(2):479-86.
22. Schiaffino S, Reggiani C. Molecular diversity of myofibrillar proteins: gene regulation and functional significance. Physiological reviews. 1996;76(2):371-423.
23. Schiaffino S, Reggiani C. Myosin isoforms in mammalian skeletal muscle. J Appl Physiol. 1994;77(2):493-501.
24. Thomason DB, Baldwin KM, Herrick RE. Myosin isozyme distribution in rodent hindlimb skeletal muscle. J Appl Physiol. 1986;60(6):1923-31.
25. Fry AC, Allemeier CA, Staron RS. Correlation between percentage fiber type area and myosin heavy chain content in human skeletal muscle. Eur J Appl Physiol Occup Physiol. 1994;68(3):246-51.
26. DeNardi C, Ausoni S, Moretti P, Gorza L, Velleca M, Buckingham M, et al. Type 2X-myosin heavy chain is coded by a muscle fiber type-specific and developmentally regulated gene. J Cell Biol. 1993;123(4):823-35. PMCID: 2200149.
27. Stephenson GM. Hybrid skeletal muscle fibres: a rare or common phenomenon? Clin Exp Pharmacol Physiol. 2001;28(8):692-702.
28. Castorena CM, Mackrell JG, Bogan JS, Kanzaki M, Cartee GD. Clustering of GLUT4, TUG, and RUVBL2 protein levels correlate with myosin heavy chain isoform pattern in skeletal muscles, but AS160 and TBC1D1 levels do not. J Appl Physiol. 2011;111(4):1106-17. PMCID: 3191788.
29. Caiozzo VJ, Baker MJ, Baldwin KM. Modulation of myosin isoform expression by mechanical loading: role of stimulation frequency. J Appl Physiol. 1997;82(1):211-8.
30. Caiozzo VJ, Baker MJ, Huang K, Chou H, Wu YZ, Baldwin KM. Single-fiber myosin heavy chain polymorphism: how many patterns and what proportions? American journal of physiology. 2003;285(3):R570-80.
31. DeFronzo RA. Lilly lecture 1987. The triumvirate: beta-cell, muscle, liver. A collusion responsible for NIDDM. Diabetes. 1988;37(6):667-87.
32. Perseghin G, Price TB, Petersen KF, Roden M, Cline GW, Gerow K, et al. Increased glucose transport-phosphorylation and muscle glycogen synthesis after exercise training in insulin-resistant subjects. N Engl J Med. 1996;335(18):1357-62.
33. Perseghin G, Ghosh S, Gerow K, Shulman GI. Metabolic defects in lean nondiabetic offspring of NIDDM parents: a cross-sectional study. Diabetes. 1997;46(6):1001-9.
34. Defronzo RA. Banting Lecture. From the triumvirate to the ominous octet: a new paradigm for the treatment of type 2 diabetes mellitus. Diabetes. 2009;58(4):773-95.
35. American Diabetes Association. Economic Costs of Diabetes in the U.S. in 2007. Diabetes Care. 2008;31(3):596-615.

36. Colditz GA. Economic costs of obesity and inactivity. Med Sci Sports Exerc. 1999;31(11 Suppl):S663-7.
37. Type 2 diabetes in children and adolescents. American Diabetes Association. Pediatrics. 2000;105(3 Pt 1):671-80.
38. Facchini FS, Hua N, Abbasi F, Reaven GM. Insulin resistance as a predictor of age-related diseases. J Clin Endocrinol Metab. 2001;86(8):3574-8.
39. Haffner SM. Epidemiology of insulin resistance and its relation to coronary artery disease. Am J Cardiol. 1999;84(1A):11J-4J.

40. Kumari M, Brunner E, Fuhrer R. Minireview: mechanisms by which the metabolic syndrome and diabetes impair memory. J Gerontol A Biol Sci Med Sci. 2000;55(5):B228-32.
41. Sinacore DR, Gulve EA. The role of skeletal muscle in glucose transport, glucose homeostasis, and insulin resistance: implications for physical therapy. Phys Ther. 1993;73(12):878-91.
42. Birnbaum MJ. The insulin-sensitive glucose transporter. Int Rev Cytol. 1992;137:239-97.
43. Lavan BE, Lienhard GE. Insulin signalling and the stimulation of glucose transport. Biochem Soc Trans. 1994;22(3):676-80.
44. DeFronzo RA, Jacot E, Jequier E, Maeder E, Wahren J, Felber JP. The effect of insulin on the disposal of intravenous glucose. Results from indirect calorimetry and hepatic and femoral venous catheterization. Diabetes. 1981;30(12):1000-7.
45. Ziel FH, Venkatesan N, Davidson MB. Glucose transport is rate limiting for skeletal muscle glucose metabolism in normal and STZ-induced diabetic rats. Diabetes. 1988;37(7):885-90.
46. Constable SH, Favier RJ, Cartee GD, Young DA, Holloszy JO. Muscle glucose transport: interactions of in vitro contractions, insulin, and exercise. J Appl Physiol. 1988;64(6):2329-32.
47. Cartee GD, Young DA, Sleeper MD, Zierath J, Wallberg-Henriksson H, Holloszy JO. Prolonged increase in insulin-stimulated glucose transport in muscle after exercise. The American journal of physiology. 1989;256(4 Pt 1):E494-9.
48. Holloszy JO, Hansen PA. Regulation of glucose transport into skeletal muscle. Rev Physiol Biochem Pharmacol. 1996;128:99-193.
49. Henriksen EJ, Bourey RE, Rodnick KJ, Koranyi L, Permutt MA, Holloszy JO. Glucose transporter protein content and glucose transport capacity in rat skeletal muscles. The American journal of physiology. 1990;259(4 Pt 1):E593-8.
50. Cartee GD, Holloszy JO. Exercise increases susceptibility of muscle glucose transport to activation by various stimuli. The American journal of physiology. 1990;258(2 Pt 1):E390-3.
51. Holloszy JO. A forty-year memoir of research on the regulation of glucose transport into muscle. Am J Physiol Endocrinol Metab. 2003;284(3):E453-67.
52. Cushman SW, Wardzala LJ. Potential mechanism of insulin action on glucose transport in the isolated rat adipose cell. Apparent translocation of intracellular transport systems to the plasma membrane. J Biol Chem. 1980;255(10):4758-62.
53. Suzuki K, Kono T. Evidence that insulin causes translocation of glucose transport activity to the plasma membrane from an intracellular storage site. Proceedings of the National Academy of Sciences of the United States of America. 1980;77(5):2542-5. PMCID: 349437.
54. Birnbaum MJ. Identification of a novel gene encoding an insulin-responsive glucose transporter protein. Cell. 1989;57(2):305-15.
55. Taniguchi CM, Emanuelli B, Kahn CR. Critical nodes in signalling pathways: insights into insulin action. Nature reviews. 2006;7(2):85-96.
56. Huang S, Czech MP. The GLUT4 glucose transporter. Cell metabolism. 2007;5(4):237-52.

57. Myers MG, Jr., Sun XJ, White MF. The IRS-1 signaling system. Trends in biochemical sciences. 1994;19(7):289-93.
58. Tamemoto H, Kadowaki T, Tobe K, Yagi T, Sakura H, Hayakawa T, et al. Insulin resistance and growth retardation in mice lacking insulin receptor substrate-1. Nature. 1994;372(6502):182-6.
59. Barbieri M, Bonafe M, Franceschi C, Paolisso G. Insulin/IGF-I-signaling pathway: an evolutionarily conserved mechanism of longevity from yeast to humans. Am J Physiol Endocrinol Metab. 2003;285(5):E1064-71.
60. Taha C, Klip A. The insulin signaling pathway. J Membr Biol. 1999;169(1):1-12.
61. Storgaard H, Song XM, Jensen CB, Madsbad S, Bjornholm M, Vaag A, et al. Insulin signal transduction in skeletal muscle from glucose-intolerant relatives of type 2 diabetic patients [corrected]. Diabetes. 2001;50(12):2770-8.
62. Calera MR, Martinez C, Liu H, Jack AK, Birnbaum MJ, Pilch PF. Insulin increases the association of Akt-2 with Glut4-containing vesicles. J Biol Chem. 1998;273(13):7201-4.
63. Cho H, Thorvaldsen JL, Chu Q, Feng F, Birnbaum MJ. Akt1/PKBalpha is required for normal growth but dispensable for maintenance of glucose homeostasis in mice. J Biol Chem. 2001;276(42):38349-52.
64. Hill MM, Clark SF, Tucker DF, Birnbaum MJ, James DE, Macaulay SL. A role for protein kinase Bbeta/Akt2 in insulin-stimulated GLUT4 translocation in adipocytes. Mol Cell Biol. 1999;19(11):7771-81.
65. Whiteman EL, Cho H, Birnbaum MJ. Role of Akt/protein kinase B in metabolism. Trends Endocrinol Metab. 2002;13(10):444-51.
66. Vanhaesebroeck B, Alessi DR. The PI3K-PDK1 connection: more than just a road to PKB. The Biochemical journal. 2000;346 Pt 3:561-76.
67. Sarbassov DD, Guertin DA, Ali SM, Sabatini DM. Phosphorylation and regulation of Akt/PKB by the rictor-mTOR complex. Science. 2005;307(5712):1098-101.
68. Sano H, Kane S, Sano E, Miinea CP, Asara JM, Lane WS, et al. Insulin-stimulated phosphorylation of a Rab GTPase-activating protein regulates GLUT4 translocation. J Biol Chem. 2003;278(17):14599-602.
69. Kane S, Sano H, Liu SC, Asara JM, Lane WS, Garner CC, et al. A method to identify serine kinase substrates. Akt phosphorylates a novel adipocyte protein with a Rab GTPase-activating protein (GAP) domain. J Biol Chem. 2002;277(25):22115-8.
70. Roach WG, Chavez JA, MÃ®inea CP, Lienhard GE. Substrate specificity and effect on GLUT4 translocation of the Rab GTPase-activating protein Tbc1d1. The Biochemical journal. 2007;403(2):353-8.
71. Chavez JA, Roach WG, Keller SR, Lane WS, Lienhard GE. Inhibition of GLUT4 translocation by Tbc1d1, a Rab GTPase activating protein abundant in skeletal muscle, is partially relieved by AMPK activation. J Biol Chem. 2008:M708934200.
72. Cartee GD, Wojtaszewski JF. Role of Akt substrate of 160 kDa in insulin-stimulated and contraction-stimulated glucose transport. Appl Physiol Nutr Metab. 2007;32(3):557-66.
73. Kern M, Wells JA, Stephens JM, Elton CW, Friedman JE, Tapscott EB, et al. Insulin responsiveness in skeletal muscle is determined by glucose transporter (Glut4) protein level. The Biochemical journal. 1990;270(2):397-400.

74. Miinea CP, Sano H, Kane S, Sano E, Fukuda M, Peranen J, et al. AS160, the Akt substrate regulating GLUT4 translocation, has a functional Rab GTPase-activating protein domain. The Biochemical journal. 2005;391(Pt 1):87-93.
75. Yeh JI, Gulve EA, Rameh L, Birnbaum MJ. The effects of wortmannin on rat skeletal muscle. Dissociation of signaling pathways for insulin- and contraction-activated hexose transport. J Biol Chem. 1995;270(5):2107-11.
76. Liu ML, Gibbs EM, McCoid SC, Milici AJ, Stukenbrok HA, McPherson RK, et al. Transgenic mice expressing the human GLUT4/muscle-fat facilitative glucose transporter protein exhibit efficient glycemic control. Proceedings of the National Academy of Sciences of the United States of America. 1993;90(23):11346-50. PMCID: 47979.
77. Ren JM, Marshall BA, Mueckler MM, McCaleb M, Amatruda JM, Shulman GI. Overexpression of Glut4 protein in muscle increases basal and insulin-stimulated whole body glucose disposal in conscious mice. J Clin Invest. 1995;95(1):429-32. PMCID: 295454.
78. Charron MJ, Katz EB. Metabolic and therapeutic lessons from genetic manipulation of GLUT4. Mol Cell Biochem. 1998;182(1-2):143-52.
79. Katz EB, Burcelin R, Tsao TS, Stenbit AE, Charron MJ. The metabolic consequences of altered glucose transporter expression in transgenic mice. J Mol Med (Berl). 1996;74(11):639-52.
80. Tsao TS, Burcelin R, Katz EB, Huang L, Charron MJ. Enhanced insulin action due to targeted GLUT4 overexpression exclusively in muscle. Diabetes. 1996;45(1):28-36.
81. Cleasby ME, Davey JR, Reinten TA, Graham MW, James DE, Kraegen EW, et al. Acute bidirectional manipulation of muscle glucose uptake by in vivo electrotransfer of constructs targeting glucose transporter genes. Diabetes. 2005;54(9):2702-11.
82. Bonen A, Tan MH, Watson-Wright WM. Insulin binding and glucose uptake differences in rodent skeletal muscles. Diabetes. 1981;30(8):702-4.
83. James DE, Jenkins AB, Kraegen EW. Heterogeneity of insulin action in individual muscles in vivo: euglycemic clamp studies in rats. The American journal of physiology. 1985;248(5 Pt 1):E567-74.
84. Ploug T, Galbo H, Vinten J, Jorgensen M, Richter EA. Kinetics of glucose transport in rat muscle: effects of insulin and contractions. The American journal of physiology. 1987;253(1 Pt 1):E12-20.
85. Merrill GF, Kurth EJ, Hardie DG, Winder WW. AICA riboside increases AMP-activated protein kinase, fatty acid oxidation, and glucose uptake in rat muscle. The American journal of physiology. 1997;273(6 Pt 1):E1107-12.
86. Bergeron R, Russell RR, 3rd, Young LH, Ren JM, Marcucci M, Lee A, et al. Effect of AMPK activation on muscle glucose metabolism in conscious rats. The American journal of physiology. 1999;276(5 Pt 1):E938-44.
87. Ai H, Ihlemann J, Hellsten Y, Lauritzen HP, Hardie DG, Galbo H, et al. Effect of fiber type and nutritional state on AICAR- and contraction-stimulated glucose transport in rat muscle. Am J Physiol Endocrinol Metab. 2002;282(6):E1291-300.
88. Hayashi T, Hirshman MF, Kurth EJ, Winder WW, Goodyear LJ. Evidence for 5' AMP-activated protein kinase mediation of the effect of muscle contraction on glucose transport. Diabetes. 1998;47(8):1369-73.

89. Mayor P, Maianu L, Garvey WT. Glucose and insulin chronically regulate insulin action via different mechanisms in BC3H1 myocytes. Effects on glucose transporter gene expression. Diabetes. 1992;41(3):274-85.
90. Mitsumoto Y, Burdett E, Grant A, Klip A. Differential expression of the GLUT1 and GLUT4 glucose transporters during differentiation of L6 muscle cells. Biochemical and biophysical research communications. 1991;175(2):652-9.
91. Tortorella LL, Pilch PF. C2C12 myocytes lack an insulin-responsive vesicular compartment despite dexamethasone-induced GLUT4 expression. Am J Physiol Endocrinol Metab. 2002;283(3):E514-24.
92. Nedachi T, Kanzaki M. Regulation of glucose transporters by insulin and extracellular glucose in C2C12 myotubes. Am J Physiol Endocrinol Metab. 2006;291(4):E817-28.
93. Yaffe D. Retention of differentiation potentialities during prolonged cultivation of myogenic cells. Proceedings of the National Academy of Sciences of the United States of America. 1968;61(2):477-83. PMCID: 225183.
94. Rudich A, Klip A. Push/pull mechanisms of GLUT4 traffic in muscle cells. Acta Physiol Scand. 2003;178(4):297-308.
95. Ueyama A, Yaworsky KL, Wang Q, Ebina Y, Klip A. GLUT-4myc ectopic expression in L6 myoblasts generates a GLUT-4-specific pool conferring insulin sensitivity. The American journal of physiology. 1999;277(3 Pt 1):E572-8.
96. Yaffe D, Saxel O. Serial passaging and differentiation of myogenic cells isolated from dystrophic mouse muscle. Nature. 1977;270(5639):725-7.
97. Cooper ST, Maxwell AL, Kizana E, Ghoddusi M, Hardeman EC, Alexander IE, et al. C2C12 co-culture on a fibroblast substratum enables sustained survival of contractile, highly differentiated myotubes with peripheral nuclei and adult fast myosin expression. Cell Motil Cytoskeleton. 2004;58(3):200-11.
98. Kislinger T, Gramolini AO, Pan Y, Rahman K, MacLennan DH, Emili A. Proteome dynamics during C2C12 myoblast differentiation. Mol Cell Proteomics. 2005;4(7):887-901.
99. Moran JL, Li Y, Hill AA, Mounts WM, Miller CP. Gene expression changes during mouse skeletal myoblast differentiation revealed by transcriptional profiling. Physiol Genomics. 2002;10(2):103-11.
100. Sarabia V, Ramlal T, Klip A. Glucose uptake in human and animal muscle cells in culture. Biochem Cell Biol. 1990;68(2):536-42.
101. Gulve EA, Cartee GD, Zierath JR, Corpus VM, Holloszy JO. Reversal of enhanced muscle glucose transport after exercise: roles of insulin and glucose. The American journal of physiology. 1990;259(5 Pt 1):E685-91.
102. Young DA, Uhl JJ, Cartee GD, Holloszy JO. Activation of glucose transport in muscle by prolonged exposure to insulin. Effects of glucose and insulin concentrations. J Biol Chem. 1986;261(34):16049-53.
103. Robinson R, Robinson LJ, James DE, Lawrence JC, Jr. Glucose transport in L6 myoblasts overexpressing GLUT1 and GLUT4. J Biol Chem. 1993;268(29):22119-26.
104. Thong FSL, Bilan PJ, Klip A. The Rab GTPase-Activating Protein AS160 Integrates Akt, Protein Kinase C, and AMP-Activated Protein Kinase Signals Regulating GLUT4 Traffic

105. Yamada K, Saito M, Matsuoka H, Inagaki N. A real-time method of imaging glucose uptake in single, living mammalian cells. Nat Protoc. 2007;2(3):753-62.

106. Antonescu CN, Randhawa VK, Klip A. Dissecting GLUT4 traffic components in L6 myocytes by fluorescence-based, single-cell assays. Methods Mol Biol. 2008;457:367-78.
107. Lauritzen HP, Schertzer JD. Measuring GLUT4 translocation in mature muscle fibers. Am J Physiol Endocrinol Metab. 2010;299(2):E169-79.
108. Watchko JF, Daood MJ, Sieck GC. Myosin heavy chain transitions during development. Functional implications for the respiratory musculature. Comp Biochem Physiol B Biochem Mol Biol. 1998;119(3):459-70.
109. Bekoff A, Betz W. Properties of isolated adult rat muscle fibres maintained in tissue culture. J Physiol. 1977;271(2):537-47. PMCID: 1353585.
110. Rosenblatt JD, Lunt AI, Parry DJ, Partridge TA. Culturing satellite cells from living single muscle fiber explants. In Vitro Cell Dev Biol Anim. 1995;31(10):773-9.
111. Geiger PC, Cody MJ, Sieck GC. Force-calcium relationship depends on myosin heavy chain and troponin isoforms in rat diaphragm muscle fibers. J Appl Physiol. 1999;87(5):1894-900.
112. Geiger PC, Cody MJ, Macken RL, Sieck GC. Maximum specific force depends on myosin heavy chain content in rat diaphragm muscle fibers. J Appl Physiol. 2000;89(2):695-703.
113. Geiger PC, Cody MJ, Macken RL, Bayrd ME, Sieck GC. Effect of unilateral denervation on maximum specific force in rat diaphragm muscle fibers. J Appl Physiol. 2001;90(4):1196-204.
114. Sieck GC, Zhan WZ, Han YS, Prakash YS. Effect of denervation on ATP consumption rate of diaphragm muscle fibers. J Appl Physiol. 2007;103(3):858-66.
115. Guth K, Wojciechowski R. Perfusion cuvette for the simultaneous measurement of mechanical, optical and energetic parameters of skinned muscle fibres. Pflugers Arch. 1986;407(5):552-7.
116. Hoyle G, Smyth T, Jr. Neuromuscular Physiology of Giant Muscle Fibers of a Barnacle, Balanus Nubilus Darwin. Comp Biochem Physiol. 1963;10:291-314.
117. Hoyle G, Smyth T, Jr. Giant Muscle Fibers in a Barnacle, Balanus nubilus Darwin. Science. 1963;139(3549):49-50.
118. Carruthers A. Sugar transport in giant barnacle muscle fibres. J Physiol. 1983;336:377-96. PMCID: 1198975.
119. Baker PF, Carruthers A. Insulin regulation of sugar transport in giant muscle fibres of the barnacle. J Physiol. 1983;336:397-431. PMCID: 1198994.
120. James DE, Brown R, Navarro J, Pilch PF. Insulin-regulatable tissues express a unique insulin-sensitive glucose transport protein. Nature. 1988;333(6169):183-5.
121. Gaster M, Poulsen P, Handberg A, Schroder HD, Beck-Nielsen H. Direct evidence of fiber type-dependent GLUT-4 expression in human skeletal muscle. Am J Physiol Endocrinol Metab. 2000;278(5):E910-6.
122. Daugaard JR, Nielsen JN, Kristiansen S, Andersen JL, Hargreaves M, Richter EA. Fiber type-specific expression of GLUT4 in human skeletal muscle: influence of exercise training. Diabetes. 2000;49(7):1092-5.

123. Kong X, Manchester J, Salmons S, Lawrence JC, Jr. Glucose transporters in single skeletal muscle fibers. Relationship to hexokinase and regulation by contractile activity. J Biol Chem. 1994;269(17):12963-7.
124. Lauritzen HP. In vivo imaging of GLUT4 translocation. Appl Physiol Nutr Metab. 2009;34(3):420-3.
125. Lauritzen HP, Ploug T, Prats C, Tavare JM, Galbo H. Imaging of insulin signaling in skeletal muscle of living mice shows major role of T-tubules. Diabetes. 2006;55(5):1300-6.
126. Lauritzen HP. Imaging of protein translocation in situ in skeletal muscle of living mice. Methods Mol Biol. 2010;637:231-44.
127. Lanner JT, Bruton JD, Assefaw-Redda Y, Andronache Z, Zhang SJ, Severa D, et al. Knockdown of TRPC3 with siRNA coupled to carbon nanotubes results in decreased insulin-mediated glucose uptake in adult skeletal muscle cells. FASEB J. 2009;23(6):1728-38.
128. Brown LD, Schneider MF. Delayed dedifferentiation and retention of properties in dissociated adult skeletal muscle fibers in vitro. In Vitro Cell Dev Biol Anim. 2002;38(7):411-22.
129. Wagers AJ, Conboy IM. Cellular and molecular signatures of muscle regeneration: current concepts and controversies in adult myogenesis. Cell. 2005;122(5):659-67.
130. Brown LD, Rodney GG, Hernandez-Ochoa E, Ward CW, Schneider MF. Ca2+ sparks and T tubule reorganization in dedifferentiating adult mouse skeletal muscle fibers. Am J Physiol Cell Physiol. 2007;292(3):C1156-66. PMCID: 2654399.
131. Mu X, Brown LD, Liu Y, Schneider MF. Roles of the calcineurin and CaMK signaling pathways in fast-to-slow fiber type transformation of cultured adult mouse skeletal muscle fibers. Physiol Genomics. 2007;30(3):300-12.
132. Huang C, Thirone AC, Huang X, Klip A. Differential contribution of insulin receptor substrates 1 versus 2 to insulin signaling and glucose uptake in l6 myotubes. J Biol Chem. 2005;280(19):19426-35.
133. Sarabia V, Lam L, Burdett E, Leiter LA, Klip A. Glucose transport in human skeletal muscle cells in culture. Stimulation by insulin and metformin. J Clin Invest. 1992;90(4):1386-95.
134. Klip A, Ramlal T, Bilan PJ, Marette A, Liu Z, Mitsumoto Y. What signals are involved in the stimulation of glucose transport by insulin in muscle cells? Cell Signal. 1993;5(5):519-29.
135. Sargeant R, Mitsumoto Y, Sarabia V, Shillabeer G, Klip A. Hormonal regulation of glucose transporters in muscle cells in culture. J Endocrinol Invest. 1993;16(2):147-62.
136. Klip A, Tsakiridis T, Marette A, Ortiz PA. Regulation of expression of glucose transporters by glucose: a review of studies in vivo and in cell cultures. Faseb J. 1994;8(1):43-53.
137. Foster LJ, Klip A. Mechanism and regulation of GLUT-4 vesicle fusion in muscle and fat cells. Am J Physiol Cell Physiol. 2000;279(4):C877-90.
138. Krook A, Zierath JR. Specificity of insulin signalling in human skeletal muscle as revealed by small interfering RNA. Diabetologia. 2009;52(7):1231-9.
139. Edman KA. Contractile performance of striated muscle. Adv Exp Med Biol. 2010;682:7-40.

140. Wang Y, Beydoun MA. The obesity epidemic in the United States--gender, age, socioeconomic, racial/ethnic, and geographic characteristics: a systematic review and meta-regression analysis. Epidemiol Rev. 2007;29:6-28.
141. Pan DA, Lillioja S, Kriketos AD, Milner MR, Baur LA, Bogardus C, et al. Skeletal muscle triglyceride levels are inversely related to insulin action. Diabetes. 1997;46(6):983-8.
142. Malenfant P, Joanisse DR, Theriault R, Goodpaster BH, Kelley DE, Simoneau JA. Fat content in individual muscle fibers of lean and obese subjects. Int J Obes Relat Metab Disord. 2001;25(9):1316-21.
143. Shulman GI. Cellular mechanisms of insulin resistance. J Clin Invest. 2000;106(2):171-6. PMCID: 314317.
144. Bonadonna RC, Del Prato S, Bonora E, Saccomani MP, Gulli G, Natali A, et al. Roles of glucose transport and glucose phosphorylation in muscle insulin resistance of NIDDM. Diabetes. 1996;45(7):915-25.
145. Kelley DE, Mintun MA, Watkins SC, Simoneau JA, Jadali F, Fredrickson A, et al. The effect of non-insulin-dependent diabetes mellitus and obesity on glucose transport and phosphorylation in skeletal muscle. J Clin Invest. 1996;97(12):2705-13. PMCID: 507362.
146. Aleixandre de Artinano A, Miguel Castro M. Experimental rat models to study the metabolic syndrome. Br J Nutr. 2009;102(9):1246-53.
147. Brozinick JT, Jr., Etgen GJ, Jr., Yaspelkis BB, 3rd, Ivy JL. Glucose uptake and GLUT-4 protein distribution in skeletal muscle of the obese Zucker rat. The American journal of physiology. 1994;267(1 Pt 2):R236-43.
148. Sherman WM, Katz AL, Cutler CL, Withers RT, Ivy JL. Glucose transport: locus of muscle insulin resistance in obese Zucker rats. The American journal of physiology. 1988;255(3 Pt 1):E374-82.
149. Etgen GJ, Jr., Wilson CM, Jensen J, Cushman SW, Ivy JL. Glucose transport and cell surface GLUT-4 protein in skeletal muscle of the obese Zucker rat. The American journal of physiology. 1996;271(2 Pt 1):E294-301.
150. Rowe JW, Minaker KL, Pallotta JA, Flier JS. Characterization of the insulin resistance of aging. J Clin Invest. 1983;71(6):1581-7. PMCID: 370364.
151. Nishimura H, Kuzuya H, Okamoto M, Yoshimasa Y, Yamada K, Ida T, et al. Change of insulin action with aging in conscious rats determined by euglycemic clamp. The American journal of physiology. 1988;254(1 Pt 1):E92-8.
152. Goodman MN, Dluz SM, McElaney MA, Belur E, Ruderman NB. Glucose uptake and insulin sensitivity in rat muscle: changes during 3-96 weeks of age. The American journal of physiology. 1983;244(1):E93-100.
153. Escriva F, Gavete ML, Fermin Y, Perez C, Gallardo N, Alvarez C, et al. Effect of age and moderate food restriction on insulin sensitivity in Wistar rats: role of adiposity. J Endocrinol. 2007;194(1):131-41.
154. Sharma N, Arias EB, Sajan MP, MacKrell JG, Bhat AD, Farese RV, et al. Insulin resistance for glucose uptake and Akt2 phosphorylation in the soleus, but not epitrochlearis, muscles of old vs. adult rats. J Appl Physiol. 2010;108(6):1631-40. PMCID: 2886681.
155. Cartee GD, Briggs-Tung C, Kietzke EW. Persistent effects of exercise on skeletal muscle glucose transport across the life-span of rats. J Appl Physiol. 1993;75(2):972-8.

156. Cartee GD. Influence of age on skeletal muscle glucose transport and glycogen metabolism. Med Sci Sports Exerc. 1994;26(5):577-85.
157. Cartee GD, Bohn EE. Growth hormone reduces glucose transport but not GLUT-1 or GLUT-4 in adult and old rats. The American journal of physiology. 1995;268(5 Pt 1):E902-9.
158. Gulve EA, Henriksen EJ, Rodnick KJ, Youn JH, Holloszy JO. Glucose transporters and glucose transport in skeletal muscles of 1- to 25-mo-old rats. The American journal of physiology. 1993;264(3 Pt 1):E319-27.
159. Gulve EA, Rodnick KJ, Henriksen EJ, Holloszy JO. Effects of wheel running on glucose transporter (GLUT4) concentration in skeletal muscle of young adult and old rats. Mech Ageing Dev. 1993;67(1-2):187-200.
160. Cartee GD, Kietzke EW, Briggs-Tung C. Adaptation of muscle glucose transport with caloric restriction in adult, middle-aged, and old rats. The American journal of physiology. 1994;266(5 Pt 2):R1443-7.
161. Twigger SN. Of rats and men. Genome Biol. 2004;5(3):314. PMCID: 395761.
162. Rats! Nature Methods. 2010;7(6):413.
163. Clause BT. The Wistar Rat as a right choice: establishing mammalian standards and the ideal of a standardized mammal. J Hist Biol. 1993;26(2):329-49.
164. Zucker TF, Zucker LM. Fat accretion and growth in the rat. J Nutr. 1963;80:6-19.
165. Zucker LM, Antoniades HN. Insulin and obesity in the Zucker genetically obese rat "fatty". Endocrinology. 1972;90(5):1320-30.
166. Ionescu E, Sauter JF, Jeanrenaud B. Abnormal oral glucose tolerance in genetically obese (fa/fa) rats. The American journal of physiology. 1985;248(5 Pt 1):E500-6.
167. Muller S, Cleary MP. Glucose metabolism in isolated adipocytes from ad Libitum- and restricted-fed lean and obese Zucker rats at two different ages. Proc Soc Exp Biol Med. 1988;187(4):398-407.
168. Karlsson HK, Ahlsen M, Zierath JR, Wallberg-Henriksson H, Koistinen HA. Insulin signaling and glucose transport in skeletal muscle from first-degree relatives of type 2 diabetic patients. Diabetes. 2006;55(5):1283-8.
169. Christ CY, Hunt D, Hancock J, Garcia-Macedo R, Mandarino LJ, Ivy JL. Exercise training improves muscle insulin resistance but not insulin receptor signaling in obese Zucker rats. J Appl Physiol. 2002;92(2):736-44.
170. Benton CR, Holloway GP, Han XX, Yoshida Y, Snook LA, Lally J, et al. Increased levels of peroxisome proliferator-activated receptor gamma, coactivator 1 alpha (PGC-1alpha) improve lipid utilisation, insulin signalling and glucose transport in skeletal muscle of lean and insulin-resistant obese Zucker rats. Diabetologia. 2010.
171. Thyfault JP, Cree MG, Zheng D, Zwetsloot JJ, Tapscott EB, Koves TR, et al. Contraction of insulin-resistant muscle normalizes insulin action in association with increased mitochondrial activity and fatty acid catabolism. Am J Physiol Cell Physiol. 2007;292(2):C729-39.
172. Andreollo NA, Santos EF, Araujo MR, Lopes LR. Rat's age versus human's age: what is the relationship? Arq Bras Cir Dig. 2012;25(1):49-51.
173. Catalano KJ, Bergman RN, Ader M. Increased susceptibility to insulin resistance associated with abdominal obesity in aging rats. Obes Res. 2005;13(1):11-20.

174. Chiasson RB. Laboratory Anatomy of the White Rat. Dubuque, Iowa, USA: WMC Brown Company Publishers. 1969.
175. Delp MD, Duan C. Composition and size of type I, IIA, IID/X, and IIB fibers and citrate synthase activity of rat muscle. J Appl Physiol. 1996;80(1):261-70.
176. Armstrong RB, Phelps RO. Muscle fiber type composition of the rat hindlimb. Am J Anat. 1984;171(3):259-72.
177. Wallberg-Henriksson H. Glucose transport into skeletal muscle. Influence of contractile activity, insulin, catecholamines and diabetes mellitus. Acta Physiol Scand Suppl. 1987;564:1-80.
178. Magee TR, Artaza JN, Ferrini MG, Vernet D, Zuniga FI, Cantini L, et al. Myostatin short interfering hairpin RNA gene transfer increases skeletal muscle mass. The journal of gene medicine. 2006;8(9):1171-81.
179. Gronevik E, von Steyern FV, Kalhovde JM, Tjelle TE, Mathiesen I. Gene expression and immune response kinetics using electroporation-mediated DNA delivery to muscle. The journal of gene medicine. 2005;7(2):218-27.
180. Mir LM, Bureau MF, Gehl J, Rangara R, Rouy D, Caillaud JM, et al. High-efficiency gene transfer into skeletal muscle mediated by electric pulses. Proceedings of the National Academy of Sciences of the United States of America. 1999;96(8):4262-7.
181. McMahon JM, Wells DJ. Electroporation for gene transfer to skeletal muscles: current status. BioDrugs. 2004;18(3):155-65.

CHAPTER III

STUDY 1

A Novel Method to Measure Glucose Uptake and Myosin Heavy Chain Isoform Expression of Single Fibers from Rat Skeletal Muscle

Abstract

Skeletal muscle includes many individual fibers with diverse phenotypes. A barrier to understanding muscle glucose uptake (GU) at the cellular level has been the absence of a method to measure GU by single fibers (SF) from mammalian skeletal muscle. This study's primary objective was to develop a procedure to measure GU by SF from rat skeletal muscle. Rat epitrochlearis muscles were incubated ex vivo with [^{3}H]-2-deoxy-D-glucose, with or without insulin or AICAR, before isolation of ~10-30 SF from each muscle. Fiber type (myosin heavy chain, MHC, isoform) and GU were determined for each SF. Insulin-stimulated GU (which was cytochalasin B-inhibitable) varied according to MHC isoform expression with ~2-fold greater values for IIA versus IIB or IIX fibers, and ~1.3-fold greater for hybrid (IIB/X) versus IIB fibers. In contrast, AICAR-stimulated GU was ~1.5-fold greater for IIB versus IIA fibers. A secondary objective was to assess insulin resistance of SF from obese versus lean Zucker rats. Genotype differences were observed for insulin-stimulated GU and IκB-β abundance in

SF (lean>obese), with decrements for GU (44-58%) and IκB-β (25-32%) in each fiber type. This novel method creates a unique opportunity for future research focused on understanding muscle GU at the cellular level.

Introduction

Skeletal muscle is the major tissue for insulin-mediated disposal of blood glucose (1). Accordingly, the capacity for insulin-stimulated glucose disposal by skeletal muscle is a crucial determinant of glucoregulation. However, glucose uptake is not uniform across all muscles (2). Even when muscles are studied ex vivo to minimize the direct effects of microvascular perfusion and muscle contractile activity, muscle-dependent differences in glucose uptake remain (3).

Each muscle includes hundreds or thousands of cells known as muscle fibers. There can be substantial heterogeneity in the metabolic characteristics of individual fibers within a particular muscle (4). The gold-standard for classifying fiber type relies on identifying the myosin heavy chain (MHC) isoform(s) expressed by each fiber (5). The MHC isoforms expressed by adult rat muscle fibers are types I, IIA, IIB and IIX (6-9). Henriksen et al. studied isolated rat muscles with diverse fiber type compositions (3). They reported similar insulin-stimulated glucose uptake for soleus (predominantly type I) compared with flexor digitorum longus (FDB; predominantly type IIA) (3). The insulin-stimulated glucose uptake for the soleus or FDB was ~2-fold greater than the predominantly type IIB epitrochlearis (3).

The study of cultured myocytes has provided important insights into mechanisms that regulate glucose uptake (10-16). However, because cultured cells fail to replicate all

properties of adult muscle, the ability to measure glucose uptake by single fibers from authentic muscle would prove valuable. No methods are available for measuring glucose uptake by single fibers from mammalian muscle. To fully understand muscle glucose uptake at the cellular level, it will be essential to develop such a method. Therefore, our first aim was to develop and validate a novel method to measure glucose uptake by single fibers from rat muscle. Because the results from muscle tissue research provide evidence that glucose uptake capacity varies according to fiber type, it was important to also identify the MHC isoform expressed in the same fibers used for glucose uptake measurements. We hypothesized that insulin-stimulated glucose uptake would vary among the fibers, with fibers expressing type I or IIA MHC having greater values than fibers expressing IIB or IIX MHC. Our second aim was to use the single fiber glucose uptake method to gain insights into insulin resistance by measuring glucose uptake of single fibers from Obese Zucker (OZ) vs. Lean Zucker (LZ) rats. We hypothesized that when single fibers expressing the same MHC isoform were compared, insulin-stimulated glucose uptake for fibers from LZ rats would exceed the values for fibers from OZ rats.

Research Design & Methods

Materials.

Human recombinant insulin was from Eli Lilly (Indianapolis, IN). 5-Aminoimidazole-4-carboxamide-1-β-D-ribofuranoside (AICAR) and cytochalasin B were from Calbiochem/EMD Chemicals (Gibbstown, NJ). Reagents for SDS-PAGE and immunoblotting were from Bio-Rad (Hercules, CA). Bicinchoninic acid protein assay reagent and T-PER reagent were from Pierce Biotechnology (Rockford, IL). [^{3}H]-2-

Deoxy-D-glucose ([^{3}H]-2-DG) was from Perkin Elmer (Waltham, MA). Collagenase (type II) was from Worthington Biochem Corp. (Lakewood, NJ). Trypan Blue was from Invitrogen (Carlsbad, CA). Other reagents were from Sigma-Aldrich (St. Louis, MO) or Fisher Scientific (Pittsburgh, PA). Reagents and apparatus for SDS-PAGE and immunoblotting were purchased from Bio-Rad (Hercules, CA). West Dura Extended Duration Substrate was from Pierce Biotechnology (Rockford, IL). Anti-APPL1 antibody (#ab59592) was from Abcam (Cambridge, MA), anti-IκB-β antibody (#sc-945) was from Santa Cruz (Santa Cruz, CA), and anti-rabbit IgG horseradish peroxidase (#7074) was from Cell Signaling Technology (Danvers, MA).

Animal Treatment.

Procedures for animal care were approved by the University of Michigan Committee on Use and Care of Animals. Male Wistar rats, (7-10weeks) were from Harlan (Indianapolis, IN). Lean (Fa/_) and obese (fa/fa) male Zucker rats (7-8weeks) were from Charles River Laboratories (Wilmington, MA). Animals were provided with rodent chow ad libitum until 1700 the night before the experiment, when food was removed. The next day, between 1000 and 1300, rats were anesthetized (intraperitoneal injection of sodium pentobarbital) and both epitrochlearis muscles were extracted.

Muscle Incubation.

Isolated muscles underwent a series of incubation steps (see below). Unless otherwise noted, vials were shaken (45rpm), gassed (95% O_2/5% CO_2), and heated (35°C) in a water bath.

Standard Incubation Protocol.

Isolated muscles were incubated in vials containing 2ml of Media-1 [Krebs Henseleit buffer (KHB) supplemented with 0.1% BSA (KHB-BSA), 2mM sodium pyruvate and 6mM mannitol] with 0 or 12nM insulin for 20min. Each muscle was then transferred to a second vial for 60min incubation in 2ml of Media-2 [KHB-BSA, 1mM 2-DG (specific activity of 2.25mCi/mmol [^{3}H]-2-DG) and 9mM mannitol (specific activity of 0.022 mCi/mol [^{14}C]mannitol)] and the same insulin concentration as the previous step. Muscles were blotted, freeze-clamped, and stored at -80°C.

Revised Incubation Protocol.

Isolated muscles were incubated in vials containing 2ml of Media-1 with 0 or 12nM insulin for 20min. Each muscle was transferred to a second vial for 60min incubation in 2ml of Media-3 [KHB-BSA, 1mM 2-DG (specific activity of 13.5mCi/mmol [^{3}H]-2-DG), and 9mM mannitol] and the same insulin concentration as the previous step. Muscles underwent 3x5min washes (100rpm) in ice-cold KHB-BSA to clear extracellular space (ECS) of 2-DG (17). Muscles were placed in Collagenase Media (Ca^{2+}-free KHB and 1.5% type II collagenase) for 60min for enzymatic digestion of collagen (enzymatically digested muscles are hereafter referred to as fiber bundles). Some muscles were incubated with cytochalasin B (CB, 25μM in 0.4% DMSO). One

muscle per rat was incubated with CB for sequential incubations in Media-1 and -3. The contralateral muscle served as a control (vehicle, 0.4% DMSO). CB or vehicle remained at the same concentration in incubation Media-1 and -3. Some muscles were incubated with 2mM AICAR using the revised protocol described above, except AICAR was substituted for insulin.

Single Fiber Isolation and Processing.

Following collagenase incubation, fiber bundles were removed from solution, washed with Ca^{2+}-free KHB, and placed in a petri-dish containing Ca^{2+}-free KHB plus Trypan Blue (TB, 0.25%). Under a dissecting microscope, single fibers were teased from the bundle using forceps. Only fibers non-permeable to TB (TB-permeable fibers were very rare) were isolated (~10-30 fibers per fiber bundle). Each fiber was imaged using a camera-enabled microscope with Leica Application Suite EZ software after isolation. Fiber dimensions were measured using Image J software. Width (mean value for width measured at 3 locations per fiber: near fiber midpoint and approximately halfway between midpoint and each end of the fiber) and length of each fiber were used to estimate volume ($V= \pi r^2 l$; r=radius as determined by half of the width measurement, l=length). Following imaging, each fiber was transferred by pipette with 10µl of solution to a micro-centrifuge tube containing 40µl of lysis buffer (T-PER, 1mM EDTA, 1mM EGTA, 2.5 mM sodium pyrophosphate, 1mM Na_3VO_4, 1 mM β-glycerophosphate, 1µg/ml leupeptin, and 1mM PMSF). Laemmli buffer (2X, 50µl) was added to each tube. Tubes were vortexed. Aliquots of lysed fiber were used for 2-DG uptake and MHC characterization.

Single Fiber 2-DG Uptake.

An aliquot of the lysed fiber was pipetted into a vial with 10ml of scintillation cocktail. Aliquots of Media-3 (in which muscles had been incubated with [^{3}H]-2-DG) and Ca^{2+}-free KHB (used to isolate fibers) were added to separate vials containing 10ml of scintillation cocktail. [^{3}H]-2-DG disintegrations per minute (dpm) for each vial were determined using a scintillation counter. ^{3}H dpm accumulation was calculated as fiber ^{3}H dpm minus ^{3}H dpm in Ca^{2+}-free KHB rinse solution. This difference was used as the corrected dpm value to calculate 2-DG accumulation by fibers essentially as previously performed for muscles (18, 19), (corrected total ^{3}H dpm per fiber $\bullet \frac{\mu mol\ 2-DG\ per\ ml\ incubation\ media}{^3H\ dpm\ per\ ml\ incubation\ media}$). Measured 2-DG accumulation was normalized to calculated fiber volume and expressed as nmol $\bullet$ μl^{-1}.

Myosin Heavy Chain Isoform Expression.

Myosin heavy chain (MHC) isoforms were separated and identified by SDS-PAGE (20). An aliquot of fiber homogenate was run on gels at constant voltage (70V) for ~24h. A mixture of homogenized soleus and extensor digitorum longus muscles (Sol/EDL; containing all four MHC isoforms) was used as a standard on each gel. Gels were stained with Coomassie Brilliant Blue for ~1h and destained in 20% methanol & 10% acetic acid mixture.

Immunoblotting.

Prior to immunoblotting epitrochlearis single fiber lysates from LZ and OZ rats were fiber typed based on MHC expression. Relative protein abundance of each fiber was calculated using a three-point MHC standard curve from a Sol/EDL lysate loaded on each gel. A similar amount of MHC protein for each fiber sample was loaded onto 9% SDS-PAGE gels. Following electrophoretic transfer to nitrocellulose, gels were Coomassie-stained, and post-transfer MHC bands were quantified by densitometry (AlphaEase FC, Alpha Innotech, San Leandro, CA) as previously described (21). After immunoblotting the membranes, the immunoreactive protein bands (IκB-β and APPL1) were visualized by enhanced chemiluminescence and quantified by densitometry as previously described (22). IκB-β and APPL1 protein levels for each fiber were expressed relative to the fiber's respective post-transfer MHC density.

Muscle and Fiber Bundle Homogenization.

Intact muscles and fiber bundles used for 2-DG uptake were processed in 1ml ice-cold lysis buffer using glass-on-glass grinding tubes. Homogenates were rotated (4°C, 1h) before being centrifuged (12,000*g*, 10 min, 4°C). Aliquots of supernatant used for 2-DG uptake were pipetted into vials for scintillation counting, and 2-DG uptake was determined. A portion of supernatant was used to determine protein concentration (BCA protein assay). 2-DG uptake was normalized to either muscle weight ($\mu mol \cdot g^{-1}$ for intact muscles) or protein content ($\mu mol \cdot \mu g^{-1}$ protein for fiber bundles). Remaining supernatant was stored at −80°C until further analysis.

Statistical Analysis.

Data are expressed as mean ±SEM. Differences between two groups were determined by student's *t*-test. Pearson's correlation coefficient was used for correlation analysis. One-way ANOVA was used to evaluate the effect of fiber type on 2-DG uptake. Two-way ANOVA was used for the CB experiment and the Zucker rat experiment. Tukey's post hoc *t*-test was applied to determine the source of significant variance. A P-value of ≤ 0.05 was considered statistically significant.

Results

2-DG values were similar for whole muscles using revised vs. standard protocols.

The standard incubation protocol for 2-DG uptake uses [^{14}C]mannitol to calculate ECS, which is used to calculate extracellular 2-DG, which is subtracted from whole muscle 2-DG to calculate intracellular 2-DG accumulation (19). To confirm that the standard vs. revised protocols resulted in similar values for 2-DG uptake, paired muscles from Wistar rats were studied with both protocols. Both muscles from some rats were incubated with insulin, and both muscles from other rats were incubated without insulin. KHB was supplemented with [^{3}H]-2-DG and [^{14}C]mannitol for one muscle while KHB was supplemented with [^{3}H]-2-DG only for the contralateral muscle. The muscle incubated in [^{14}C]mannitol + [^{3}H]-2-DG was immediately freeze-clamped following incubation, while the contralateral muscle (incubated in [^{3}H]-2-DG only) underwent 3 rinses (5min each) in ice cold KHB. 2-DG uptake did not differ significantly between muscles incubated using the standard vs. revised protocol (Fig.3.1A). 2-DG values were significantly correlated (Basal: $R=0.88$, $P<0.05$; Insulin-stimulated $R=0.91$, $P<0.05$)

between paired muscles undergoing the standard vs. revised protocol (Fig.3.1B). 2-DG uptake for muscles undergoing the standard protocol can also be expressed as nmol • μl^{-1}: Basal=1.86±0.41, and Insulin-stimulated=5.89±0.82.

Incubation with collagenase did not alter 2-DG uptake.

Paired muscles were dissected from Wistar rats. Both muscles from some rats were incubated with insulin, and both muscles from other rats were incubated without insulin. KHB was supplemented with [^{3}H]-2-DG for the second incubation step. After 3 rinses to remove extracellular 2-DG, one muscle per rat was incubated with collagenase, and the other was incubated without collagenase. Collagenase did not alter 2-DG uptake (Fig.3.1C).

Insulin-stimulated 2-DG uptake by single fibers was correlated with 2-DG for fiber bundles.

2-DG that enters muscle fibers is rapidly phosphorylated by hexokinase, while resultant 2-DG-6P is trapped intracellularly without further metabolization. After collagenase-treatment, muscles from Wistar rats were incubated in Ca^{2+} -free KHB with TB. A bundle of several hundred fibers from each muscle used to harvest single fibers was also processed for 2-DG uptake without insulin or with 12nM insulin. 2-DG uptake was also determined from ~10-30 single fibers per bundle. Fig.3.1D illustrates the significant correlations (Basal: $R=0.68$, $P<0.05$; Insulin-stimulated $R= 0.63$, $P<0.05$) between mean 2-DG uptake by single fibers from each bundle vs. 2-DG uptake by the donor bundle from which fibers were isolated.

Differences in insulin-stimulated 2-DG uptake by single fibers.

Relative numbers of fibers (%) for each MHC isoform in single fibers isolated from Wistar rats were 9% IIA, 61% IIB, 8% IIX, and 22% IIB/X (see Figure 3.2 for representative gel). These values compare to the relative abundance of MHC composition of whole epitrochlearis muscles from 7-10wk-old, Wistar rats (8% I, 13% IIA, 51% IIB, and 28% IIX) (23). Fig.3.3 illustrates data from single fibers from Wistar rats used to measure both insulin-stimulated 2-DG uptake and MHC isoform expression. We found no significant fiber type differences for basal 2-DG uptake. ANOVA revealed a significant difference ($P<0.05$) for insulin-stimulated 2-DG uptake of IIA fibers vs. fibers expressing each of the other MHC isoforms, and a significant difference between IIB/X vs. IIB fibers (IIB/X > IIB).

Insulin-stimulated 2-DG uptake by single fibers was inhibited by CB.

For 2-DG uptake by single fibers from muscles incubated without insulin, there were significant main effects ($P<0.05$) of CB and fiber type. The only statistically significant difference ($P<0.05$) identified by post-hoc analysis was in IIB/X fibers (no CB > with CB; Fig. 3.4). For 2-DG uptake by single fibers from insulin-stimulated muscles, there was a significant main effect of CB ($P<0.001$). Post-hoc analysis ($P<0.001$) indicated values without CB exceeded values with CB for each fiber type. For 2-DG uptake by single fibers from insulin-stimulated muscles, there was a significant main effect of fiber type ($P<0.001$), and a significant interaction between CB status and fiber type ($P<0.001$). Post-hoc analysis indicated that for insulin-stimulated muscles

incubated without CB, 2-DG values for IIA fibers were significantly ($P<0.05$) greater than values for all other fiber types, and 2-DG values for IIB/X fibers were significantly ($P<0.05$) greater than values for IIB fibers. For 2-DG uptake by single fibers from muscles incubated with insulin and CB, post-hoc analysis detected no significant differences among fiber types.

AICAR-stimulated 2-DG uptake by single fibers.

Fig. 3.5 illustrates data from single fibers used to measure AICAR-stimulated 2-DG uptake and MHC isoform expression. There were no significant fiber type differences for basal 2-DG uptake. ANOVA revealed a significant difference ($p<0.05$) for AICAR-stimulated 2-DG uptake between fiber types. Post-hoc analysis indicated a significant difference for IIB fibers vs. IIA fibers (IIB> IIA).

2-DG uptake by single fibers from epitrochlearis of obese Zucker (OZ) vs. lean Zucker (LZ) rats.

Basal 2-DG uptake values by single fibers were not significantly different between OZ and LZ, regardless of MHC isoform expression (Fig. 3.6). For 2-DG uptake by single fibers from insulin-stimulated muscles, there was a significant main effect of genotype ($P<0.001$), and post-hoc analysis indicated that insulin-stimulated 2-DG values for each fiber type were significantly greater for LZ vs. OZ rats ($P<0.05$). For 2-DG uptake by single fibers from insulin-stimulated muscles, there was also a significant main effect of fiber type ($P<0.001$), and a significant interaction (genotype x fiber type; $P<0.001$). Post-hoc analysis indicated that within the LZ fibers from insulin-stimulated

muscles, 2-DG uptake for IIA fibers exceeded values for all other fiber types ($P<0.05$). However, for single fibers from insulin-stimulated OZ muscles, post-hoc analysis did not reveal significant differences among fiber types. Relative decrements for 2-DG uptake of insulin-stimulated OZ vs. LZ muscles were estimated by calculating differences between the mean LZ value for each fiber type and individual OZ values for the same fiber type. Calculated reductions for insulin-stimulated 2-DG uptake for the fiber types (IIA = 44.4±3.0%, IIB = 58.0±10.0%, IIX = 52.0±8.01%, IIB/X = 52.3±5.0%) did not differ significantly.

IκB-β and APPL1 abundance in single fibers.

For IκB-β, we observed a significant main effect of genotype ($P<0.005$;LZ>OZ), regardless of fiber type. No fiber type difference for IκB-β was detected, and the calculated reductions in IκB-β content for LZ vs. OZ were similar across fiber types (IIB=24.8±10.7%, IIA=27.5±7.1%, IIX=30.0±9.1%, IIB/X=31.9±4.0%; Figure 3.7A). For APPL1, there was no significant genotype or fiber type difference (Figure 3.7B).

Discussion

Skeletal muscle is a heterogeneous tissue primarily composed of muscle fibers that can have diverse phenotypes. However, there was previously no method to evaluate glucose uptake by single mammalian fibers. The current study filled this gap. Importantly, the novel method includes identification of MHC isoform expression in each fiber used for glucose uptake assay. The results indicated that insulin-stimulated glucose uptake varied among fibers according to fiber type, with 2-fold greater insulin-mediated glucose uptake for IIA vs. IIB or IIX fibers. These data extend earlier research using

tissue analyses in which rat muscles primarily composed of IIA fibers had ~2 to 3-fold greater insulin-mediated glucose uptake than muscles mostly composed of IIB fibers (3). The current results also revealed that hybrid fibers, which expressed more than one MHC isoform (IIB/X), had higher insulin-induced glucose uptake than IIB fibers. In contrast to the results of insulin-stimulated glucose uptake, AICAR-stimulated glucose uptake was greater in IIB versus IIA fibers. These data coincide with results for whole epitrochlearis (predominantly IIB) that had greater AICAR-stimulated glucose uptake versus whole FDB (predominantly IIA) (24). The relative magnitude of insulin resistance in OZ vs. LZ rats was substantial (from 44 to 58% for fibers expressing each of the fiber types evaluated, IIA, IIB, IIX, and IIB/X). Furthermore, for OZ vs. LZ rats IκB-β content was also reduced (25-32%) across each fiber type.

We performed a series of experiments to validate the procedure for assessing glucose uptake by single fibers. We demonstrated that glucose uptake was unaltered by collagenase-treatment and documented that glucose uptake by single fibers was highly correlated with values for donor muscles from which single fibers were isolated. Using CB, a compound that inhibits glucose transporter protein-mediated glucose transport, we established that 2-DG accumulation by single fibers was attributable to transporter-specific glucose uptake.

The MHC isoform profile of single fibers isolated from Wistar rats (9% IIA, 61% IIB, 8% IIX, and 22% IIB/X) compares to the relative abundance of MHC composition of whole epitrochlearis from Wistar rats (8% I, 13% IIA, 51% IIB, and 28% IIX) (23). It is uncertain why type I fibers were not included among the hundreds of fibers isolated using collagenase. It may relate to the greater collagen levels surrounding type I compared to

type II fibers in rat muscle (25). Consistent with this interpretation, despite repeated attempts to use collagenase with isolated soleus, a muscle composed of ~90% type I fibers (26), we were unable to isolate any single fibers. Regardless, the protocol successfully isolated single fibers expressing each of the other MHC isoforms (representing >90% of MHC expressed by the epitrochlearis) in proportions roughly comparable to their respective abundance in whole epitrochlearis.

Glucose uptake measurement by traditional tissue analysis has limitations that are avoided using the single fiber method. 1) No muscles in rats have been found to exclusively express a single MHC isoform. Therefore, tissue comparisons are limited to muscles or regions of muscles largely composed of a particular fiber type. 2) No rat muscle has been identified in which type IIX fibers account for most of the MHC. 3) Tissue analysis cannot reveal the glucose uptake of hybrid fibers. 4) Tissue analysis includes the contribution of other cell types in skeletal muscle (vascular, neural, adipose, fibroblasts, etc.). 5) Various conditions alter fiber type composition of muscles (27-31), confounding interpretation of between-group comparisons. The single fiber procedure makes comparisons possible between fibers matched for MHC expression.

Full understanding of muscle insulin resistance will require elucidation of insulin resistance at the cellular level. Cultured myocytes provide valuable insights into the mechanisms for insulin resistance (32-34), however they are imperfect models of fibers in adult muscle. To probe muscle insulin resistance, we compared glucose uptake in single fibers from LZ and OZ rats. Insulin-stimulated glucose uptake is reduced by 67% in isolated intact epitrochlearis (35). Using the perfused rat hindlimb procedure, Sherman et al. (36) found similar relative deficits for OZ vs. LZ rats in glucose uptake for a muscle

composed of predominantly type I fibers (soleus, 47% decline), a region of muscle with a high portion of IIA fibers (red quadriceps, 66% decline), and a region of muscle that is mostly IIB fibers (white quadriceps, 54% decline). In single fibers that expressed known MHC isoforms, the relative decrements were similar to these published results for tissue glucose uptake. Furthermore, the relative decrements were similar for each fiber type that was assessed. The results from perfused and isolated muscles indicate that all fiber types contribute to the insulin resistance in OZ rats.

The correspondence for the magnitude of insulin resistance in single fibers compared to published data for isolated epitrochlearis and perfused hindlimb (35, 36) provides further support for the validity of the single fiber method. However, various interventions, including exercise, dietary manipulations, or pharmaceutical treatments may not uniformly modulate single fiber glucose uptake. The single fiber method could be especially valuable for experiments that using vivo gene delivery (by electroporation or gene gun) to muscle. These approaches have provided important information about the regulation of muscle glucose uptake. However, because gene delivery using these approaches is not 100% efficient, the interpretation can be imprecise. For example, if gene delivery induces a 50% reduction in glucose uptake, it is possible that only 50% of the fibers were transfected, and glucose uptake was completely inhibited in each transfected fiber. Alternatively, it is possible that most of the fibers were transfected, but glucose uptake was only partly inhibited in each transfected fiber. The single fiber method can turn this complication into an advantage by allowing isolation of those fibers expressing the gene of interest (facilitated by a fluorescent reporter). Moreover, the non-transfected fibers could provide an invaluable internal control from the same muscle. It

is also possible that transfection efficiency will vary by fiber type, or that the consequences of transfection will be fiber-type specific. The single fiber model offers the opportunity to address these possible outcomes.

Obesity-associated inflammation is considered a likely contributor to muscle insulin resistance (37, 38). Over-activation of the inhibitor κB (IκB)/ nuclear factor κB (NFκB) pathway is hypothesized to trigger insulin resistance, and reduced IκB-β protein abundance is commonly used as a marker of this activation. For example, IκB-β content was decreased in muscle of insulin resistant humans with type 2 diabetes (39). Previous studies using whole skeletal muscles or regions of muscles have suggested that activation of the IκB-NFκB pathway may be modulated by obesity in a fiber-type dependent manner (40, 41). The current results demonstrate significantly lower IκB-β levels in single fibers from obese rats, regardless of fiber type. When these novel observations are coupled with our demonstrated decline in glucose uptake by single fibers from OZ rats, the results provide new evidence that supports the idea that the insulin resistance found in fibers from the obese rats, regardless of fiber type, is linked to greater activation of the IκB/NFκB pathway. Another novel result was the lack of a significant fiber type difference for IκB-β levels, indicating the fiber type differences in glucose transport are independent of differences in expression of this protein. APPL1 mediates adiponectin signaling and has been linked to enhanced insulin-stimulated Akt activation, GLUT4 translocation and glucose uptake (42, 43). The lack of significant effects of either obesity or fiber type on APPL1 abundance, taken together with the single fiber glucose uptake data, demonstrate that neither the obesity-related insulin resistance nor the fiber

type differences in glucose uptake are attributable to differential expression of this regulatory protein.

In conclusion, the current study provides new insights into the relationship between MHC isoform expression and glucose uptake in rat muscle. In addition, the results demonstrated that in OZ rats, the extent of insulin resistance was similar for single fibers expressing different MHC isoforms. More importantly, the study validated an innovative approach that has the potential to provide unique information about muscle glucose uptake to be used for understanding, preventing and treating insulin resistance.

ACKNOWLEDGEMENTS.

This research was supported by grants from the National Institutes of Health (DK071771 and AG10026 to G.D.C.). No potential conflicts of interest relevant to this article were reported. Author contributions: J.G.M. researched data, contributed to discussion, wrote manuscript, reviewed/edited manuscript. G.D.C. contributed to discussion, wrote manuscript, reviewed/edited manuscript, and is the guarantor. The authors would like to thank Edward Arias (University of Michigan) for his assistance with the muscle dissections.

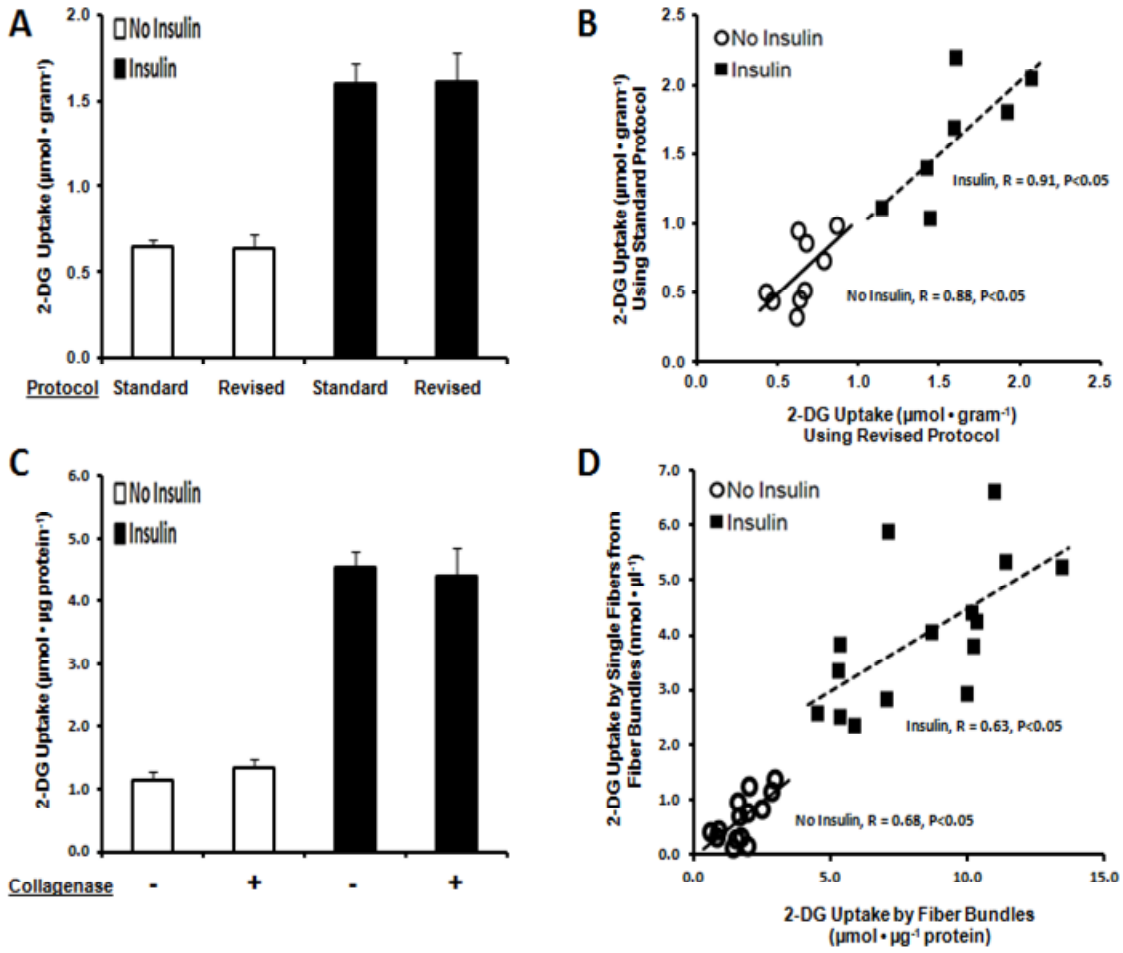

Figure 3.1 Glucose Uptake and Correlations Describing Results for Novel Single Fiber Method Validation. **A.** 2-DG uptake by epitrochlearis muscle with (filled bars) or without (open bars) insulin stimulation. Paired epitrochlearis muscles from the same rat underwent either the standard incubation protocol ([^{3}H]-2-DG and [^{14}C]mannitol) or the revised incubation protocol ([^{3}H]-2-DG only, with 3 washes). Data are means ± SEM (n=7-9 muscles per protocol at each insulin concentration). **B.** Correlations between the standard and revised protocols from muscles used in Fig. 3.1A (n=7-9 muscles per protocol and insulin concentration). Each symbol represents data from paired muscles after incubation in the respective protocol, with (filled squares) or without insulin (open circles). Without insulin R=0.88, P<0.05; With insulin R=0.91, P<0.05. **C.** 2-DG uptake by epitrochlearis muscles with (filled bars) or without (open bars) insulin stimulation, followed by a 60 minute incubation in media with collagenase (+) or without collagenase (-). Data are means ± SEM (n=6 per bar). **D.** Correlations between the 2-DG uptake by fiber bundles (expressed as µmol per µg protein) vs. mean 2-DG uptake by single fibers isolated from their corresponding fiber bundle (~10-20 fibers, expressed as nmol per µl), represented by each symbol, with (filled squares) or without insulin (open circles). Without insulin R=0.68, P<0.05; With insulin R= 0.63, P<0.05.

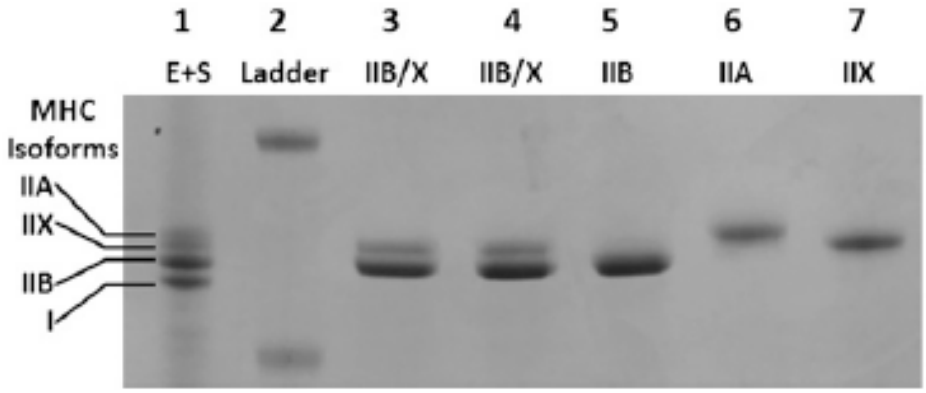

Figure 3.2 Representative SDS-polyacrylamide Gel of Single Fibers. Representative SDS-polyacrylamide gel of single fibers (SF) isolated from rat epitrochlearis muscle visualized using Coomassie Blue Staining. *Lane 1*, E+S, pooled sample from rat extensor digitorum longus and soleus muscles expressing MHC (myosin heavy chain) types I, IIA, IIB and IIX; *lane 2*, Ladder, molecular mass standard; *lane 3*, epitrochlearis SF expressing type IIB/X (hybrid fiber); *lane 4*, epitrochlearis SF expressing type IIB/X (hybrid fiber); *lane 5*, epitrochlearis SF expressing type IIB; *lane 6*, epitrochlearis SF expressing type IIA; *lane 7*, epitrochlearis SF expressing type IIX.

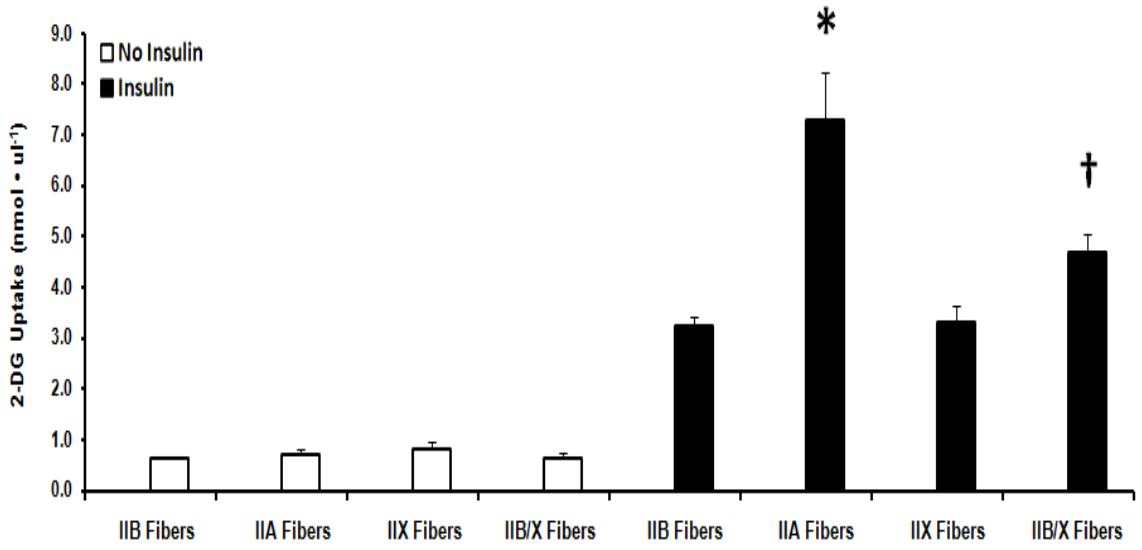

Figure 3.3 Mean Basal and Insulin-stimulated 2-DG Uptake by Fibers Expressing the Same MHC isoform. Mean 2-DG uptake by fibers expressing the same myosin heavy chain (MHC) isoform, with (filled bars) or without (open bars) insulin stimulation. For basal (no insulin) fibers the number of fibers for each MHC-type is in parentheses: IIB (105), IIA (16), IIX (7), IIB/X (30). For insulin-stimulated fibers, the number of fibers for each MHC-type is in parentheses: IIB (117), IIA (15), IIX (13), IIB/X (41). Data are means ± SEM. ANOVA revealed a significant difference related to MHC expression for insulin-stimulated fibers ($P<0.05$). Post-hoc analysis of insulin-stimulated fibers revealed significant differences ($P<0.05$) for: 1) *IIA vs. all other fiber types; and 2) †IIB/X vs. IIB fibers**.**

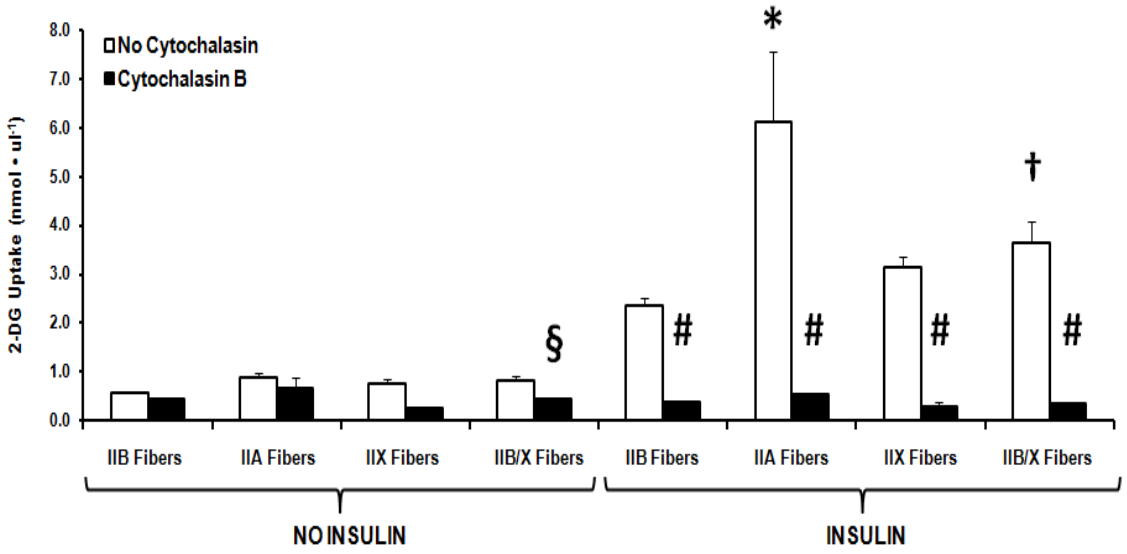

Figure 3.4 Mean 2-DG Uptake by Fibers Isolated from Epitrochlearis Muscles that were Incubated With or Without Cytochalasin B (CB). Mean 2-DG uptake by fibers isolated from epitrochlearis muscles that were incubated without cytochalasin B (No CB; open bars) or with cytochalasin B (CB; filled bars). For basal (no insulin) fibers, without CB, the number of fibers for each MHC-type is in parentheses: IIB (56), IIA (11), IIX (9), IIB/X (23). For basal fibers, with CB, the number of fibers for each MHC-type is in parentheses: IIB (58), IIA (6), IIX (11), IIB/X (25). For insulin-stimulated fibers, without CB, the number of fibers for each MHC-type is in parentheses: IIB (37), IIA (5), IIX (6), IIB/X (19). For insulin-stimulated fibers, with CB, the number of fibers for each MHC-type is in parentheses: IIB (40), IIA (6), IIX (5), IIB/X (16). Data are means ± SEM. For fibers without insulin, there were significant main effects of CB status (No CB > with CB; $P<0.001$) and fiber type ($P<0.001$). Post-hoc analysis indicated for fibers without insulin, No CB > with CB for IIB/X fibers ($^{\S}P<0.05$). For fibers with insulin, there were significant main effects of CB status (No CB > CB; $P<0.001$) and fiber type ($P<0.001$) and a significant CB x fiber type interaction ($P<0.001$). Post-hoc analysis revealed that for insulin-stimulated fibers: 1) $^{\#}P<0.05$ for CB vs. No CB for all fiber types; and 2) for fibers with No CB, $^{*}P<0.05$ for IIA vs. IIB, IIX, IIB/X fibers, and $^{\dagger}P<0.05$ for IIB/X vs. IIB fibers**.**

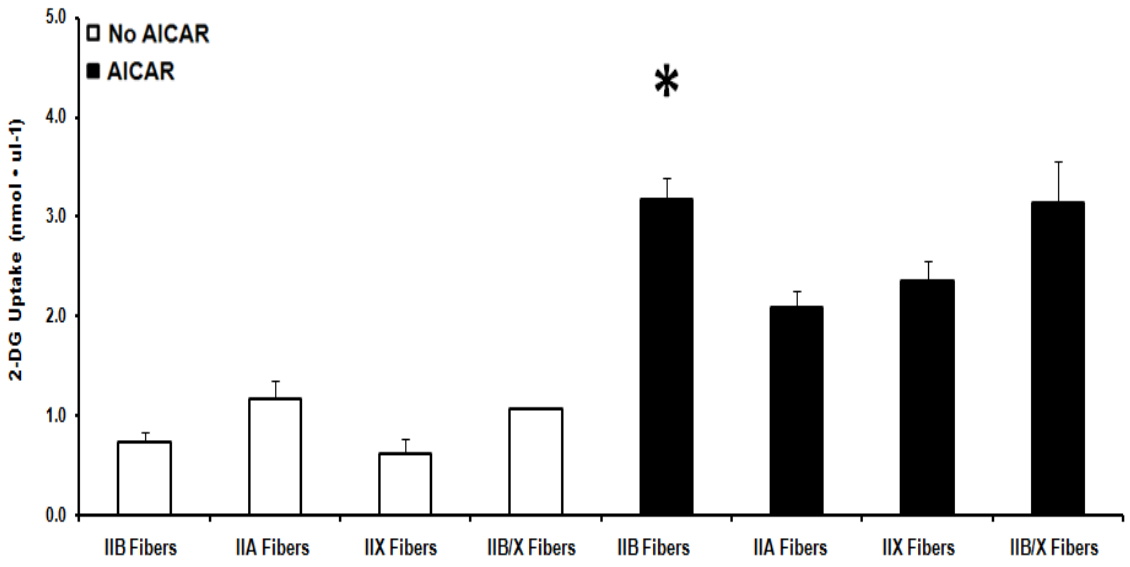

Figure 3.5 Mean 2-DG Uptake by Fibers Expressing the Same MHC Isoform, With or Without AICAR Stimulation. Mean 2-DG uptake by fibers expressing the same myosin heavy chain (MHC) isoform, with (filled bars) or without (open bars) AICAR stimulation. For basal (no AICAR) fibers the number of fibers for each MHC-type is in parentheses: IIB (27), IIA (6), IIX (6), IIB/X (1). For AICAR-stimulated fibers, the number of fibers for each MHC-type is in parentheses: IIB (51), IIA (21), IIX (13), IIB/X (15). Data are means ± SEM. ANOVA revealed a significant difference related to MHC expression for AICAR-stimulated fibers ($P<0.05$). Post-hoc analysis of AICAR-stimulated fibers revealed a significant difference, *$P<0.05$ for IIB vs. IIA fibers**.**

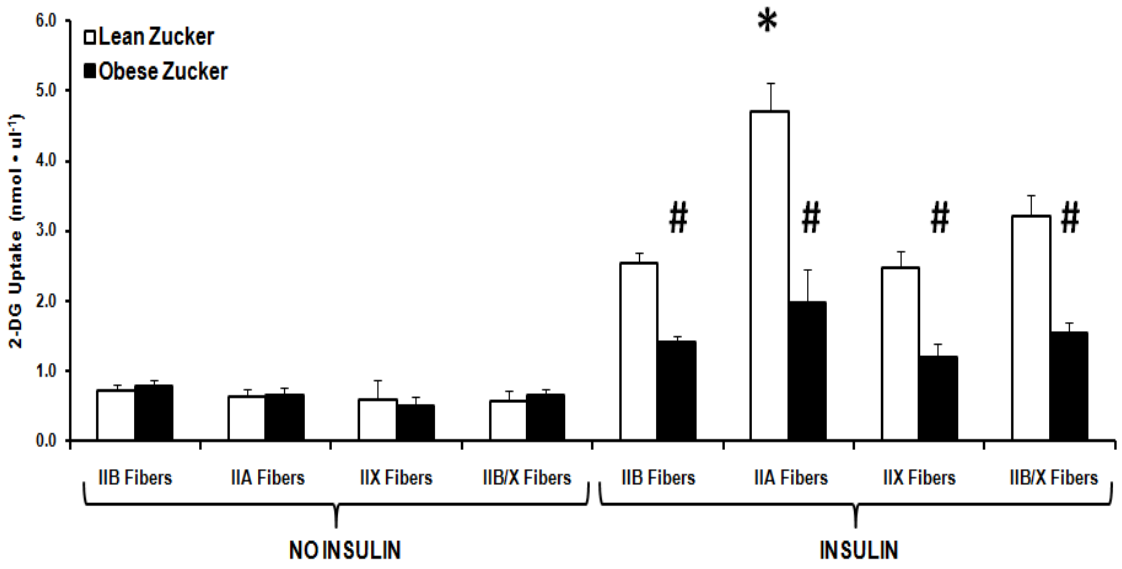

Figure 3.6 Mean 2-DG Uptake by Fibers Isolated from Epitrochlearis Muscles from Lean Zucker (LZ) or Obese Zucker (OZ) Rats. Mean 2-DG uptake by fibers isolated from epitrochlearis muscles from lean Zucker (LZ, open bars) or obese Zucker (OZ, filled bars) rats. For basal (no insulin) fibers from LZ rat muscles, the number of fibers for each MHC-type is in parentheses: IIB (51), IIA (10), IIX (8), IIB/X (11). For basal fibers from OZ rat muscles, the number of fibers for each MHC-type is in parentheses: IIB (71), IIA (10), IIX (5), IIB/X (14). For insulin-stimulated fibers, from LZ rat muscles, the number of fibers for each MHC-type is in parentheses: IIB (73), IIA (13), IIX (15), IIB/X (19). For insulin-stimulated fibers from OZ rat muscles, the number of fibers for each MHC-type is in parentheses: IIB (99), IIA (9), IIX (7), IIB/X (25). Data are means ± SEM. For fibers with insulin, there were significant main effects of genotype (LZ > OZ; $P<0.001$) and fiber type ($P<0.001$) and a significant genotype x fiber type interaction ($P<0.01$). Post-hoc analysis of insulin-stimulated fibers revealed: 1) $^{\#}P<0.05$ for insulin-stimulated OZ vs. LZ for all fiber types; and 2) for insulin-stimulated fibers within only the LZ group, $*P<0.05$ for insulin-stimulated IIA vs. IIB, IIX, IIB/X fibers.

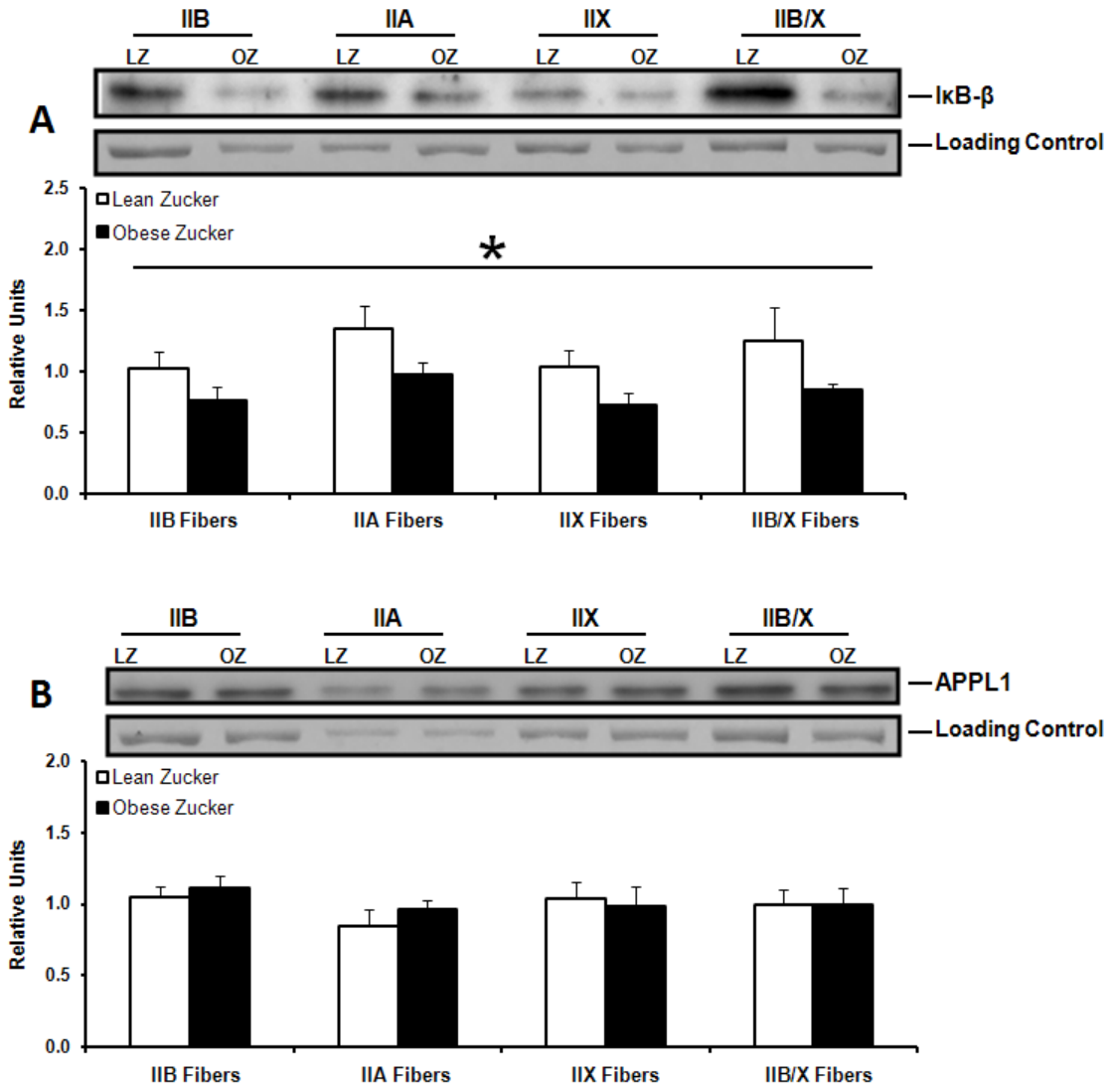

Figure 3.7 IκB-β and APPL1 Protein Abundance in Single Fibers Isolated from Epitrochlearis Muscles from Lean Zucker (LZ) or Obese Zucker (OZ) Rats. Representative blots of protein abundance (IκB-β or APPL1) and corresponding Coomassie stained gels of post-transfer MHC (loading control) are provided. The density value for each protein (IκB-β or APPL1) was normalized to the density value for the loading control. **A.** There was a significant main effect of genotype (LZ > OZ; *P<0.005), but no significant fiber type difference for IκB-β. Data are means ± SEM. n=8 fibers per bar. **B.** There was no significant genotype or fiber type difference for APPL1. Data are means ± SEM. n=8 fibers per bar.

References

1. DeFronzo RA. Lilly lecture 1987. The triumvirate: beta-cell, muscle, liver. A collusion responsible for NIDDM. Diabetes. 1988;37(6):667-87.
2. James DE, Jenkins AB, Kraegen EW. Heterogeneity of insulin action in individual muscles in vivo: euglycemic clamp studies in rats. The American journal of physiology. 1985;248(5 Pt 1):E567-74.
3. Henriksen EJ, Bourey RE, Rodnick KJ, Koranyi L, Permutt MA, Holloszy JO. Glucose transporter protein content and glucose transport capacity in rat skeletal muscles. The American journal of physiology. 1990;259(4 Pt 1):E593-8.
4. Pette D, Staron RS. Mammalian skeletal muscle fiber type transitions. Int Rev Cytol. 1997;170:143-223.
5. Pandorf CE, Caiozzo VJ, Haddad F, Baldwin KM. A rationale for SDS-PAGE of MHC isoforms as a gold standard for determining contractile phenotype. J Appl Physiol. 2010;108(1):222-2; author reply 6.
6. Bigard AX, Sanchez H, Birot O, Serrurier B. Myosin heavy chain composition of skeletal muscles in young rats growing under hypobaric hypoxia conditions. J Appl Physiol. 2000;88(2):479-86.
7. Schiaffino S, Reggiani C. Molecular diversity of myofibrillar proteins: gene regulation and functional significance. Physiological reviews. 1996;76(2):371-423.
8. Schiaffino S, Reggiani C. Myosin isoforms in mammalian skeletal muscle. J Appl Physiol. 1994;77(2):493-501.
9. Thomason DB, Baldwin KM, Herrick RE. Myosin isozyme distribution in rodent hindlimb skeletal muscle. J Appl Physiol. 1986;60(6):1923-31.
10. Huang C, Thirone AC, Huang X, Klip A. Differential contribution of insulin receptor substrates 1 versus 2 to insulin signaling and glucose uptake in l6 myotubes. J Biol Chem. 2005;280(19):19426-35.
11. Sarabia V, Lam L, Burdett E, Leiter LA, Klip A. Glucose transport in human skeletal muscle cells in culture. Stimulation by insulin and metformin. J Clin Invest. 1992;90(4):1386-95.
12. Klip A, Ramlal T, Bilan PJ, Marette A, Liu Z, Mitsumoto Y. What signals are involved in the stimulation of glucose transport by insulin in muscle cells? Cell Signal. 1993;5(5):519-29.
13. Sargeant R, Mitsumoto Y, Sarabia V, Shillabeer G, Klip A. Hormonal regulation of glucose transporters in muscle cells in culture. J Endocrinol Invest. 1993;16(2):147-62.
14. Klip A, Tsakiridis T, Marette A, Ortiz PA. Regulation of expression of glucose transporters by glucose: a review of studies in vivo and in cell cultures. Faseb J. 1994;8(1):43-53.
15. Foster LJ, Klip A. Mechanism and regulation of GLUT-4 vesicle fusion in muscle and fat cells. Am J Physiol Cell Physiol. 2000;279(4):C877-90.
16. Krook A, Zierath JR. Specificity of insulin signalling in human skeletal muscle as revealed by small interfering RNA. Diabetologia. 2009;52(7):1231-9.
17. Wang C. Insulin-stimulated glucose uptake in rat diaphragm during postnatal development: lack of correlation with the number of insulin receptors and of intracellular glucose transporters. Proceedings of the National Academy of Sciences of the United States of America. 1985;82(11):3621-5.

18. Cartee GD, Bohn EE. Growth hormone reduces glucose transport but not GLUT-1 or GLUT-4 in adult and old rats. The American journal of physiology. 1995;268(5 Pt 1):E902-9.
19. Hansen PA, Gulve EA, Holloszy JO. Suitability of 2-deoxyglucose for in vitro measurement of glucose transport activity in skeletal muscle. J Appl Physiol. 1994;76(2):979-85.
20. Talmadge RJ, Roy RR. Electrophoretic separation of rat skeletal muscle myosin heavy-chain isoforms. J Appl Physiol. 1993;75(5):2337-40.
21. Murphy RM. Enhanced technique to measure proteins in single segments of human skeletal muscle fibers: fiber-type dependence of AMPK-alpha1 and -beta1. J Appl Physiol. 2011;110(3):820-5.
22. Sharma N, Arias EB, Bhat AD, Sequea DA, Ho S, Croff KK, et al. Mechanisms for increased insulin-stimulated Akt phosphorylation and glucose uptake in fast- and slow-twitch skeletal muscles of calorie-restricted rats. Am J Physiol Endocrinol Metab. 2011;300(6):E966-78. PMCID: 3118592.
23. Castorena CM, Mackrell JG, Bogan JS, Kanzaki M, Cartee GD. Clustering of GLUT4, TUG and RUVBL2 Protein Levels Correlate with Myosin Heavy Chain Isoform Pattern in Skeletal Muscles, but AS160 and TBC1D1 Levels Do Not. J Appl Physiol. 2011.
24. Ai H, Ihlemann J, Hellsten Y, Lauritzen HP, Hardie DG, Galbo H, et al. Effect of fiber type and nutritional state on AICAR- and contraction-stimulated glucose transport in rat muscle. Am J Physiol Endocrinol Metab. 2002;282(6):E1291-300.
25. Kovanen V, Suominen H, Heikkinen E. Collagen of slow twitch and fast twitch muscle fibres in different types of rat skeletal muscle. Eur J Appl Physiol Occup Physiol. 1984;52(2):235-42.
26. Castorena CM, Mackrell JG, Bogan JS, Kanzaki M, Cartee GD. Clustering of GLUT4, TUG and RUVBL2 Protein Levels Correlate with Myosin Heavy Chain Isoform Pattern in Skeletal Muscles, but AS160 and TBC1D1 Levels Do Not. J Appl Physiol. 2011;[Epub ahead of print].
27. Pellegrino MA, D'Antona G, Bortolotto S, Boschi F, Pastoris O, Bottinelli R, et al. Clenbuterol antagonizes glucocorticoid-induced atrophy and fibre type transformation in mice. Exp Physiol. 2004;89(1):89-100.
28. Schiaffino S, Sandri M, Murgia M. Activity-dependent signaling pathways controlling muscle diversity and plasticity. Physiology (Bethesda). 2007;22:269-78.
29. Baldwin KM, Haddad F. Effects of different activity and inactivity paradigms on myosin heavy chain gene expression in striated muscle. J Appl Physiol. 2001;90(1):345-57.
30. Diffee GM, McCue S, LaRosa A, Herrick RE, Baldwin KM. Interaction of various mechanical activity models in regulation of myosin heavy chain isoform expression. J Appl Physiol. 1993;74(5):2517-22.
31. Diffee GM, Caiozzo VJ, McCue SA, Herrick RE, Baldwin KM. Activity-induced regulation of myosin isoform distribution: comparison of two contractile activity programs. J Appl Physiol. 1993;74(5):2509-16.
32. Zierath JR, He L, Guma A, Odegoard Wahlstrom E, Klip A, Wallberg-Henriksson H. Insulin action on glucose transport and plasma membrane GLUT4 content in skeletal muscle from patients with NIDDM. Diabetologia. 1996;39(10):1180-9.

33. Klip A, Ramlal T, Walker D. Insulin stimulation of glucose uptake and the transmembrane potential of muscle cells in culture. FEBS Lett. 1986;205(1):11-4.
34. Sarabia V, Ramlal T, Klip A. Glucose uptake in human and animal muscle cells in culture. Biochem Cell Biol. 1990;68(2):536-42.
35. Etgen GJ, Jr., Wilson CM, Jensen J, Cushman SW, Ivy JL. Glucose transport and cell surface GLUT-4 protein in skeletal muscle of the obese Zucker rat. The American journal of physiology. 1996;271(2 Pt 1):E294-301.
36. Sherman WM, Katz AL, Cutler CL, Withers RT, Ivy JL. Glucose transport: locus of muscle insulin resistance in obese Zucker rats. The American journal of physiology. 1988;255(3 Pt 1):E374-82.
37. Gregor MF, Hotamisligil GS. Inflammatory mechanisms in obesity. Annu Rev Immunol. 2011;29:415-45.
38. Schenk S, Saberi M, Olefsky JM. Insulin sensitivity: modulation by nutrients and inflammation. J Clin Invest. 2008;118(9):2992-3002. PMCID: 2522344.
39. Sriwijitkamol A, Christ-Roberts C, Berria R, Eagan P, Pratipanawatr T, DeFronzo RA, et al. Reduced skeletal muscle inhibitor of kappaB beta content is associated with insulin resistance in subjects with type 2 diabetes: reversal by exercise training. Diabetes. 2006;55(3):760-7.
40. Bhatt BA, Dube JJ, Dedousis N, Reider JA, O'Doherty RM. Diet-induced obesity and acute hyperlipidemia reduce IkappaBalpha levels in rat skeletal muscle in a fiber-type dependent manner. American journal of physiology. 2006;290(1):R233-40.
41. Bikman BT, Zheng D, Kane DA, Anderson EJ, Woodlief TL, Price JW, et al. Metformin Improves Insulin Signaling in Obese Rats via Reduced IKKbeta Action in a Fiber-Type Specific Manner. J Obes. 2010;2010. PMCID: 2925476.
42. Saito T, Jones CC, Huang S, Czech MP, Pilch PF. The interaction of Akt with APPL1 is required for insulin-stimulated Glut4 translocation. J Biol Chem. 2007;282(44):32280-7.
43. Deepa SS, Dong LQ. APPL1: role in adiponectin signaling and beyond. Am J Physiol Endocrinol Metab. 2009;296(1):E22-36. PMCID: 2636986.

CHAPTER IV

STUDY 2

Fiber Type-specific Differences in Glucose Uptake by Single Fibers from Skeletal Muscles of 9 and 25 Month-old Rats

Abstract

The primary purpose of this study was to assess the feasibility of applying a novel approach to measure myosin heavy chain (MHC) isoform expression, glucose uptake, fiber volume, and protein abundance in single muscle fibers of adult (9-month) and old (25-month) rats. Epitrochlearis muscle fibers were successfully isolated and analyzed for MHC isoform expression, glucose uptake, fiber volume, and protein (COXIV, APPL1, IκB-β) abundance. Insulin-stimulated glucose uptake by single fibers did not differ between age groups, but there was a significant difference between fiber types (IIA>IIX>IIB/X≈IIB). There were also significant main effects of fiber type on APPL1 (IIX>IIB) and COXIV (IIA>IIX>IIB/X≈IIB) abundance, and IIB fibers were significantly larger than IIA fibers. This study established the feasibility of a new approach for assessing age-related differences in muscle at the single fiber level and

demonstrated the magnitude and rank-order for fiber type differences in insulin-stimulated glucose uptake of 9-month-old and 25-month-old rats.

Introduction

Many of the most prevalent and devastating age-related diseases in humans (including hypertension, coronary heart disease, stroke, some forms of cancer, and type 2 diabetes) have been linked to insulin resistance (1). Whole body glucose disposal during a euglycemic-hyperinsulinemic clamp has been reported to be moderately (~15-35%) lower for old rats (20-25 months old) compared to adult rats (6-10 month old) (2, 3). Skeletal muscle is the major tissue for insulin-mediated glucose clearance, but the magnitude of age-related insulin resistance does not appear to be uniform in all skeletal muscles. Previous studies have compared 8-9 month-old and 24-25 month-old rats for glucose uptake by multiple muscles under in vivo conditions (during euglycemic-hyperinsulinemic clamp) (4) and under ex vivo conditions (in isolated muscles) (5). In both conditions, relatively greater age-related decrements in glucose uptake were reported for skeletal muscles that were mostly composed of type I and type IIA fibers, and lesser levels of age-related insulin resistance in muscles that were largely composed of type IIB and IIX fibers. However, it is uncertain if the variable extent of age-related insulin resistance is solely attributable to differences in fiber type composition or if there may be a contribution of other differences between the particular skeletal muscles that have been studied. In this context, it would be informative to measure glucose uptake by muscle fibers of differing fiber types from the same muscle.

There is striking diversity in fiber type composition between different muscles from the same animal. Furthermore, each skeletal muscle is composed of hundreds or thousands of muscle fibers that can also be diverse in fiber type and metabolic characteristics. We recently developed and validated the first method allowing for the isolation of single mammalian skeletal muscle fibers to be used for measurement of fiber type, fiber size, and glucose uptake (6). Using isolated epitrochlearis muscles from 2-3 month-old rats, we found fiber type-dependent differences in insulin-stimulated glucose uptake. Fibers expressing the IIA myosin heavy chain (MHC) isoform had significantly greater glucose uptake than all other fiber types measured (IIA>IIB, IIX, IIB/X). Furthermore, our novel single fiber method provided the first information about the glucose uptake capacity of hybrid fibers (expressing more than one MHC isoform; IIB/X) (6) that have been reported to account for ~5 to 30% of fibers in some rodent muscles (7). In a series of studies using isolated whole epitrochlearis muscles from adult (8-13 months old) compared to old (23-31 months old), we have found age-related differences in insulin-stimulated glucose uptake ranging from 0 to 18% (8-11). It seemed possible that the small fraction of highly oxidative fibers in this muscle [including ~6-13% type IIA fibers and ~6-8% type I fibers (12, 13) may account for a disproportionate amount of the modest age-related insulin resistance that has sometimes been detected in the whole muscle. In our earlier study using 2-3 mo-old rats, we were able to isolate and measure glucose uptake of single fibers expressing type IIA, IIB, IIX and IIB/X MHC (6). Accordingly, this new method offered the opportunity to evaluate the idea that the extent of age-related insulin resistance might be variable among these fiber types.

The overall goal of the current study was to advance the currently limited understanding of the relationship between fiber type, and age-associated insulin resistance in skeletal muscle by studying muscle glucose uptake of adult and old rats for the first time at the level of the single fiber. The first aim was to determine if our novel single fiber method for measuring glucose uptake and MHC isoform expression could be successfully applied to epitrochlearis muscles from adult (9 month-old) and old (25 month-old) rats. The second aim was to determine if insulin-stimulated glucose uptake differs among fiber types in either adult or old rats. The third aim was to determine if the extent of age-associated insulin resistance for glucose uptake is fiber type dependent. Our final aim was to determine possible age and fiber type differences for expression of selected proteins: cytochrome C oxidase subunit IV (COXIV, mitochondrial electron transport chain protein), IκB-β (marker of IκB/Nuclear factor-κB, NFκB, pathway activation), and Appl1 (an adapter protein involved in mediating signaling and metabolic effects of adiponectin).

Research Design & Methods

Materials

Human recombinant insulin was from Eli Lilly (Indianapolis, IN). Bicinchoninic acid (BCA) protein assay reagents and T-PER reagent were from Pierce Biotechnology (Rockford, IL). [^{3}H]-2-Deoxy-D-glucose ([^{3}H]-2-DG) was from Perkin Elmer (Waltham, MA). Collagenase (type II) was from Worthington Biochem Corp. (Lakewood, NJ). Trypan Blue was from Invitrogen (Carlsbad, CA). Reagents and apparatus for SDS-PAGE and immunoblotting were purchased from Bio-Rad (Hercules,

CA). West Dura Extended Duration Substrate was from Pierce Biotechnology (Rockford, IL). Anti-APPL1 antibody (#ab59592) and anti-COXIV (#ab16506) were from Abcam (Cambridge, MA), anti-IκB-β antibody (#sc-945) was from Santa Cruz (Santa Cruz, CA), and anti-rabbit IgG horseradish peroxidase (#7074) was from Cell Signaling Technology (Danvers, MA). Other reagents were from Sigma-Aldrich (St. Louis, MO) or Fisher Scientific (Pittsburgh, PA).

Animal Treatment

Procedures for animal care were approved by the University of Michigan Committee on Use and Care of Animals. Male Fisher-344 x Brown Norway, F1 generation rats were obtained at 9 or 25 month-old from Harlan (Indianapolis, IN). Animals were provided with rodent chow ad libitum until 1700 the night before the experiment, when food was removed. The next day, between 1000 and 1300, rats were anesthetized (intraperitoneal injection of sodium pentobarbital) and both epitrochlearis muscles were extracted.

Muscle Incubation

Isolated muscles underwent a series of incubation steps as previously described (6). In brief, isolated muscles were incubated in vials containing 2ml of Krebs Henseleit buffer (KHB) supplemented with 0.1% BSA (KHB-BSA), 2mM sodium pyruvate and 6mM mannitol with 0 or 12nM insulin for 20min, then transferred to a second vial for 60min incubation in 2ml of KHB-BSA, 1mM 2-DG (specific activity of 13.5mCi/mmol [^{3}H]-2-DG), and 9mM mannitol and the same insulin concentration as the previous step.

Muscles underwent 3x5min washes (100rpm) in ice-cold KHB-BSA to clear the extracellular space of 2-DG (14), followed by incubation in Collagenase Media (Ca^{2+}-free KHB and 1.5% type II collagenase) for 60min (collagenase-treated muscles are hereafter referred to as fiber bundles). Unless otherwise noted, vials were shaken (45rpm), gassed (95% O_2/5% CO_2), and maintained at 35°C in a water bath.

Single Fiber Isolation and Processing

Following collagenase incubation, fiber bundles were removed from solution and single fibers were isolated as previously described (6). In brief, single fibers were teased from the fiber bundle using forceps and imaged using a camera-enabled microscope with Leica Application Suite EZ software after isolation. Fiber width (mean value for width measured at 3 locations per fiber: near the fiber midpoint and approximately halfway between midpoint and each end of the fiber) and length of each fiber was used to estimate volume ($V = \pi \cdot r^2 \cdot l$; r = fiber radius as determined by half of the width measurement, l = fiber length). Each fiber was transferred by pipette with 10µl of solution to a micro-centrifuge tube containing 40µl of lysis buffer (T-PER, 1mM EDTA, 1mM EGTA, 2.5 mM sodium pyrophosphate, 1mM Na_3VO_4, 1 mM β-glycerophosphate, 1µg/ml leupeptin, and 1mM PMSF). Laemmli buffer (2X, 50µl) was added to each tube.

Single Fiber 2-DG Uptake, Myosin Heavy Chain (MHC) Isoform Characterization, and Immunoblotting

Separate aliquots of a lysed fiber were used for 2-DG uptake, MHC characterization, and protein abundance (immunoblotting) for single fibers as previously

described (6). In brief, an aliquot of lysed fiber was used to determine [^{3}H]-2-DG disintegrations per minute (dpm) using a scintillation counter. Measured 2-DG accumulation was normalized to calculated fiber volume and expressed as nanomoles per microliter (nmol • μl^{-1}). A separate aliquot of fiber lysate was used to determine MHC isoform expression via SDS-PAGE. Using the relative abundance of MHC expressed per fiber, a similar amount of MHC protein for each fiber aliquot was loaded onto 9% SDS-PAGE gels for subsequent immunoblotting and measurements of COXIV, Appl1, and IκB-β content as previously described (6). After immunoblotting, membranes were washed and subjected to enhanced chemiluminescence (West Dura Extended Duration Substrate; #34075; Pierce) to visualize protein bands. Immunoreactive proteins were quantified by densitometry (AlphaEase FC; Alpha Innotech, San Leandro, CA). Values for protein abundance of single fibers were normalized to the average of the Adult (9 month-old) samples on each blot and expressed relative to the fiber's respective post-transfer MHC density determined in the gel (6) .

Fiber Bundle Homogenization, 2-DG Uptake, and Immunoblotting

Following fiber isolation, the donor fiber bundles from which fibers were isolated were processed for 2-DG uptake and immunoblotting in 1ml ice-cold lysis buffer using glass-on-glass grinding tubes (6). Homogenates were rotated (4°C, 1h) before being centrifuged (12,000*g*, 10 min, 4°C). A portion of supernatant was used to determine protein concentration (BCA protein assay). Aliquots of supernatant used for 2-DG uptake were pipetted into vials for scintillation counting, and 2-DG uptake was determined and normalized to protein content ($\mu mol \bullet \mu g^{-1}$ protein for fiber bundles) as

previously described (6). Immunoblotting was performed as previously described (5). Values are expressed relative to the normalized average of the Adult (9 month-old) samples on each blot. Remaining supernatant was stored at −80°C until further analysis.

Statistical Analysis

Data are expressed as mean ±SEM. Two-way ANOVA was used to identify significant main effects (age and fiber type) and interactions for glucose uptake, fiber size (estimated volume), and protein abundance (Appl1, IκB-β, and COXIV) in single fibers. Tukey's post hoc *t*-test was applied to determine the source of significant variance. A Student's *t*-test was used to identify age differences for body mass, fiber bundle protein abundance and fiber type composition. A P-value of ≤0.05 was considered statistically significant.

Results

Body Mass, Epitrochlearis Myosin Heavy Chain (MHC) Composition and Estimated Fiber Volume

Body mass was 18% greater ($p<0.05$) in old (530.2 ± 11.6 g) vs. adult (432.4 ± 7.2 g) rats. The relative abundance of each MHC isoform (I, IIB, IIX, and IIA) in the whole epitrochlearis muscles did not differ between adult (type I = 10.5% ± 0.6, IIB = 42.3% ± 3.4, IIX = 34.8% ± 2.0, IIA = 12.3% ± 1.2) and old (type I = 8.7% ± 0.7, IIB = 40.9% ± 1.8, IIX = 39.4% ± 2.2, IIA = 11.0% ± 1.1) rats. The volume of each isolated single fiber was estimated using width and length measurements. There was no significant effect of age on fiber volume, but there was a significant main effect of fiber

type on fiber volume. Post-hoc analysis revealed that the volume of IIB fibers was significantly greater ($p<0.05$) than the volume of IIA fibers from adult and old rat muscle (Fig. 4.1).

2-DG Uptake by Fiber Bundles and Single Fibers

No significant effect of age was detected for 2-DG uptake by the "donor" fiber bundles (from which single fibers had been previously isolated) incubated in either the absence or presence of insulin (Fig. 4.2A). Basal (no insulin) 2-DG uptake values by single fibers were not significantly different between adult and old rats within any of the fiber types (Fig. 4.2B). There was also no significant age-related difference for insulin-stimulated 2-DG uptake within any of the fiber types. However, in single fibers from insulin-stimulated muscles, there was a significant main effect of fiber type ($p<0.001$) on 2-DG uptake. Post-hoc analysis revealed that for single fibers from insulin-stimulated muscles (either adult or old), 2-DG uptake was greater for IIA fibers compared to all other fiber types (IIA > IIB, IIX and IIB/X; $p<0.001$). In addition, 2-DG uptake was significantly greater ($p<0.05$) for IIX versus IIB fibers from insulin-stimulated muscles.

COXIV Abundance in Fiber Bundles and Single Fibers

In fiber bundles, there was no significant effect of age on COXIV abundance (Fig. 4.3A). In single fibers, there were significant main effects of age ($p<0.05$) and fiber type ($p<0.001$; Fig. 4.3B). Post-hoc analysis revealed that COXIV content in IIA was significantly greater ($p<0.001$) than in IIB, IIX, and IIB/X fibers (IIA > IIB, IIX IIB/X;

Fig. 4.3B) and COXIV content in IIX fibers was significantly greater ($p<0.01$) than IIB and IIB/X fibers (IIX > IIB and IIB/X; Fig. 4.3B).

Appl1 Abundance in Fiber Bundles and Single Fibers

In fiber bundles, there was no significant effect of age on Appl1 abundance (Fig. 4.4A). In single fibers, there was no main effect of age on Appl1 abundance, but there was significant main effect of fiber type ($p<0.01$; Fig. 4.4B). Post-hoc analysis revealed the source of significant differences ($p<0.05$) for APPL1 abundance among fiber types was IIX fibers vs. IIB fibers (IIX > IIB).

IκB-β Abundance in Fiber Bundles and Single Fibers

In fiber bundles, there was no significant effect of age on IκB-β abundance (Fig. 4.5A). There were also no significant effects of either age or fiber type on IκB-β abundance in single fibers (Fig. 4.5B).

Discussion

A major outcome of the current study was demonstrating the feasibility of measuring glucose uptake, MHC isoform expression, estimated fiber volume and protein abundance in single fibers of adult (9 month-old) and old (25 month-old) rats. Another significant and novel result was that in single fibers from both age groups, the rank-order for insulin-stimulated glucose uptake by single fibers was found to be: IIA > IIX > IIB/X ≈ IIB. The magnitude of fiber type-related differences for insulin-stimulated glucose uptake of adult and old rats was striking with values for type IIA fibers found to be more

than 2-fold greater than IIX fibers and more than 3-4-fold greater than type IIB or IIB/X fibers from the same muscle. An additional valuable finding was the lack of age-related differences for insulin-stimulated glucose uptake by single fibers within any of the type II fiber types. There were also no age-related differences for MHC isoform content of whole muscles or for abundance of Appl1 and IκB-β at either the whole muscle level or within any of the fiber types. COXIV protein abundance was greater in both IIA and IIX fibers versus both IIB and IIB/X fibers in each age-group. As expected, estimated fiber volume for type IIB fibers exceeded type IIA fibers in both age groups. No significant age-related differences in fiber volume were identified for any of the fiber types. Taken together, the current data demonstrate substantial fiber-type related differences for insulin-stimulated glucose uptake, COXIV protein abundance and fiber volume.

Because of the phenotypic heterogeneity of different fiber types, it is essential to evaluate single fibers identified by fiber type to understand skeletal muscle at the cellular level. Previous studies have characterized single fibers from old individuals with regard to contractile properties, morphology, enzymatic activity, MHC expression and mitochondrial deletions (15-23). However, the influence of aging on single fiber glucose uptake was unknown because there was previously no method to measure glucose uptake of mammalian single fibers. The results of the current study demonstrated that insulin-stimulated glucose uptake measured at the single fiber level within any type II MHC isoform is not lower for 25 month-old compared to 9 month-old rats. Earlier studies found age-related insulin resistance in whole muscles appeared to be greater for muscles with a high abundance of type I and IIA fibers compared to muscles that were largely composed of fibers with high abundance of type IIB and IIX fibers (4, 5). Therefore, we

expected that we might find age-related insulin resistance in type IIA fibers, but the data did not support this expectation. It remains possible that type I fibers may be susceptible to age-related insulin resistance. However, the data from the current study do not provide direct information about this idea because, as in our earlier study of younger (2-3 month-old rats) (6), no type I fibers were isolated. We are unsure of the reason for the lack of type I fiber isolation, but it may be related to the higher level of collagen that is reported to surround type I versus type II fibers (24). In support of this idea, despite multiple attempts to use collagenase with isolated soleus muscles (composed of approximately 90% type I fibers), we were unable to isolate type I fibers. Regardless, our current protocol was successful in isolating single fibers expressing each of the other MHC isoforms in (which account for more than 90% of the total MHC isoforms expressed in the rat epitrochlearis) (13, 25).

Significant age-related differences in glucose uptake were not detected in either whole muscles or single fibers. We evaluated the influence of age on insulin-stimulated glucose uptake by the whole epitrochlearis muscle in several previous studies. We recently found a small (18%) reduction in glucose uptake of the whole epitrochlearis of 25 versus 9 month-old rats (5), but in several earlier studies of old (23-31 month-old) compared to adult (8 to 13 month-old) rats, similar to the results of the current study, we did not detect significant age-related differences in glucose uptake by the whole epitrochlearis (8-10). These results indicate there is not profound insulin resistance in the whole epitrochlearis of rats across this portion of the adult lifespan. It is notable that in many rodents with experimentally introduced genetic modifications (i.e., mice that express a mutated protein or that are null for expression of particular protein), insulin

sensitivity can be normal under usual experimental conditions (e.g., eating a standard rodent chow diet), with insulin resistance revealed only when the animals are metabolically challenged by eating a high fat diet. Various interventions can also markedly influence insulin sensitivity of adult and old rats. For example, consuming a high fat diet, reducing normal muscle contractile activity (e.g., by hindlimb unloading, denervation or immobilization) or various drugs that are often used to treat adult and older individuals can induce insulin resistance (2, 26-29). Conversely, either calorie restriction or exercise can substantially improve insulin sensitivity in skeletal muscle of old rats (9-11, 30-32). Our new approach makes it possible, for the first time, to determine the fiber type-specific influence of these various interventions on skeletal muscle from adult or old rats at the cellular level.

Although our primary focus in the current study was on glucose uptake, the results also demonstrated that this experimental approach has the potential value for understanding other issues related to aging in skeletal muscle. Sarcopenia refers to an age-related loss of muscle mass or muscle function. The extent of age-related muscle atrophy varies by fiber type, with type IIB fibers often found to be highly susceptible to loss of cross-sectional area. In the current study, there were no significant differences in the volume of any of the fiber types studied. Some skeletal muscles are characterized by age-related decrements in various mitochondrial markers, including enzyme activity and protein abundance (33). However, previous studies measuring mitochondrial enzymes in the whole epitrochlearis muscle reported no age-related changes in rats of ages similar to those in the current study (34-36). Consistent with these earlier results, we also found no significant difference of age in COXIV abundance in the whole epitrochlearis fiber

bundle. However, there was a small, but significant main effect of age on COXIV abundance at the single fiber level, with a greater COXIV levels in the fibers from 25 month-old rats. This result provides an example of the ability of single fiber analysis to reveal differences that may be overlooked with whole tissue analysis.

Hybrid fibers have been reported to account for up to 5 to 30% of fibers of some rodent skeletal muscles (7). Because conventional tissue analysis cannot reveal information about the metabolic properties of hybrid fibers, single fiber analysis is uniquely valuable to provide insights into the metabolism of hybrid fibers. In the current study, insulin-stimulated glucose uptake of IIB/X fibers did not differ significantly from type IIB fibers, whereas in our previous study of younger (2-3 month-old rats), we found insulin-stimulated glucose uptake of type IIB/X fibers was slightly (25%) but significantly greater than for type IIB fibers. It is uncertain if the reason for the differing results from the current study compared to the earlier study is attributable to the difference in age of the rats. The IIB/X and IIB fibers in the current study were similar with regard to some characteristics (COXIV abundance and glucose uptake), but they differed with regard to others (APPL1 abundance and fiber volume). It would be useful to further characterize the protein expression profile of hybrid fibers from adult and old rats.

In conclusion, age-related changes in the structure and function of skeletal muscle do not occur uniformly across the different muscle fiber types. It is essential to develop and employ new experimental approaches to fully understand the effects of aging on skeletal muscle at the cellular and molecular level. In this context, the results of the current study provide a unique opportunity for future research focused on the metabolic

properties of single fibers from adult and old rats. This new method will be valuable to test for possible age-dependent and fiber type-specific effects of various clinically relevant interventions (e.g., dietary manipulations, exercise, limb immobilization, treatment with drugs, etc.) on glucose uptake, MHC isoform expression, fiber size, and protein abundance in adult and old rats.

Acknowledgments

This work was supported by the National Institutes of Health (AG-010026 to G.D.C.); and the American Heart Association (12PRE9270001 to J.G.M.)

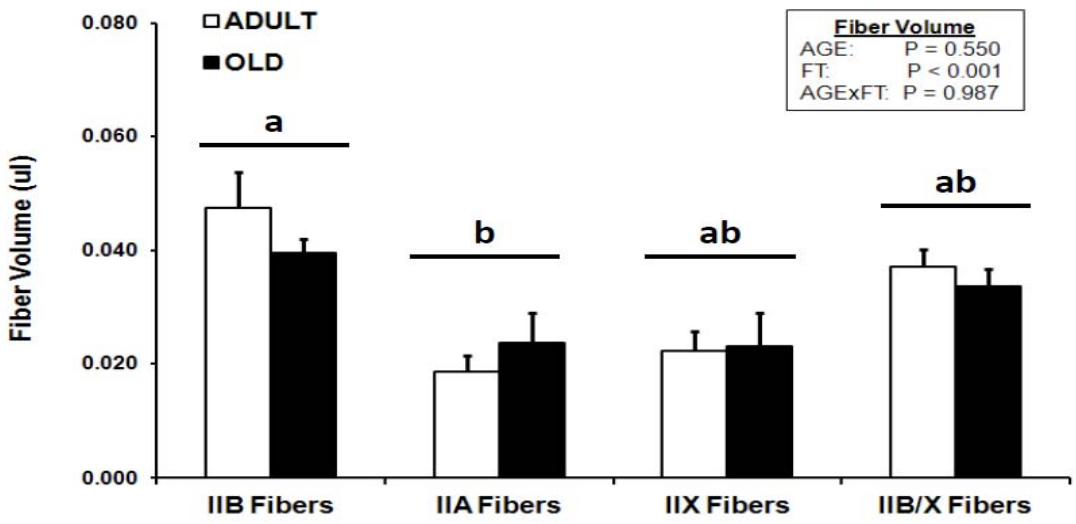

Figure 4.1 Size (volume, µl) of Single Fibers Expressing the Same MHC Isoform From Adult Vs. Old Epitrochlearis Muscles. For fibers from adult rat muscle, the number of fibers for each MHC isoform is in parentheses: IIB (109), IIA (19), IIX (18), IIB/X (54). For fibers from old rat muscle, the number of fibers for each MHC isoform is in parentheses: IIB (103), IIA (11), IIX (11), IIB/X (35). Data are means ± SEM and were analyzed by two-way ANOVA. AGE, main effect of age (9-mo vs. 25-mo); FT, main effect of fiber type; AGExFT, interaction between main effects. There was a main effect of fiber type ($p<0.05$). MHC isoforms that were revealed by post-hoc analysis to be significantly different from each other ($p<0.05$ for IIB vs. IIA) are designated by not having the same letter above their respective bars, while isoforms that were not significantly different are designated by having the same letter above their respective bars.

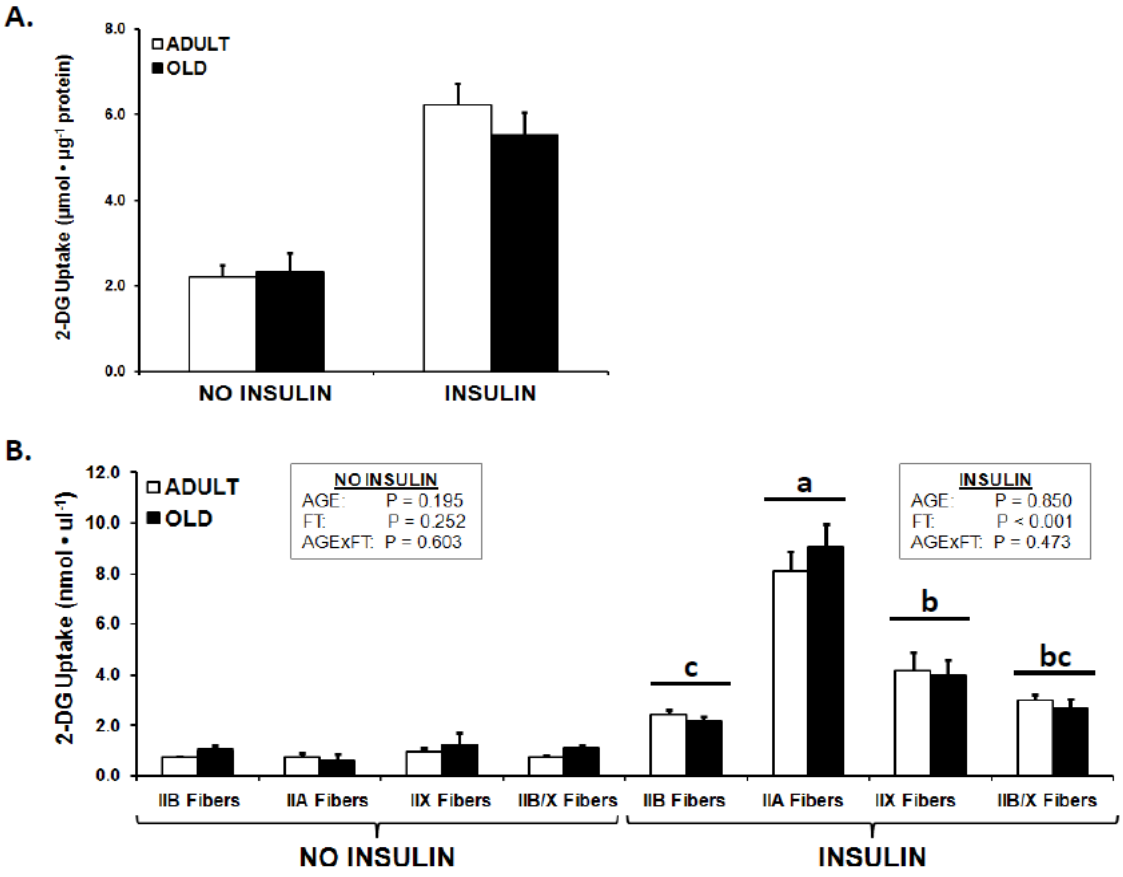

Figure 4.2 Glucose Uptake by Fiber Bundles and Single Fibers Adult and Old Rats. **A.** Basal and insulin-stimulated 2-DG uptake by adult (open bars) vs. old (closed bars) fiber bundles (from which single fibers had been previously isolated). Data are means ± SEM (n = 5-6 muscles per age group at each insulin concentration). **B.** Mean 2-DG uptake by single muscle fibers expressing the same MHC isoform from adult (open bars) vs. old (closed bars) epitrochlearis muscles. For basal fibers, from adult rat muscle, the number of fibers for each MHC isoform is in parentheses: IIB (56), IIA (5), IIX (9), IIB/X (20). For basal fibers, from old rat muscle, the number of fibers for each MHC isoform is in parentheses: IIB (46), IIA (4), IIX (5), IIB/X (15). For insulin-stimulated fibers, from adult rat muscle the number of fibers for each MHC isoform is in parentheses: IIB (53), IIA (14), IIX (9), IIB/X (34). For insulin-stimulated fibers, from old rat muscle, the number of fibers for each MHC isoform is in parentheses: IIB (57), IIA (7), IIX (6), IIB/X (20). Data are means ± SEM and were analyzed by two-way ANOVA within each insulin level. AGE, main effect of age (9-mo vs. 25-mo); FT, main effect of fiber type; AGExFT, interaction between main effects. For fibers with insulin, there was a main effect of fiber type ($p<0.001$). MHC isoforms that were significantly different from each other ($p<0.001$ for IIA vs. IIB, IIX, and IIB/X; and $p<0.05$ for IIX vs. IIB) are designated by not having the same letter above their respective bars, while isoforms that were not significantly different from each other are designated by having the same letter above their respective bars.

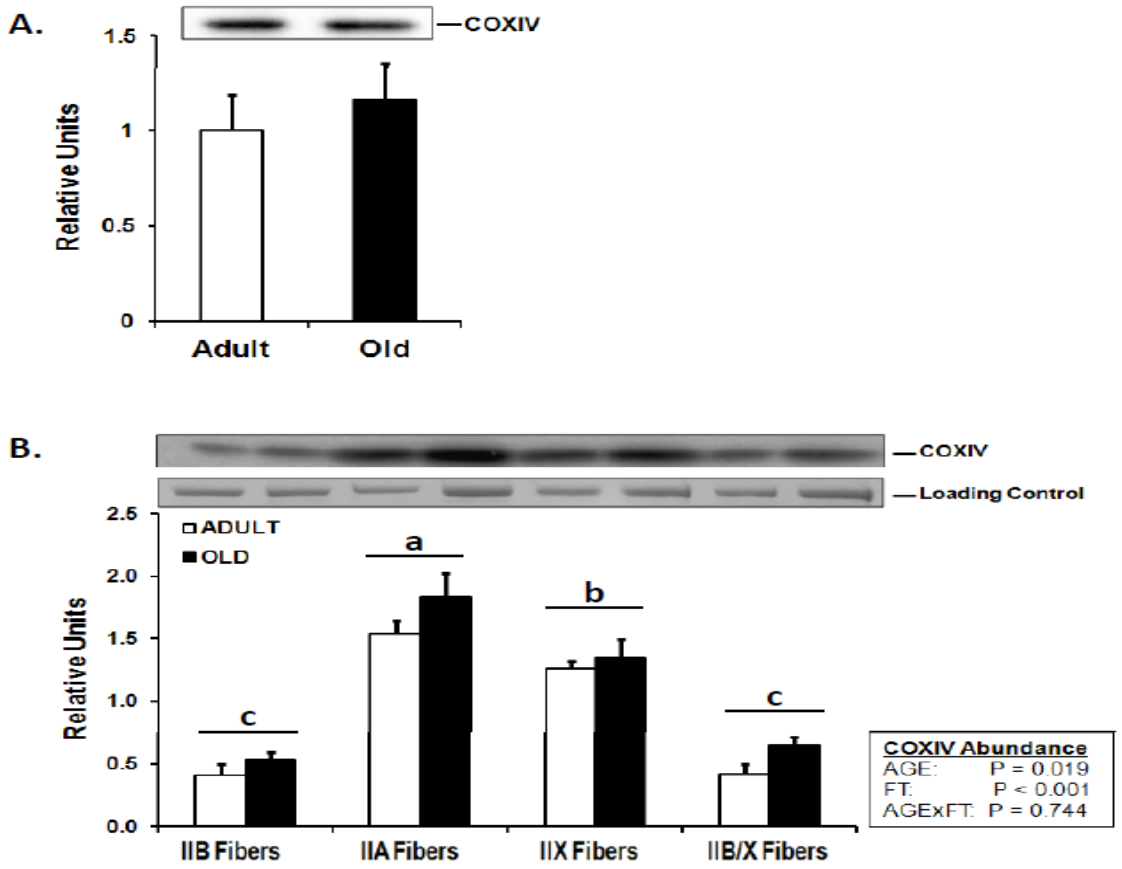

Figure 4.3 COXIV Protein Abundance in Fiber Bundles and Single Fibers From Adult and Old Rats. A. Data are means ± SEM (n = 6 fiber bundles per age group). Representative blots of protein abundance are provided. **B.** Data are means ± SEM (n = 8 fibers of each MHC isoform per age group) and were analyzed by two-way ANOVA. AGE, main effect of age (9-mo vs. 25-mo); FT, main effect of fiber type; AGExFT, interaction between main effects. Representative blots of protein abundance and corresponding Coomassie Brilliant Blue-stained gels of post transfer MHC (loading control) are provided. The density value for each protein was normalized to the density value for the loading control. There was a significant main effect of age ($p<0.05$) and fiber type (FT; $p<0.001$). Post-hoc analysis revealed 1). MHC isoform that were significantly different from each other ($p<0.001$ for IIA vs. IIB, IIX, and IIB/X; and $p<0.001$ for IIX vs. IIB and IIB/X) are designated by not having the same letter above their respective bars, while isoforms that were not significantly different from each other are designated by having the same letter above their respective bars.

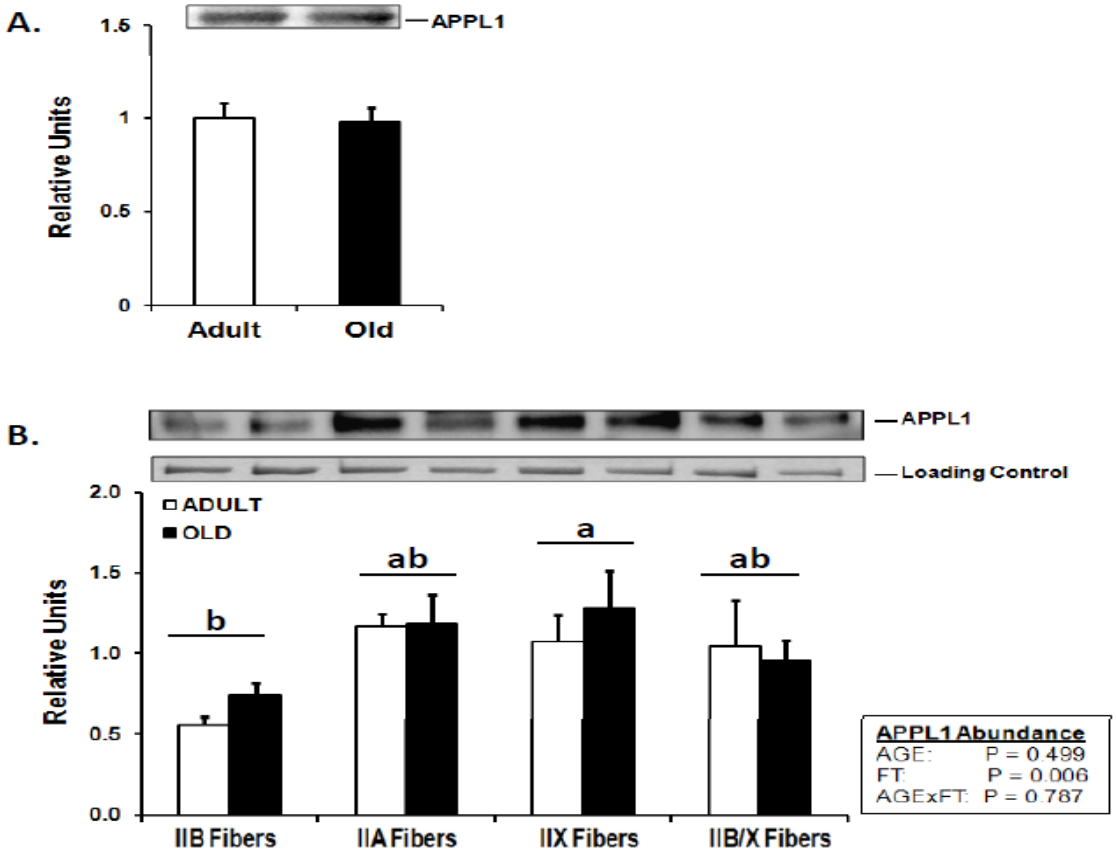

Figure 4.4 Appl1 Protein Abundance in Fiber Bundles and Single Fibers From Adult and Old Rats. A. Data are means ± SEM (n = 6 fiber bundles per age group). Representative blots of protein abundance are provided. **B.** Data are means ± SEM (n = 8 fibers of each MHC isoform per age group) and were analyzed by two-way ANOVA. AGE, main effect of age (9-mo vs. 25-mo); FT, main effect of fiber type; AGExFT, interaction between main effects. Representative blots of protein abundance and corresponding Coomassie Brilliant Blue-stained gels of post transfer MHC (loading control) are provided. The density value for each protein was normalized to the density value for the loading control. There was significant main effect of fiber type ($p<0.01$). MHC isoforms that were revealed by post-hoc analysis to be significantly different from each other ($p<0.05$ for IIX vs. IIB) are designated by not having the same letter above their respective bars , while isoforms that were not significantly different from each other are designated by having the same letter above their respective bars.

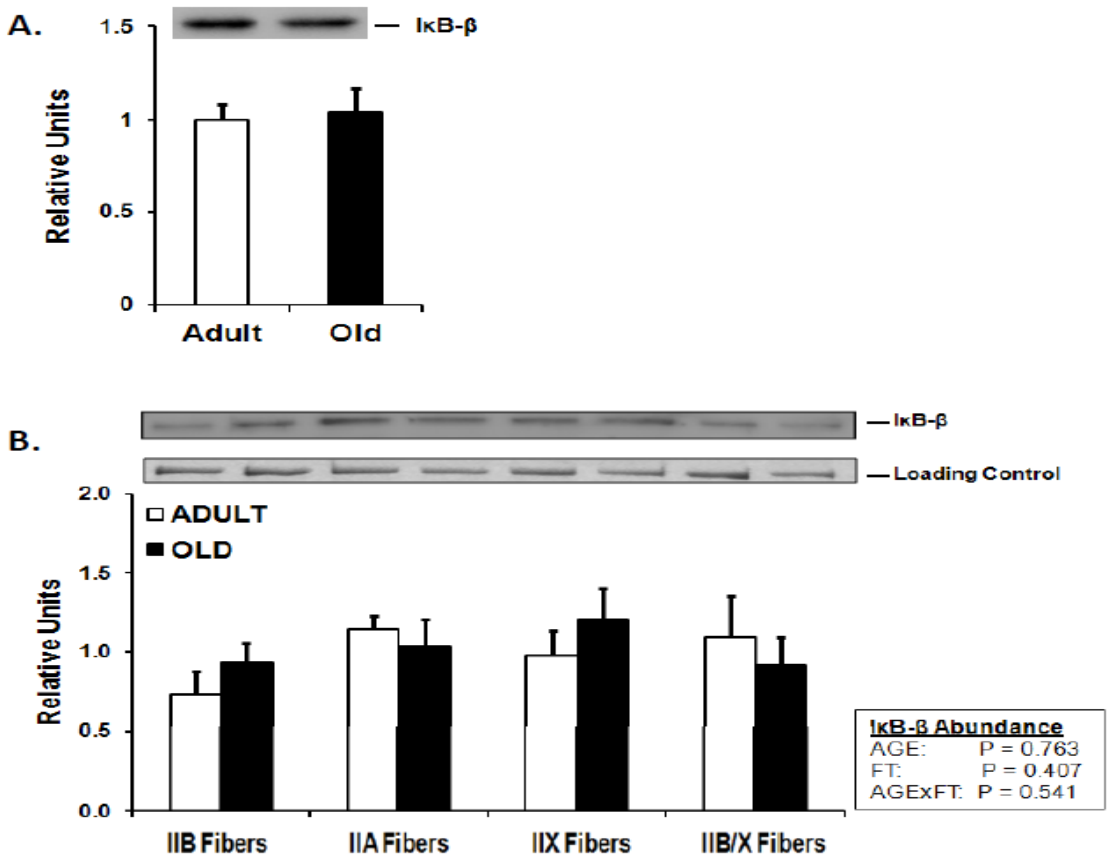

Figure 4.5 IκB-β Protein Abundance in Fiber Bundles and Single Fibers From Adult and Old Rats. A. Data are means ± SEM (n = 6 fiber bundles per age group) and were analyzed by two-way ANOVA. AGE, main effect of age (9-mo vs. 25-mo); FT, main effect of fiber type; AGExFT, interaction between main effects. Representative blots of protein abundance are provided. **B.** Data are means ± SEM (n = 8 fibers of each MHC isoform per age group). Representative blots of protein abundance and corresponding Coomassie Brilliant Blue-stained gels of post transfer MHC (loading control) are provided. The density value for each protein was normalized to the density value for the loading control.

References

1. Facchini FS, Hua N, Abbasi F, Reaven GM. Insulin resistance as a predictor of age-related diseases. J Clin Endocrinol Metab. 2001;86(8):3574-8.
2. Catalano KJ, Bergman RN, Ader M. Increased susceptibility to insulin resistance associated with abdominal obesity in aging rats. Obes Res. 2005;13(1):11-20.
3. Nishimura H, Kuzuya H, Okamoto M, Yoshimasa Y, Yamada K, Ida T, et al. Change of insulin action with aging in conscious rats determined by euglycemic clamp. The American journal of physiology. 1988;254(1 Pt 1):E92-8.
4. Escriva F, Gavete ML, Fermin Y, Perez C, Gallardo N, Alvarez C, et al. Effect of age and moderate food restriction on insulin sensitivity in Wistar rats: role of adiposity. J Endocrinol. 2007;194(1):131-41.
5. Sharma N, Arias EB, Sajan MP, MacKrell JG, Bhat AD, Farese RV, et al. Insulin resistance for glucose uptake and Akt2 phosphorylation in the soleus, but not epitrochlearis, muscles of old vs. adult rats. J Appl Physiol. 2010;108(6):1631-40. PMCID: 2886681.
6. Mackrell JG, Cartee GD. A novel method to measure glucose uptake and Myosin heavy chain isoform expression of single fibers from rat skeletal muscle. Diabetes. 2012;61(5):995-1003.
7. Bloemberg D, Quadrilatero J. Rapid determination of Myosin heavy chain expression in rat, mouse, and human skeletal muscle using multicolor immunofluorescence analysis. PLoS One. 2012;7(4):e35273. PMCID: 3329435.
8. Cartee GD, Bohn EE. Growth hormone reduces glucose transport but not GLUT-1 or GLUT-4 in adult and old rats. The American journal of physiology. 1995;268(5 Pt 1):E902-9.
9. Cartee GD, Briggs-Tung C, Kietzke EW. Persistent effects of exercise on skeletal muscle glucose transport across the life-span of rats. J Appl Physiol. 1993;75(2):972-8.
10. Cartee GD, Kietzke EW, Briggs-Tung C. Adaptation of muscle glucose transport with caloric restriction in adult, middle-aged, and old rats. The American journal of physiology. 1994;266(5 Pt 2):R1443-7.
11. Sharma N, Arias EB, Bhat AD, Sequea DA, Ho S, Croff KK, et al. Mechanisms for increased insulin-stimulated Akt phosphorylation and glucose uptake in fast- and slow-twitch skeletal muscles of calorie-restricted rats. Am J Physiol Endocrinol Metab. 2011;300(6):E966-78. PMCID: 3118592.
12. Allaf O, Goubel F, Marini JF. A curve-fitting procedure to explain changes in muscle force-velocity relationship induced by hyperactivity. Journal of biomechanics. 2002;35(6):797-802.
13. Castorena CM, Mackrell JG, Bogan JS, Kanzaki M, Cartee GD. Clustering of GLUT4, TUG, and RUVBL2 protein levels correlate with myosin heavy chain isoform pattern in skeletal muscles, but AS160 and TBC1D1 levels do not. J Appl Physiol. 2011;111(4):1106-17. PMCID: 3191788.
14. Wang C. Insulin-stimulated glucose uptake in rat diaphragm during postnatal development: lack of correlation with the number of insulin receptors and of intracellular glucose transporters. Proceedings of the National Academy of Sciences of the United States of America. 1985;82(11):3621-5.

15. Brooks SV, Faulkner JA. Skeletal muscle weakness in old age: underlying mechanisms. Med Sci Sports Exerc. 1994;26(4):432-9.
16. Hook P, Sriramoju V, Larsson L. Effects of aging on actin sliding speed on myosin from single skeletal muscle cells of mice, rats, and humans. Am J Physiol Cell Physiol. 2001;280(4):C782-8.
17. Gonzalez E, Delbono O. Recovery from fatigue in fast and slow single intact skeletal muscle fibers from aging mouse. Muscle Nerve. 2001;24(9):1219-24.
18. Thompson LV. Contractile properties and protein isoforms of single skeletal muscle fibers from 12- and 30-month-old Fischer 344 brown Norway F1 hybrid rats. Aging (Milano). 1999;11(2):109-18.
19. Fisher JS, Brown M. Immobilization effects on contractile properties of aging rat skeletal muscle. Aging (Milano). 1998;10(1):59-66.
20. Groskreutz JJ, Thompson LV. Enzymatic alterations in single type IIB skeletal muscle fibers with inactivity and exercise in 12- and 30-month-old rats. Aging Clin Exp Res. 2002;14(5):347-53.
21. Cao Z, Wanagat J, McKiernan SH, Aiken JM. Mitochondrial DNA deletion mutations are concomitant with ragged red regions of individual, aged muscle fibers: analysis by laser-capture microdissection. Nucleic acids research. 2001;29(21):4502-8. PMCID: 60181.
22. Larsson L, Li X, Frontera WR. Effects of aging on shortening velocity and myosin isoform composition in single human skeletal muscle cells. The American journal of physiology. 1997;272(2 Pt 1):C638-49.
23. Snow LM, McLoon LK, Thompson LV. Adult and developmental myosin heavy chain isoforms in soleus muscle of aging Fischer Brown Norway rat. Anat Rec A Discov Mol Cell Evol Biol. 2005;286(1):866-73.
24. Kovanen V, Suominen H, Heikkinen E. Collagen of slow twitch and fast twitch muscle fibres in different types of rat skeletal muscle. Eur J Appl Physiol Occup Physiol. 1984;52(2):235-42.
25. Delp MD, Duan C. Composition and size of type I, IIA, IID/X, and IIB fibers and citrate synthase activity of rat muscle. J Appl Physiol. 1996;80(1):261-70.
26. Stump CS, Tipton CM, Henriksen EJ. Muscle adaptations to hindlimb suspension in mature and old Fischer 344 rats. J Appl Physiol. 1997;82(6):1875-81.
27. Henriksen EJ, Rodnick KJ, Mondon CE, James DE, Holloszy JO. Effect of denervation or unweighting on GLUT-4 protein in rat soleus muscle. J Appl Physiol. 1991;70(5):2322-7.
28. van Raalte DH, Ouwens DM, Diamant M. Novel insights into glucocorticoid-mediated diabetogenic effects: towards expansion of therapeutic options? Eur J Clin Invest. 2009;39(2):81-93.
29. Flint OP, Noor MA, Hruz PW, Hylemon PB, Yarasheski K, Kotler DP, et al. The role of protease inhibitors in the pathogenesis of HIV-associated lipodystrophy: cellular mechanisms and clinical implications. Toxicol Pathol. 2009;37(1):65-77. PMCID: 3170409.
30. Xiao Y, Sharma N, Arias EB, Castorena CM, Cartee GD. A persistent increase in insulin-stimulated glucose uptake by both fast-twitch and slow-twitch skeletal muscles after a single exercise session by old rats. Age (Dordr). 2012.

31. Sequea DA, Sharma N, Arias EB, Cartee GD. Calorie Restriction Enhances Insulin-Stimulated Glucose Uptake and Akt Phosphorylation in Both Fast-Twitch and Slow-Twitch Skeletal Muscle of 24-Month-Old Rats. J Gerontol A Biol Sci Med Sci. 2012.
32. Dean DJ, Cartee GD. Brief dietary restriction increases skeletal muscle glucose transport in old Fischer 344 rats. J Gerontol A Biol Sci Med Sci. 1996;51(3):B208-13.
33. Cartee GD. Aging skeletal muscle: response to exercise. Exerc Sport Sci Rev. 1994;22:91-120.
34. Young JC, Chen M, Holloszy JO. Maintenance of the adaptation of skeletal muscle mitochondria to exercise in old rats. Med Sci Sports Exerc. 1983;15(3):243-6.
35. Barazzoni R, Short KR, Nair KS. Effects of aging on mitochondrial DNA copy number and cytochrome c oxidase gene expression in rat skeletal muscle, liver, and heart. J Biol Chem. 2000;275(5):3343-7.
36. Gulve EA, Rodnick KJ, Henriksen EJ, Holloszy JO. Effects of wheel running on glucose transporter (GLUT4) concentration in skeletal muscle of young adult and old rats. Mech Ageing Dev. 1993;67(1-2):187-200.

CHAPTER V

STUDY 3

Effects of Electroporation and Expression of DsRed on Glucose Uptake, Fiber Size and Protein Abundance in Rat Skeletal Muscle Single Fibers

Abstract

Skeletal muscle acts as a useful tissue for studying localized genetic manipulation using the in vivo electroporation (IVE) method of gene delivery. Because of the important role that skeletal muscle plays in whole body glucoregulation, the glucose uptake capacity of this tissue is widely studied, with recent advances allowing for studying the glucose uptake by single fibers from a muscle. In addition, the effect that a specific genetic modification has on skeletal muscle glucose uptake is an area of focus. The primary purpose of this study was to gain novel insight on glucose uptake, fiber volume, myosin heavy chain (MHC) isoform expression (fiber type), and abundance of key proteins (GLUT4 and COXIV) by rat epitrochlearis single fibers that express a fluorescent reporter gene (DsRed) following delivery by IVE. Rat epitrochlearis muscles underwent IVE to deliver a plasmid containing the gene encoding the DsRed protein

(termed IVE/pDsRed), while contralateral muscles were utilized for sham procedural controls (termed control). Twelve to fourteen days after IVE, the muscles were isolated and underwent a protocol to allow for measuring glucose uptake by single fibers. From the IVE/pDsRed muscle, only those single fibers expressing the DsRed protein were studied, while fibers from the control muscle were used for comparison. No significant differences were observed between fibers from the IVE/pDsRed muscle versus control muscle for: 1) glucose uptake capacity, 2) GLUT4 abundance, or 3) COXIV abundance. Fibers from the IVE/pDsRed muscle were significantly larger than control fibers, but posthoc analysis did not indicate the source of significance. There was a significant main effect of fiber type for: 1) Insulin-stimulated glucose uptake (IIA>IIB, IIX, IIB/X; IIX>IIB; IIB/X>IIB), 2) Fiber volume (IIB>IIA), 3) GLUT4 abundance (IIA>IIB, IIB/X; IIX>IIB), and 4) COXIV abundance (IIA>IIB, IIX, IIB/X). In conclusion, IVE delivery of the DsRed fluorescent reporter gene, and subsequent expression of the gene, did not alter the important measurement endpoints of single fiber glucose uptake and abundance of key metabolic proteins (GLUT4 and COXIV). These results provide validation for future studies combining single fiber analysis with the IVE approach for genetic manipulation.

Introduction

In vivo electroporation (IVE) of genetic material is a commonly used method for ectopic gene expression in skeletal muscle. This non-viral method of gene delivery is more effective than injection of plasmid DNA alone (1, 2). Furthermore, IVE avoids the pitfalls associated with other genetic approaches such as viral delivery techniques

(possible immunogenic/toxicity effects) or transgenic models (inability for localized gene expression in specific muscle and time intensive requirements). Conversely, IVE allows for the localized expression of genetic material within days of introduction, without the toxicity effects observed with viral expression techniques.

However, IVE does not have 100% transfection efficiency, meaning that not all fibers within a skeletal muscle are transfected and express the ectopic genetic material. Relative transfection efficiency is dependent on many variables including, but not limited to, the specific muscle/tissue, type of electrode (needle vs. paddle) and stimulation pattern (pulse strength and length) of electroporation, and the characteristics of the plasmid to be expressed. Thus, previous studies using IVE have reported between 10 to 85% of skeletal muscle fibers express the exogenous gene of interest (1, 3-7). However, the relative inefficiency of IVE makes it an attractive approach when combined with the method we recently developed and validated for the isolation of single rat skeletal muscle fibers to be used for measurement of fiber type, fiber size, and glucose uptake (8). By isolating only those fibers which are expressing the ectopic genetic material (via a fluorescent reporter visualization), focus can be placed squarely on the genetically manipulated fibers. In addition, those fibers not transfected (i.e., not expressing the ectopic genetic material) within the same IVE muscle can be used as a valuable internal control.

Because skeletal muscle plays a significant role in glucose homeostasis, the genetic manipulation of muscle for purposes of altering glucose uptake capacity is an area of considerable interest. Thus a logical connection is combining the IVE method of altering genetic material in muscle with our single fiber glucose uptake method to study

the positively transfected fibers as well as non-transfected fibers to serve as controls. In addition, the ability to fiber type each fiber based on myosin heavy chain (MHC) isoform expression will provide valuable information about potential fiber type-related differences that may occur as the result of the experimental treatment. Furthermore, application of this single fiber approach circumvents those questions related to lower transfection efficiency of IVE when analyzing results from whole muscles.

In this study, epitrochlearis muscles from rats underwent IVE of pDsRed (termed "IVE/pDsRed"), while the contralateral epitrochlearis underwent a sham surgery (no IVE; termed "control"). Fibers expressing the DsRed protein (visualized using a fluorescent microscope) were isolated from the IVE/pDsRed muscle, while fibers were isolated at random from the contralateral sham-treated control muscle. The aims of this study were to: 1) evaluate feasibility of IVE on the rat epitrochlearis muscle for genetic manipulation studies, and 2) compare single fibers from control muscles vs. IVE/pDsRed muscles with regard to glucose uptake, fiber size, and abundance of selected endogenous proteins.

Research Design & Methods

Materials

The ECM 830 Square Wave Electroporator and ruled calipers were from BTX Harvard Apparatus (San Diego, CA). The plasmid DNA for electroporation, pCMV DsRed-Express2 (Cat. # 632539), was from Clontech (Mountain View, CA). Human recombinant insulin was from Eli Lilly (Indianapolis, IN). Bicinchoninic acid (BCA) protein assay reagents and T-PER reagent were from Pierce Biotechnology (Rockford,

IL). [^{3}H]-2-Deoxy-D-glucose ([^{3}H]-2-DG) was from Perkin Elmer (Waltham, MA). Collagenase (type II) was from Worthington Biochem Corp. (Lakewood, NJ). Trypan Blue was from Invitrogen (Carlsbad, CA). Reagents and apparatus for SDS-PAGE and immunoblotting were purchased from Bio-Rad (Hercules, CA). West Dura Extended Duration Substrate was from Pierce Biotechnology (Rockford, IL). Anti-COXIV (#ab16506) was from Abcam (Cambridge, MA), anti-GLUT (CBL243) was from Millipore, and anti-rabbit IgG horseradish peroxidase (#7074) was from Cell Signaling Technology (Danvers, MA). Other reagents were from Sigma-Aldrich (St. Louis, MO) or Fisher Scientific (Pittsburgh, PA).

Animals

Procedures for animal care were approved by the University of Michigan Committee on Use and Care of Animals. Male Wistar rats (aged 4-5 months old) were from Harlan (Indianapolis, IN). Animals were provided with rodent chow ad libitum unless otherwise stated below.

In Vivo Electroporation of DNA into Rat Epitrochlearis Muscles

In vivo electroporation (IVE) of DNA into the rat epitrochlearis was performed with modifications of protocols previously described (3, 9). Animals were anaesthetized with an intraperitoneal injection of ketamine (70–90 mg·kg^{-1}), xylazine (5–10 mg kg^{-1}), and sodium pentobarbital (35-50 mg·kg^{-1}). Once sedated, the forelimbs of the animal were shaved and sterilized (iodine and 70% ethanol). A small portion of the epitrochlearis muscle was surgically exposed; a small cut (1-2cm) was made along the

proximal side of the bicep. After the epitrochlearis muscle was exposed, approximately 250µg of plasmid DNA (pCMV DsRed-Express2, Clontech) was injected into the epitrochlearis via syringe with a 29-guage needle inserted parallel to the orientation of the muscle fibers. One minute after injection, a pair of 0.8-cm diameter platinum plate electrodes, attached to a set of ruled calipers, were applied directly onto the epitrochlearis muscle and the skin overlaying the forelimb directly behind the epitrochlearis. Electroporation was performed by delivering eight electric pulses (170V/cm, 1Hz, 20ms in duration) with anode and cathode electrodes alternating between lateral and medial aspects of the forelimb after each set of two pulses (ECM 830 Square Wave Electroporator) as previously described (3, 9). The area around the surgical site was then closed with stitches. The contralateral muscle was used as the sham surgery control by replicating the same protocol of surgical exposure after which the surgical site was sutured. Twelve to fourteen days following IVE [as previously recommended Bertrand et al. (10)], the epitrochlearis muscles from anesthetized rats were harvested and prepared for muscle incubation and analysis. The muscle that had undergone IVE of the pCMV DsRed-Express2 vector was termed IVE/pDsRed, and the sham surgery muscle was termed the control muscle.

Epitrochlearis Muscle Isolation and Incubation

Animals were subjected to gene delivery via IVE 12-14 days prior to termination experiments in which the muscles were dissected out for analysis. The night prior to the termination experiment (muscle dissection and animal sacrifice), chow was removed from the cages of the rats at 1700 h. On the following day, between 1000 and 1300 h,

rats were anesthetized (intraperitoneal injection of sodium pentobarbital), and both epitrochlearis muscles were extracted. Isolated muscles underwent a series of incubation steps as previously described (8, 11). Briefly, isolated epitrochlearis muscles were incubated for 20 min in vials containing 2ml of Krebs Henseleit buffer (KHB) with 0.1% BSA (KHB-BSA), 2mM sodium pyruvate and 6mM mannitol with either 0 or 12nM insulin. Muscles were then transferred to a second vial for 60min incubation in 2ml of KHB-BSA, 1mM 2-DG (specific activity of 13.5mCi/mmol [^{3}H]-2-DG), and 9mM mannitol, along with the same insulin concentration as the preceding step. Muscles underwent 3x5min washes (with shaking at 100 revolutions per minute) in ice-cold KHB-BSA to clear the extracellular space of 2-DG (12). The final incubation step in Collagenase Media (Ca^{2+}-free KHB and 1.5% type II collagenase) for 60min (collagenase-treated muscles are hereafter referred to as fiber bundles) allowed for enzymatic digestion of the muscle connective tissue. Unless otherwise noted, vials were shaken (45 revolutions per minute), gassed (95% O_2/5% CO_2), and maintained at 35°C in a water bath.

Single Fiber Isolation and Processing

After the collagenase incubation, fiber bundles were placed in a petri dish containing Ca^{2+}-free KHB and single fibers were isolated as previously described (8). Briefly, single fibers were teased from the fiber bundle under a dissecting microscope using forceps. For the primary experiment (from which all glucose uptake data in Figure 5.4, protein abundance data in Figs.5.5-5.6, and the fiber volume data in Fig.5.3A were obtained), only fibers expressing the DsRed protein (visualized under a fluorescent

microscope) were isolated from the IVE/pDsRed muscle, while fibers were pulled at random from the control muscle. For a secondary experiment (from which only fiber volume data in Fig. 5.3B were obtained), fibers were isolated from and IVE/pDsRed muscle only; fibers expressing the DsRed protein (termed +DsRed) and those not (termed –DsRed) were also isolated. Following isolation of a fiber, it was imaged using a camera-enabled microscope with Leica Application Suite EZ software. Fiber width (mean value for width measured at 3 locations per fiber: near the fiber midpoint and approximately halfway between midpoint and each end of the fiber) and length of each fiber was used to estimate volume ($V = \pi \cdot r^2 \cdot l$; r = fiber radius as determined by half of the width measurement, l = fiber length). Each fiber was transferred by pipette with 10µl of solution to a micro-centrifuge tube containing 40µl of lysis buffer (T-PER, 1mM EDTA, 1mM EGTA, 2.5 mM sodium pyrophosphate, 1mM Na_3VO_4, 1 mM β-glycerophosphate, 1µg/ml leupeptin, and 1mM PMSF). Laemmli buffer (2X, 50µl) was added to each tube. Tubes were placed in a heat block (100°C) to lyse the fiber via brief boiling.

Single Fiber 2-DG Uptake, Myosin Heavy Chain (MHC) Isoform Characterization, and Immunoblotting

Aliquots of a lysed fiber were used for 2-DG uptake, MHC characterization, and protein abundance (immunoblotting) as previously described (8, 11). In brief, an aliquot of the lysed fiber was used to determine [^{3}H]-2-DG disintegrations per minute (dpm). The quantified 2-DG accumulation was normalized to calculated fiber volume (from width and length measurements) and expressed as nanomoles per microliter (nmol • μl^{-1}).

A separate aliquot of fiber lysate was used to determine MHC isoform expression via SDS-PAGE and Coomassie staining. Using the relative abundance of MHC expressed per fiber, a similar amount of MHC protein for each fiber aliquot was loaded onto 9% SDS-PAGE gels for subsequent immunoblotting and measurements of COXIV and GLUT4 content as previously described (8). Immunoblotting was followed by washing of the membranes which were then subjected to enhanced chemiluminescence (West Dura Extended Duration Substrate; #34075; Pierce) to visualize protein bands. Immunoreactive proteins were quantified by densitometry (AlphaEase FC; Alpha Innotech, San Leandro, CA). Values for protein abundance of single fibers were normalized to the average of all samples on each blot and expressed relative to the fiber's respective post-transfer MHC density determined in the gel (8, 11).

Statistical Analysis

Data are expressed as mean ±SEM. Two-way ANOVA was used to identify significant main effects (fiber type and DsRed status) and interactions between fiber type and DsRed status for glucose uptake, fiber size (estimated volume), and protein abundance (COXIV and GLUT4) in single fibers. Tukey's post hoc *t*-test was applied to determine the source of significant variance. A P-value of ≤ 0.05 was considered statistically significant.

Results

Fiber Volume of Single Fibers

Fibers were isolated from epitrochlearis muscles which underwent a sham surgery (no IVE; control) and contralateral epitrochlearis muscles that underwent IVE of a vector containing pDsRed (IVE/pDsRed). Figure 5.1 shows an isolated epitrochlearis muscle 14 days after IVE of pDsRed under brightfield and the Red fluorescent cube. From the IVE/pDsRed muscle, only fibers expressing the DsRed were isolated and used to compare versus control fibers from the contralateral muscle. The volume of each isolated single fiber was estimated using width and length measurements. Although, there was a significant main effect of IVE/pDsRed on fiber volume ($p<0.05$), post hoc analysis did not reveal the source of significance within any of the specific fiber types. However, fibers expressing the IIA isoform from the IVE/pDsRed muscle (0.015 ± 0.002 μl; n=14) tended ($P = 0.077$) to be larger than IIA fibers from the control muscle (0.011 ± 0.002 μl; n=12). A similar non-significant trend ($P = 0.148$) was observed in that IIX fibers from IVE/pDsRed muscles (0.017 ± 0.002 μl; n=24) which tended to be larger than IIX fibers from the control muscle (0.013 ± 0.002 μl; n=15). The tendency for differences in volume appeared to be attributable to a trend ($P=0.174$) for greater width in the IIA fibers expressing DsRed from the IVE/pDsRed muscle (0.046 ± 0.002 mm, n=14) compared to the IIA fibers from the control muscle (0.042 ± 0.002 mm, n=12; Fig. 5.3A). Fiber width values of IIX fibers from the IVE/pDsRed muscle (0.050 ± 0.002 mm, n=24) were significantly ($P=0.029$) larger than IIX fibers from the control muscle (0.043 ± 0.003 mm, n=25). The length of each fiber type was not significantly altered between groups.

It was unclear if IVE alone or IVE together with DsRed expression was important for the apparent effects on fiber size. Therefore, to determine whether there was a causal role of the DsRed protein in the observance of increased fiber size, a separate experiment

was performed isolating –DsRed and +DsRed from the same IVE/pDsRed muscles. Figure 5.2 shows a representative image of -DsRed and +DsRed fibers isolated from same IVE/pDsRed muscle. The results of comparisons between –DsRed and +DsRed fibers indicated that IIA and IIX fibers expressing DsRed tended to be non-significantly larger than those fibers not expressing DsRed from the same IVE muscle (Fig. 5.3B). In addition, consistent with earlier studies (11), there was a significant main effect of fiber type on fiber volume. As expected, post hoc analysis revealed that the volume of IIB fibers was significantly greater ($p < 0.05$) than the volume of IIA fibers (Fig. 5.3A and 5.3B) regardless of treatment group.

2-DG Uptake Single Fibers

Basal (no insulin) 2-DG uptake values by single fibers from control muscles versus IVE/pDsRed muscles were not significantly different regardless of fiber type (Fig. 5.4). There was also no significant effect of IVE/pDsRed for insulin-stimulated 2-DG uptake within any of the fiber types. However, in single fibers from insulin-stimulated muscles, there was a significant main effect of fiber type ($p < 0.001$) on 2-DG uptake. Post hoc analysis revealed that for insulin-stimulated muscles (both control and IVE/pDsRed), 2-DG uptake was greater for IIA fibers compared with all other fiber types (IIA > IIB, IIX, and IIB/X; $p < 0$ .001). In addition, 2-DG uptake was significantly greater ($p < 0.05$) for IIX versus IIB fibers as well as IIB/X versus IIB fibers from insulin-stimulated muscles.

GLUT4 Abundance in Single Fibers

In single fibers, there was not a significant main effect of IVE/pDsRed on GLUT4 abundance. However, as seen in Figure 5.5, there was a significant main effect of fiber type ($p < 0.001$) on GLUT4 abundance. Post hoc analysis revealed that GLUT4 content in IIA fibers was significantly greater ($p < 0.001$) than in IIB and IIB/X fibers (IIA > IIB, IIB/X) and that GLUT4 content in IIX fibers was significantly greater ($p < 0.05$) than in IIB fibers (IIX > IIB).

COXIV Abundance in Single Fibers

In single fibers, there was not a significant main effect of IVE/pDsRed on COXIV abundance. However, as seen in Figure 5.6, there was a significant main effect of fiber type ($p < 0.001$) on COXIV abundance. Post hoc analysis revealed that COXIV content in IIA fibers was significantly greater ($p < 0.001$) than in IIB, IIX, and IIB/X fibers (IIA > IIB, IIX IIB/X).

Discussion

Because it is a very thin muscle, the rat epitrochlearis muscle is well-suited for ex vivo incubation studies and it has been widely used to measure glucose uptake, protein synthesis, glycogen synthesis and other metabolic endpoints (13-20). In this context, it is significant that the current study was the first to report the use of in vivo electroporation (IVE) (3, 21, 22) on the rat epitrochlearis muscle. The overall aim was to combine the IVE approach of genetic manipulation of skeletal muscle, with a single fiber glucose uptake method that we recently developed (8, 11). This method allows for measurement of glucose uptake, MHC isoform expression, estimated fiber volume, and protein

abundance in an epitrochlearis muscle single fiber. While the IVE approach of ectopic gene delivery results in less than 100% expression (i.e., not every single fiber in the muscle is transfected and expresses the gene of interest), this inefficient expression provides the opportunity to apply the single fiber method to study both positively transfected fibers, as well as those not expressing the gene of interest. For this study, the DsRed gene (encodes red fluorescent protein) was utilized to allow for proof-of-principle experiments, as well as a simple system to recognize fibers that did, and did not, express the gene of interest using fluorescent microscopy.

This was the first study to investigate glucose uptake by muscle single fibers following IVE of a protein of interest. Glucose uptake by the skeletal muscle requires activation and completion of a complex signaling pathway and multi-step process of GLUT4 vesicle trafficking. For that reason, measurement of glucose uptake provides a useful and sensitive indicator of possible artifacts in cell function that might occur as a consequence of the study intervention (IVE of a vector for DsRed protein expression). There were no significant differences in the glucose uptake capacity (basal or insulin-stimulated) among fibers that were isolated from control muscles compared to those isolated from a muscle 14 days post-IVE, expressing the DsRed protein. These results indicate that the complex, multi-step process of muscle glucose uptake was not altered by IVE, or expression of the reporter DsRed gene. Thus, these results suggest that expression of the DsRed protein as a reporter alongside another gene of interest can be used to identify fibers positively transfected without concern that DsRed expression alters glucose uptake.

Consistent with the results of previous studies investigating glucose uptake by single fibers, insulin-stimulated glucose uptake by type IIA fibers was significantly greater than all other fiber types that were studied (8, 11). However, a noteworthy divergence from previous results was that both the IIX and IIB/X fiber types displayed significantly greater insulin-stimulated glucose uptake than the IIB fibers in 4-5 month old Wistar rats. Previously, the insulin-stimulated glucose uptake of IIB fibers was shown to be significantly lower than values of IIB/X (but not IIX) fibers from 2-3 month old Wistar (8). Taking together the previous results using Wistar rats and the current results that also used Wistar rats, it appears that the IIB vs. IIX difference in insulin-stimulated glucose uptake may emerge in Wistar rats between 2-3 vs. 4-5 months of age. In another study, insulin-stimulated glucose uptake of IIB fibers was lower than values from IIX (but not IIB/X) fibers from either 9-month or 25-month old Fisher Brown Norway rat (11). It is unclear if further age-associated effects and/or strain-related effects account for the apparent differences among fiber types in the 4-5 month old Wistar rats compared to the older Fischer Brown Norway rats in the previous study. The hybrid IIB/X fibers are believed to be undergoing a transition process from IIB to IIX or vice versa. However, it is unclear if the process of fiber type transition is related to the differences observed in insulin-stimulated glucose uptake by these hybrid fibers compared to fibers expressing only one MHC isoform.

GLUT4 and COXIV were selected for study because each protein has important metabolic functions, the expression of each protein is believed to differ in a fiber type-dependent manner, and previous studies had demonstrated that their expression levels could be modified with physiologically relevant interventions that influence muscle

contractile activity or metabolic status (e.g., exercise training, denervation, immobilization, etc.). We tested if IVE of a vector expressing DsRed protein would alter the abundance of these key proteins and found no difference in the abundance of either protein (GLUT4 or COXIV) in control fibers versus intervention (IVE/pDsRed) fibers. These results do not provide any evidence for the intervention inducing an artifact that altered the metabolic status of fibers. Evidence of fiber damage and protein abundance changes have been shown in other studies (23, 24), though evidence for damage was found very shortly after IVE (2-3 days). Our data do not address the possibility of an initial and transient response in the first few days following IVE, but we have shown that 14-days after IVE the abundance of two key metabolic proteins was not altered (10).

The results for COXIV and GLUT4 in the current study confirm and extend previous research that has evaluated the relationship between fiber type and expression of these important metabolic proteins. The results of the current study are consistent with our previous work that found COXIV abundance was greater in the more oxidative IIA fibers from the epitrochlearis of an aged animal model (9-month and 25-month old rats) (11). We also found that GLUT4 abundance was greatest in type IIA fibers. These results coincide with observations using whole muscles that are composed of primarily IIA fibers (flexor digitorum brevis, FDB) which were reported to have significantly greater GLUT4 than the epitrochlearis (primarily IIB) (25). Many studies have shown a strong correlation between GLUT4 abundance and glucose uptake capacity determined at the tissue level (25-27). Consistent with these earlier results in whole muscles, in the current study, the IIA fibers were characterized by the greatest values for both insulin-stimulated glucose uptake and GLUT4 abundance. However, evidence exists to suggest

that other factors (e.g., glucose phosphorylation or glycogen synthesis) may modulate glucose uptake rates. By characterizing the abundance of GLUT4 in single fibers, along with knowing the glucose uptake capacity of the fiber, a clearer understanding for the role that this glucose transporter may have as rate limiting step in glucose uptake can be achieved.

Although no differences were observed due to the intervention (IVE of pDsRed) between fiber types for glucose uptake or abundance of measured proteins (GLUT and COXIV), there was a significant main effect of the intervention on fiber volume. Post hoc analysis did not reveal statistical significance, but IIA and IIX fibers from IVE/pDsRed muscles tended to be larger than fibers of the same fiber types from control muscles. In addition, a separate experiment revealed that IIA and IIX fibers expressing DsRed tended to be larger than those not expressing DsRed isolated from only IVE/pDsRed muscles. Using fiber cross-sectional area determined by histological analysis, one study also reported a non-significant trend for size differences between fibers undergoing IVE and expressing an exogenous reporter gene (GFP) compared to control fibers from the same muscle, but that did not express the GFP (6). It is currently unclear what the mechanism is for increased fiber size, though one study proposed that the overexpression of an exogenous protein may result in a swelling of the fibers (6). However, it will be important to monitor fiber size in future studies of genetic manipulation to determine if this size change coincides with functional change.

Many studies have investigated anatomical and physiological parameters in muscle following IVE (23, 24, 28, 29). IVE of rodent muscle has limitations in its transfection efficiency which can complicate interpretation of results using whole

muscles, but combining IVE with the study of single fibers is an approach to take these problems into account. For example, when analyzing whole muscles transfected with a mutant protein, a ~50% reduction in glucose uptake capacity compared to control muscle may indicate that only ~50% of the fibers were transfected, and glucose was nearly completely blocked in each transfected fiber. Another possibility is that almost all fibers were transfected, but GU was only reduced ~50% in each transfected fiber. Thus application and investigation using the single fiber method strategy will turn this "complication" into a major advantage. Results of the current study provide evidence to suggest that glucose uptake and abundance of two key proteins measured in single fibers of specific fibers types were unaltered following IVE. These data are very encouraging for future studies that will combine the IVE approach for genetic manipulation and study of single fibers to test specific hypotheses.

Acknowledgements

This work was supported by the National Institutes of Health (AG-010026 to G.D.C.); and the American Heart Association (12PRE9270001 to J.G.M.)

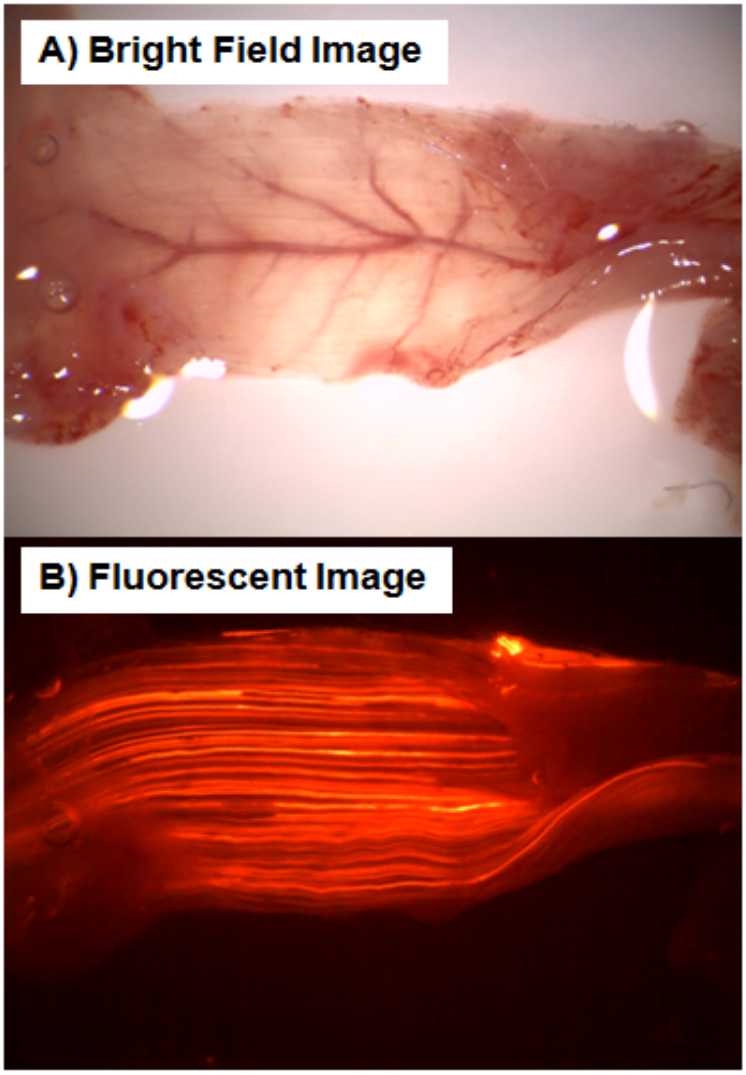

Figure 5.1 Representative Images of Epitrochlearis Muscle Isolated 14 Days after In Vivo Electroporation of the pDsRed Vector. **A.** Isolated muscle under microscope brightfield. **B.** Isolated muscle under microscope red fluorescent cube. Shows expression of DsRed protein in individual fibers.

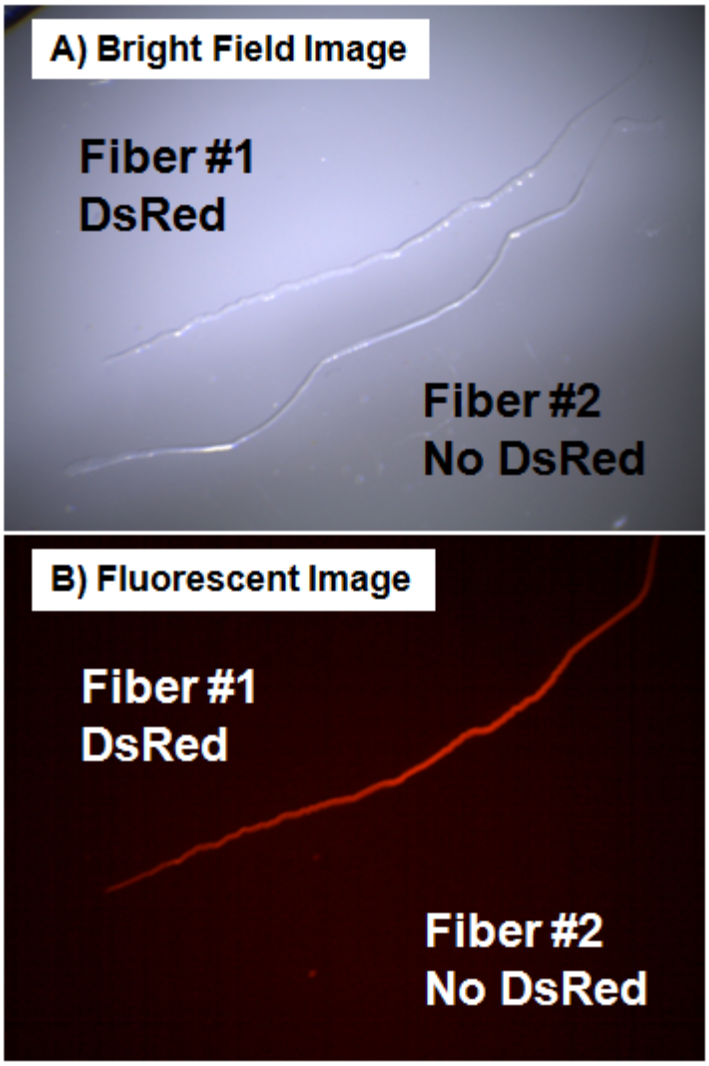

Figure 5.2 Representative Images of Single Fibers Isolated from an IVE/pDsRed Muscle 14 Days after In Vivo Electroporation of the pDsRed Vector. A. Isolated fibers (Fiber #1 & Fiber #2) under microscope bright field. **B**. Isolated fiber under microscope red fluorescent cube. Shows expression of DsRed protein in Fiber #1 (considered +DsRed) and not in Fiber #2 (considered –DsRed).

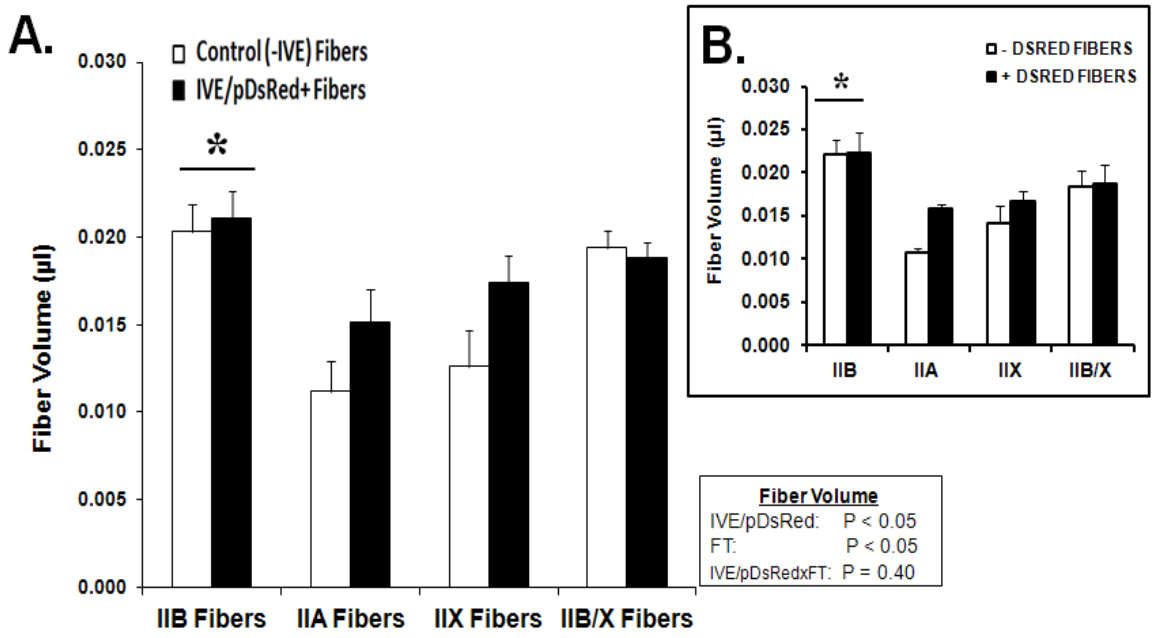

Figure 5.3 Size of Muscle Single Fibers that Express the DsRed Protein. A. Size (volume, µl) of single fibers expressing the same MHC isoform from control (no IVE; open bars) versus IVE/pDsRed+ (closed bars) epitrochlearis muscles. For fibers from control rat muscle, the number of fibers for each MHC isoform is in parentheses: IIB (48), IIA (12), IIX (15), IIB/X (55). For fibers from IVE/pDsRed+ rat muscle, the number of fibers for each MHC isoform is in parentheses: IIB (49), IIA (14), IIX (24), IIB/X (63). Data are means ± SEM and were analyzed by two-way ANOVA. IVE/pDsRed, main effect of in vivo electroporation and expression of pDsRed; FT, main effect of fiber type; IVE/pDsRedxFT, interaction between main effects. There was a main effect of IVE/pDsRed, though post-hoc analysis did not reveal the specific source of significance. There was a main effect of fiber type ($p<0.05$). Post hoc analysis revealed the IIB MHC isoform to be significantly different from IIA isoform (*$p<0.05$ for IIB vs. IIA) **B.** Size (volume, µl) of single muscle fibers expressing the same MHC isoform that expressed the DsRed protein (+DsRed; closed bars), or did not express DsRed (-DsRed; open bars), with both +DsRed and –DsRed isolated from the same muscles that underwent IVE of the pDsRed vector (IVE/pDsRed). The number of fibers that did not express DsRed (-DsRed) for each MHC isoform is in parentheses: IIB (18), IIA (3), IIX (7), IIB/X (12). The number of fibers that did express DsRed (+DsRed) for each MHC isoform is in parentheses: IIB (14), IIA (4), IIX (9), IIB/X (13). Data are means ± SEM and were analyzed by two-way ANOVA. There was not a main effect of the presence of DsRed protein. There was a main effect of fiber type ($p<0.05$). Post hoc analysis revealed the IIB MHC isoform to be significantly different from IIA isoform (*$p<0.05$ for IIB vs. IIA).

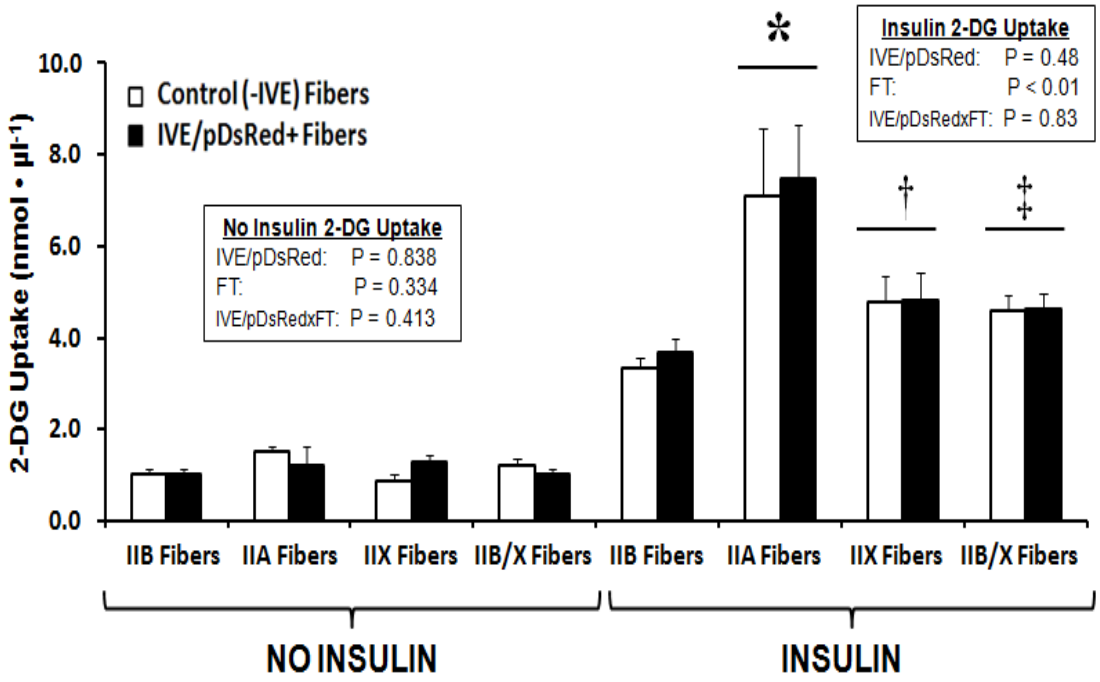

Figure 5.4 Glucose Uptake by Single Fibers that Express the DsRed Protein. Mean 2-DG uptake by single fibers expressing the same MHC isoform from control (no IVE; open bars) vs. IVE/pDsRed+ (closed bars) epitrochlearis muscles. For basal fibers, from the control rat muscle, the number of fibers for each MHC isoform is in parentheses: IIB (24), IIA (8), IIX (5), IIB/X (23). For basal fibers, from the IVE/pDsRed+ rat muscle, the number of fibers for each MHC isoform is in parentheses: IIB (23), IIA (7), IIX (14), IIB/X (26). For insulin-stimulated fibers, from the control rat muscle the number of fibers for each MHC isoform is in parentheses: IIB (24), IIA (4), IIX (10), IIB/X (32). For insulin-stimulated fibers, from the IVE/pDsRed+ rat muscle, the number of fibers for each MHC isoform is in parentheses: IIB (26), IIA (7), IIX (10), IIB/X (37). Data are means ± SEM and were analyzed by two-way ANOVA within each insulin level. IVE/pDsRed, main effect of in vivo electroporation and expression of pDsRed; FT, main effect of fiber type; IVE/pDsRedxFT, interaction between main effects. For fibers with insulin, there was a main effect of fiber type ($p<0.001$). Post hoc analysis revealed MHC isoforms that were significantly different from each other; *$p<0.001$ for IIA vs. IIB, IIX, and IIB/X; †$p<0.05$ for IIX vs. IIB; and ‡$p<0.005$ for IIB/X vs. IIB.

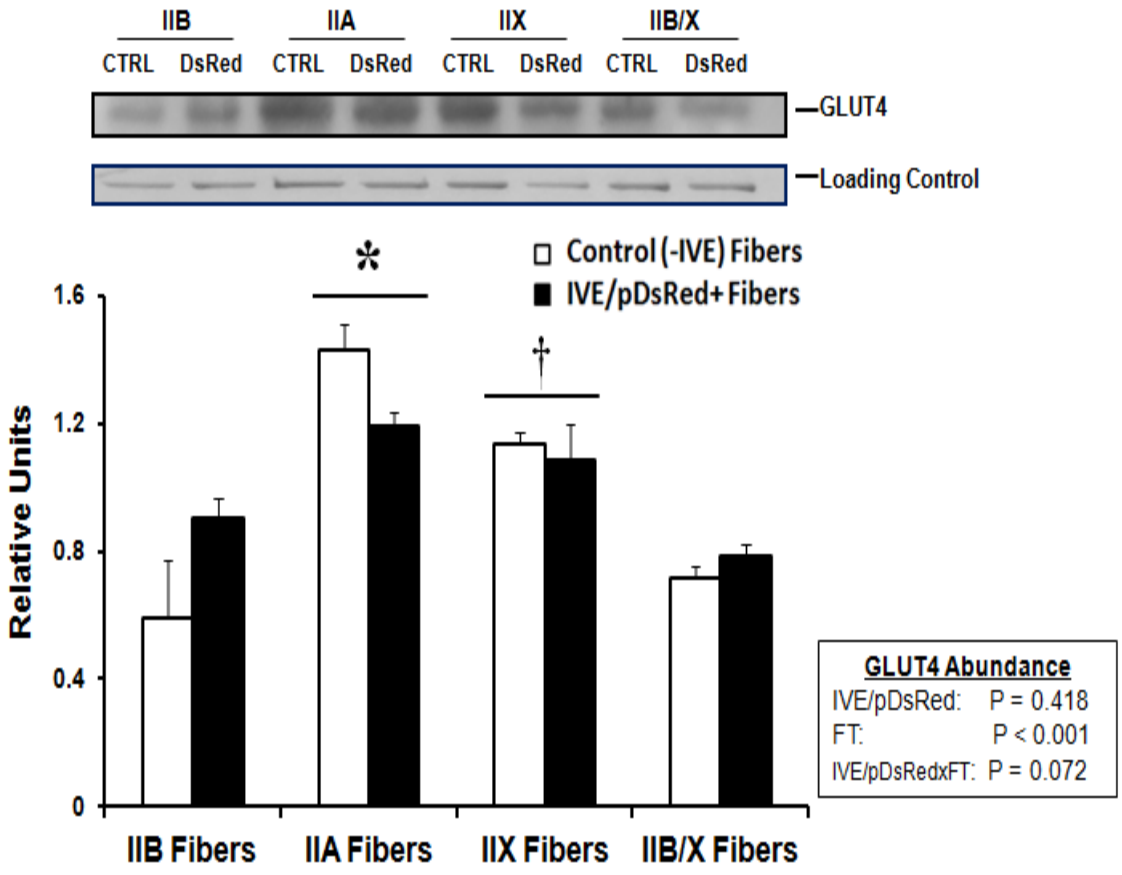

Figure 5.5 GLUT4 Protein Abundance in Single Fibers. From control (no IVE; open bars) vs. IVE/pDsRed+ (closed bars) epitrochlearis muscles. Data are means ± SEM (n = 4 fibers of each MHC isoform per group) and were analyzed by two-way ANOVA. IVE/pDsRed, main effect of in vivo electroporation and expression of pDsRed; FT, main effect of fiber type; IVE/pDsRedxFT, interaction between main effects. Representative blots of protein abundance and corresponding Coomassie Brilliant Blue-stained gels of post transfer MHC (loading control) are provided. The density value for each protein was normalized to the density value for the loading control (Coomassie stained gels of post-transfer MHC, loading control, are provided). There was a significant main effect fiber type (FT; $p<0.001$). Post hoc analysis revealed MHC isoforms that were significantly different from each other; *$p<0.001$ for IIA vs. IIB and IIB/X; and †$p<0.001$ for IIX vs. IIB.

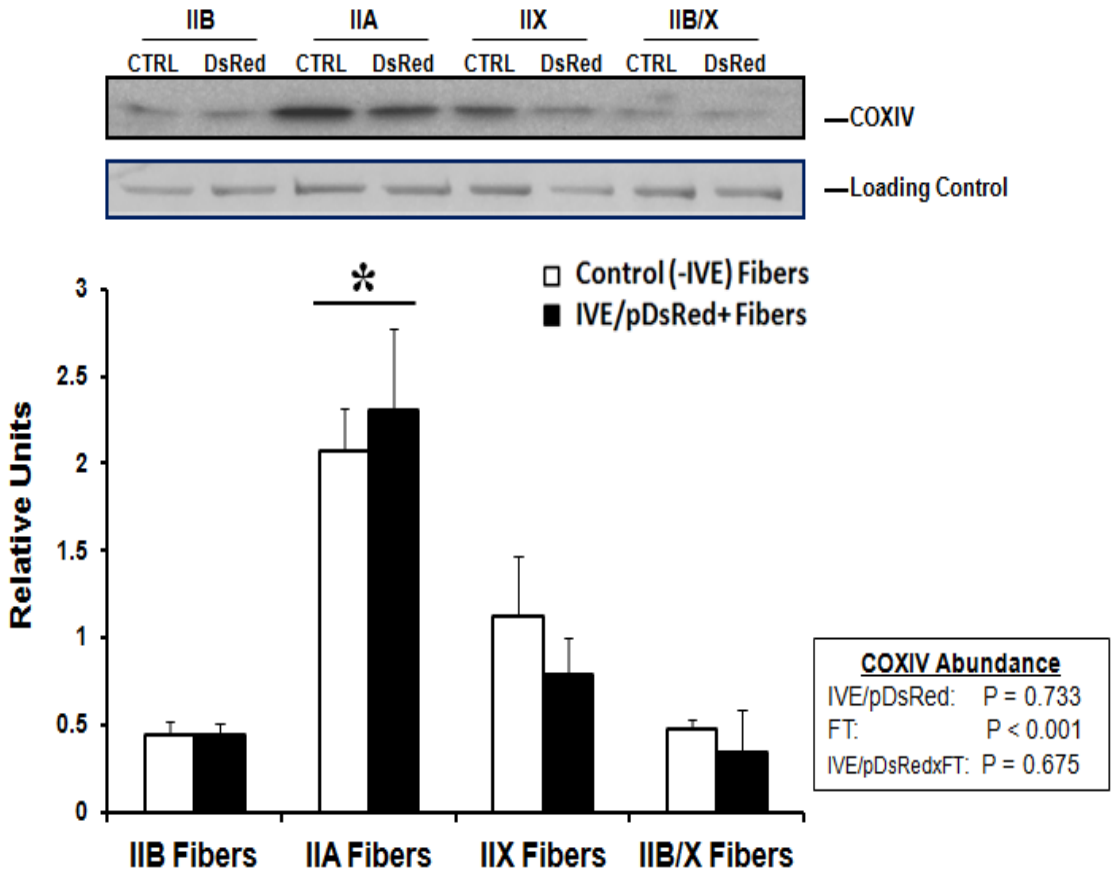

Figure 5.6. COXIV Protein Abundance in Single Fibers. From control (no IVE; open bars) vs. IVE/pDsRed+ (closed bars) epitrochlearis muscles. Data are means ± SEM (n = 4 fibers of each MHC isoform per age group) and were analyzed by two-way ANOVA. IVE/pDsRed, main effect of in vivo electroporation and expression of pDsRed; FT, main effect of fiber type; IVE/pDsRedxFT, interaction between main effects. Representative blots of protein abundance and corresponding Coomassie Brilliant Blue-stained gels of post transfer MHC (loading control) are provided. The density value for each protein was normalized to the density value for the loading control Coomassie stained gels of post-transfer MHC, loading control, are provided). There was a significant main effect fiber type (FT; $p<0.001$). Post hoc analysis revealed MHC isoforms that were significantly different from each other; *$p<0.001$ for IIA vs. IIB, IIX, and IIB/X.

References

1. Aihara H, Miyazaki J. Gene transfer into muscle by electroporation in vivo. Nat Biotechnol. 1998;16(9):867-70.
2. Mir LM, Bureau MF, Gehl J, Rangara R, Rouy D, Caillaud JM, et al. High-efficiency gene transfer into skeletal muscle mediated by electric pulses. Proceedings of the National Academy of Sciences of the United States of America. 1999;96(8):4262-7.
3. Clarke DC, Miskovic D, Han XX, Calles-Escandon J, Glatz JF, Luiken JJ, et al. Overexpression of membrane-associated fatty acid binding protein (FABPpm) in vivo increases fatty acid sarcolemmal transport and metabolism. Physiol Genomics. 2004;17(1):31-7.
4. Fujii N, Boppart MD, Dufresne SD, Crowley PF, Jozsi AC, Sakamoto K, et al. Overexpression or ablation of JNK in skeletal muscle has no effect on glycogen synthase activity. Am J Physiol Cell Physiol. 2004;287(1):C200-8.
5. Holloway GP, Lally J, Nickerson JG, Alkhateeb H, Snook LA, Heigenhauser GJ, et al. Fatty acid binding protein facilitates sarcolemmal fatty acid transport but not mitochondrial oxidation in rat and human skeletal muscle. J Physiol. 2007;582(Pt 1):393-405. PMCID: 2075306.
6. Shi H, Scheffler JM, Zeng C, Pleitner JM, Hannon KM, Grant AL, et al. Mitogen-activated protein kinase signaling is necessary for the maintenance of skeletal muscle mass. Am J Physiol Cell Physiol. 2009;296(5):C1040-8.
7. Bruce CR, Brolin C, Turner N, Cleasby ME, van der Leij FR, Cooney GJ, et al. Overexpression of carnitine palmitoyltransferase I in skeletal muscle in vivo increases fatty acid oxidation and reduces triacylglycerol esterification. Am J Physiol Endocrinol Metab. 2007;292(4):E1231-7.
8. Mackrell JG, Cartee GD. A novel method to measure glucose uptake and myosin heavy chain isoform expression of single fibers from rat skeletal muscle. Diabetes. 2012;61(5):995-1003. PMCID: 3331778.
9. Benton CR, Yoshida Y, Lally J, Han XX, Hatta H, Bonen A. PGC-1alpha increases skeletal muscle lactate uptake by increasing the expression of MCT1 but not MCT2 or MCT4. Physiol Genomics. 2008;35(1):45-54.
10. Bertrand A, Ngo-Muller V, Hentzen D, Concordet JP, Daegelen D, Tuil D. Muscle electrotransfer as a tool for studying muscle fiber-specific and nerve-dependent activity of promoters. Am J Physiol Cell Physiol. 2003;285(5):C1071-81.
11. Mackrell JG, Arias EB, Cartee GD. Fiber Type-Specific Differences in Glucose Uptake by Single Fibers From Skeletal Muscles of 9- and 25-Month-Old Rats. J Gerontol A Biol Sci Med Sci. 2012.
12. Wang C. Insulin-stimulated glucose uptake in rat diaphragm during postnatal development: lack of correlation with the number of insulin receptors and of intracellular glucose transporters. Proceedings of the National Academy of Sciences of the United States of America. 1985;82(11):3621-5.
13. Young DA, Uhl JJ, Cartee GD, Holloszy JO. Activation of glucose transport in muscle by prolonged exposure to insulin. Effects of glucose and insulin concentrations. J Biol Chem. 1986;261(34):16049-53.

14. Cartee GD, Young DA, Sleeper MD, Zierath J, Wallberg-Henriksson H, Holloszy JO. Prolonged increase in insulin-stimulated glucose transport in muscle after exercise. The American journal of physiology. 1989;256(4 Pt 1):E494-9.
15. Arias EB, Kim J, Funai K, Cartee GD. Prior Exercise Increases Phosphorylation of Akt Substrate of 160 kDa (AS160) in Rat Skeletal Muscle 10.1152/ajpendo.00602.2006. Am J Physiol Endocrinol Metab. 2006:00602.2006.
16. Ren JM, Semenkovich CF, Gulve EA, Gao J, Holloszy JO. Exercise induces rapid increases in GLUT4 expression, glucose transport capacity, and insulin-stimulated glycogen storage in muscle. J Biol Chem. 1994;269(20):14396-401.
17. Stirewalt WS, Low RB. Effects of insulin in vitro on protein turnover in rat epitrochlearis muscle. The Biochemical journal. 1983;210(2):323-30. PMCID: 1154227.
18. Clark AS, Mitch WE. Comparison of protein synthesis and degradation in incubated and perfused muscle. The Biochemical journal. 1983;212(3):649-53. PMCID: 1153139.
19. Stirewalt WS, Low RB, Slaiby JM. Insulin sensitivity and responsiveness of epitrochlearis and soleus muscles from fed and starved rats. Recognition of differential changes in insulin sensitivities of protein synthesis and glucose incorporation into glycogen. The Biochemical journal. 1985;227(2):355-62. PMCID: 1144853.
20. Davis TA, Klahr S, Tegtmeyer ED, Osborne DF, Howard TL, Karl IE. Glucose metabolism in epitrochlearis muscle of acutely exercised and trained rats. The American journal of physiology. 1986;250(2 Pt 1):E137-43.
21. Miyazaki J, Aihara H. Gene transfer into muscle by electroporation in vivo. Methods Mol Med. 2002;69:49-62.
22. Kramer HF, Taylor EB, Witczak CA, Fujii N, Hirshman MF, Goodyear LJ. Calmodulin-Binding Domain of AS160 Regulates Contraction- but Not Insulin-Stimulated Glucose Uptake in Skeletal Muscle 10.2337/db07-0681. Diabetes. 2007;56(12):2854-62.
23. Schertzer JD, Plant DR, Lynch GS. Optimizing plasmid-based gene transfer for investigating skeletal muscle structure and function. Mol Ther. 2006;13(4):795-803.
24. Roche JA, Ford-Speelman DL, Ru LW, Densmore AL, Roche R, Reed PW, et al. Physiological and histological changes in skeletal muscle following in vivo gene transfer by electroporation. Am J Physiol Cell Physiol. 2011;301(5):C1239-50. PMCID: 3213910.
25. Henriksen EJ, Bourey RE, Rodnick KJ, Koranyi L, Permutt MA, Holloszy JO. Glucose transporter protein content and glucose transport capacity in rat skeletal muscles. The American journal of physiology. 1990;259(4 Pt 1):E593-8.
26. Slentz CA, Gulve EA, Rodnick KJ, Henriksen EJ, Youn JH, Holloszy JO. Glucose transporters and maximal transport are increased in endurance-trained rat soleus. J Appl Physiol. 1992;73(2):486-92.
27. Kern M, Wells JA, Stephens JM, Elton CW, Friedman JE, Tapscott EB, et al. Insulin responsiveness in skeletal muscle is determined by glucose transporter (Glut4) protein level. The Biochemical journal. 1990;270(2):397-400.
28. Durieux AC, Bonnefoy R, Busso T, Freyssenet D. In vivo gene electrotransfer into skeletal muscle: effects of plasmid DNA on the occurrence and extent of muscle damage. The journal of gene medicine. 2004;6(7):809-16.

29. Cleasby ME, Davey JR, Reinten TA, Graham MW, James DE, Kraegen EW, et al. Acute bidirectional manipulation of muscle glucose uptake by in vivo electrotransfer of constructs targeting glucose transporter genes. Diabetes. 2005;54(9):2702-11.

CHAPTER VI

DISCUSSION

Focus of this Discussion

This chapter of the dissertation will: 1) provide an integrated interpretation of the results from all studies including a brief description of how findings in this dissertation advance the understanding of the relationship between fiber type (IIA, IIB, IIX, IIB/X) and the regulation of epitrochlearis muscle glucose uptake (including in models of insulin resistance and aging), 2) identify additional opportunities extending the study of single fibers, 3) propose future directions with a brief research plan for an experiment, and 4) provide summary and conclusions.

Insights from Integrating the Results of Dissertation Studies

Glucose Uptake by Single Fibers

Insulin-stimulated glucose uptake was analyzed for all studies and in each animal model. The MHC IIA isoform (type IIA fibers) consistently exhibited significantly greater insulin-stimulated glucose uptake compared to all other fiber types (IIB, IIX and IIB/X). Previously, there was uncertainty about the role that fiber type plays in muscle glucose uptake (i.e., are differences observed between muscles of primarily one fiber type

intrinsic to that muscle, or intrinsic to the fiber type itself?). For example, Henriksen et al. showed the flexor digitorum brevis had a greater capacity for insulin-stimulated glucose uptake than the epitrochlearis (1). Other groups that have supported these findings of muscle differences in glucose uptake capacity have commonly attributed the muscle fiber type makeup as a primary reason for the variation, (i.e., an intrinsic feature of the fiber type itself). However, without the ability to measure glucose uptake by a muscle single fiber of known fiber type, the possibility remained that glucose uptake differences among different muscles may be a result of a mechanism other than fiber type, and intrinsic to the muscles themselves. The results of this study provided evidence for fiber type differences with regards to both insulin-stimulated and AICAR-stimulated glucose uptake. Of course there is the potential that IIA fibers from the epitrochlearis muscle are not representative of IIA fibers from other muscles (e.g., the EDL or FDB). While this possibility cannot be ruled out until IIA fibers from other muscles are analyzed, combining results illustrating insulin-stimulated glucose uptake by whole muscles (FDB>epitrochlearis) with single fiber analysis (IIA>IIB) supports the conclusion that IIA fibers are more responsive to insulin. Further studies will need to be performed to better understand the mechanism for the increased responsiveness. However, results from Study 3 within this dissertation, provide evidence that the increased ability for IIA fibers to take up glucose in response to insulin may be, in part, due to greater GLUT4 abundance in IIA fibers. Although GLUT4 abundance is unlikely to be the only determinant of capacity for insulin-stimulated glucose uptake because a complex series of process are required for GLUT4 to translocate to the cell surface, the fact that IIA fibers had greater GLUT4 abundance than all other fiber types supports the

notion that a greater capacity to take up glucose under insulin-stimulated conditions is dependent on GLUT4 abundance.

However, in contrast to the apparent direct relationship between fiber type-specific values for GLUT4 abundance and insulin-stimulated glucose uptake capacity, AICAR-stimulated glucose uptake was significantly greater for IIB vs. IIA fibers in spite of lower GLUT4 levels in IIB fibers. AICAR simulation of glucose uptake occurs through an insulin-independent mechanism. Contraction-stimulated and exercise-stimulated glucose uptake are widely believed to occur through a pathway involving AMPK signaling. Whole muscle analysis indicates that AICAR-dependent glucose uptake is greater in the EDL (enriched with IIB fibers) than the FDB (enriched with IIA fibers), and this relationship is the inverse of that observed for these muscles with insulin stimulation. Previous studies have established that both insulin- and AICAR-stimulated glucose uptake are mediated by the GLUT4 transporter (2-11), so fiber type differences for AICAR-stimulated vs. insulin-stimulated glucose uptake may be explained by fiber type differences in the abundance or activation of other proteins that regulate GLUT4 translocation. There is evidence that the AMPK-α2 isoform plays an important role in the insulin-independent mechanism of glucose uptake, with AMPK-α2 knockout mice not responding to AICAR-stimulation (12). In addition, AMPK-α2 activation was shown to be increased in skeletal muscle following acute exercise (13), as well as muscle from chronically trained mice (14). In this context, one could infer that greater AMPK-α2 abundance or activation in the muscle may be important for greater insulin-independent stimulated glucose uptake capacity (knowing that exercise induces glucose uptake). Thus, perhaps the IIB fibers express greater levels of AMPK-α2 isoform than IIA fibers,

making them more sensitive to AICAR stimulation. Recently, Dr. Robyn Murphy's group classified single fibers biochemically while investigating the abundance of AMPK isoforms to better understand insulin-independent mechanisms (15). The ability to measure both glucose uptake and the abundance of key proteins in the single fibers of known fiber type offers the opportunity to test the idea that fiber type differences in AMPK isoform expression may play a role in the fiber type differences in AICAR-stimulated glucose uptake.

Although for the most part there was consistency between strains and ages of rats for fiber type effects on insulin-stimulated glucose uptake, the IIB/X fiber type was a notable exception. Glucose uptake by these hybrid fibers, which are thought to be undergoing a state of transition from IIB to IIX or vice versa, can be studied only by using the novel single fiber method. Whole muscle analysis does not allow for study of this fiber type's glucose uptake capacity, and histochemical analysis has provided little in the way of characterizing the IIB/X fiber. There is evidence to suggest these fibers are relatively abundant in skeletal muscle (16, 17), providing a rationale for future attention being placed on this fiber type. Thus, the results from Studies 1-3 are unique and provide valuable data in the small, yet growing field studying hybrid fibers. In Study 1, the IIB/X fibers exhibited significantly greater glucose uptake than the IIB fibers from the 2-3 month old Wistar as well as 2-3 month old LZ rat. In this initial study, we hypothesized that perhaps these fibers undergoing transition had greater energy requirements, and thus were more responsive to insulin, taking up more glucose (i.e., energy) than the IIB fibers. However, in Study 2 investigating single fibers from the 9 month-old and 25 month-old rats, the IIX fibers had significantly greater glucose uptake

than the IIB fibers, essentially switching rank order with the IIB/X fibers which were not significantly greater than the IIB fibers. Similarly, in Study 3, investigating single fibers from the 4-5 month old rats, the IIB/X and IIX fibers both displayed significantly greater glucose uptake than the IIB fibers. Thus, in Wistar 2-3 and 4-5 month old rats and 2-3 month old Lean Zucker rats, insulin-stimulated glucose uptake in IIB/X > IIB, however in the 9- and 25-month old FBN rats IIB/X ≈ IIB, while IIX > IIB. These results suggest two possible explanations for the IIB/X variability: 1) strain differences, and/or 2) age differences. Further research will be required to test which of these possibilities may explain the different results for hybrid fibers.

Single Fiber Volume

The studies in this dissertation were the first to investigate single fiber volume by measuring the length and width of each fiber. Previously, studies had estimated fiber volume via cross-sectional area (CSA) measurements through histology. The method provided within this dissertation allows for a more accurate description of the single fiber volume as the length of each fiber and several width measurements (three per fiber were averaged for final volume calculation) can be evaluated. When comparing the fiber volume for fibers isolated from all strains and ages studied throughout the dissertation, the results reveal that IIB fibers were significantly greater than IIA fibers. These results are consistent with those studies indicating the CSA of IIB fibers being larger than IIA fibers (18) (19, 20). Though no previous studies had investigated single fiber CSA in the epitrochlearis muscle, this dissertation provided novel analysis of single fibers from this muscle while also providing a new method to analyze fiber size (i.e., fiber volume).

The ability to measure fiber size becomes important in conditions of altered muscle mass (e.g., muscle atrophy or hypertrophy). Study 2 investigated possible sarcopenia in 25 month-old versus 9 month-old rat epitrochlearis single fibers. With 13% of the American population over the age of 65, the detrimental effects of aging are an important area of study. There has been a wealth of research investigating the effects of aging in rodents, large mammals, and humans. In general, aging has a profound role on skeletal muscle. Functionally, the force-generating capacity is known to decline (21, 22) and has been attributed to a muscle atrophy (22, 23) rather than defects in muscle activation (24) . This muscle atrophy, or reduction in muscle mass known as sarcopenia, is indicative of a decline in the fiber size and/or number, noting that muscle fat and connective tissue increase with age. Age-related patterns in fiber changes (size and/or number) are seemingly dependent on the species, muscle, and method utilized (25). For example, when comparing 19 to 73 year old human vastus lateralis muscle, there was a 41% loss in fiber number and a 26% decrease in muscle cross-sectional area (CSA) (23). However, research with rats has shown an age-related decrease in muscle mass [~15% in soleus and EDL (26, 27)] can occur with little to no decline in fiber numbers. There is evidence to suggest that the age-related CSA differences may occur on a fiber-type basis. In both rats and humans, a preferential reduction in type II fibers has been reported with little or no decline in type I fiber CSA (23, 28-30). However, it is interesting that some muscles in rats, including the epitrochlearis exhibit little atrophy with age up to 25 months old (31, 32). It was possible that the epitrochlearis muscle remained protected from the aging effects on muscle size. However, the epitrochlearis muscle size has only been assessed

via its weight, thus any changes in actual fiber size were unknown. Since fiber or muscle CSA of the epitrochlearis had not been investigated, it was possible that certain fiber types do exhibit atrophy, though not to an extent large enough to change the overall mass of the muscle. In addition, measurement of total muscle mass does not account for changes in connective tissue or lipid components of the tissue. Thus it was important to examine actual fiber size, rather than simply whole muscle weight, of the aged epitrochlearis muscle to determine possible localized, or fiber specific, sarcopenia. Although no differences were observed between the 9 month-old and 25 month-old rats, the ability to measure fiber size in other conditions of atrophy may prove to be valuable in the future.

When calculating glucose uptake by single fibers, fiber volume was used for normalization. Typically weight or protein content is used for normalization in whole muscle or cell analysis. Since the IIA fibers are the smallest of the type II fiber types, the argument could be made that normalizing to the smaller volume will mathematically create a larger glucose uptake value for the IIA fibers compared to the IIB fibers. To address this, we matched IIA and IIB fibers for similar volumes (represented in Figure 6.2) and correlated 2-DG uptake versus fiber volume. It is clear that even the smaller IIB fibers have lower insulin-stimulated glucose uptake capacity than IIA fibers. Thus the IIA fibers have greater insulin-stimulated glucose uptake that is not simply related to differences in fiber volume.

Protein Abundance in Single Fibers

The abundance of several key proteins was measured within single fibers including, COXIV (aging models and Wistar), APPL1 (LZ, OZ, aging), IkB-β (LZ, OZ, aging), and GLUT4 (Wistar). The ability to measure protein abundance in combination with fiber type and glucose uptake capacity provides for a richer phenotyping opportunity. Previous studies have measured GLUT4 in whole muscles, but the current studies display the capability to measure the abundance of this critical protein in a muscle single fiber. Because GLUT4 is the distal and functional molecule in the insulin-stimulated glucose transport pathway, measuring single fiber GLUT4 allows for a more mechanistic view of the glucose uptake by single fibers. Similarly, COXIV abundance in single fibers can be used as a mitochondrial marker at the single fiber level allowing for ability to characterize fiber type more clearly. Furthermore, although the ability to measure signaling directly in single fibers has not been developed, the measurement of indirect signaling events, such as the expression and degradation of IkB-beta is valuable. Overactivation of the NFκB pathway is indicated by lower levels of IκB-β (phosphorylation of the protein leads to degradation of the protein). Study 3 was the first to show this indirect signaling pathway event can be measured in single fibers for future phenotyping and mechanistic evaluation.

Additional Opportunities for Extending the Study of Single Fibers

The studies in this dissertation have provided novel information on single mammalian muscle fiber glucose uptake capacity, MHC isoform expression, fiber size, and abundance of key proteins. Looking forward, several opportunities present themselves for extending the study of single fibers.

Investigating Signaling Events in Single Fibers

In order to study signaling events (e.g., protein phosphorylation) in the isolated epitrochlearis fibers, culturing the fibers following isolation would be necessary for several reasons. It would likely not be informative to simply measure the signaling event in a single fiber immediately after collagenase digestion because: 1) removing the extracellular matrix will likely trigger intracellular signaling events that may affect glucose uptake; and 2) after fibers are isolated, they are more susceptible to subsequent damage. Our unpublished results indicate the collagenase digestion, along with teasing of the fibers, lends to increased phosphorylation status of Akt. It is important to note that primary endpoint measurements in this dissertation (i.e., glucose uptake and protein abundance) are not altered by the signaling events that occur during collagenase digestion and fiber isolation as evidenced by comparisons between paired whole muscles from the same rat that either did or did not undergo collagenase treatment. Culturing epitrochlearis single fibers would be a potential approach to allow for the fibers to return to a basal state following collagenase and isolation. Likewise, the use of cultured single fibers would then allow for subsequent stimulation (insulin, AICAR, etc.), and the study of the signaling pathway within each fiber. Culturing of single mammalian muscle fibers has been accomplished using the smaller, more myogenic cell like flexor digitorum brevis (FDB) muscle fibers (33-35). The studies utilizing cultured FDB fibers have investigated morphological properties, satellite cell migration, and calcium handling among other features, but no signaling events have been reported. However, these FDB culture models begin to mimic cell cultures as the FDB fibers revert to a myogenic cell

like state. Thus creating a short term culture system of epitrochlearis fibers for the study of adult skeletal muscle function may prove useful to investigate signaling events. In addition, exposure to various stimulants or therapeutic agents could provide meaningful results regarding their effects on the signaling pathways within specific muscle fiber types.

Investigating Type I Fibers

The experiments in this dissertation provided results to better characterize muscle single fibers that expressed the IIB, IIA, IIX, or IIB/X (hybrid) MHC isoforms. However, one caveat observed through all facets of this dissertation was the absence of type I fibers that were isolated by these procedures. Several modifications of the method were attempted with the goal of isolating type I fibers from the epitrochlearis muscle. Initial attempts to isolate type I fibers from the epitrochlearis involved altering the percentage of type II collagenase, providing for greater connective tissue digestion. The described incubation protocol relied on 1.5% type II collagenase used; this percentage was increased significantly in an attempt to allow type I fiber dissociation, which ultimately proved unsuccessful. Since the type I fibers within the epitrochlearis (accounting for ~9% of the MHC) are reported to be located predominantly in the central portions of the muscle (36), a greater focus was placed on isolating from that area during experiments in which the goal was to isolate type I fibers. After multiple unsuccessful attempts using the epitrochlearis muscle, which has relatively low percentage of type I fibers, a muscle of primarily type I fibers (the soleus) was used. However, repeated attempts to isolate single fibers from the soleus were unsuccessful. There is evidence that

muscles of primarily type I fibers contain greater amounts of collagen (37), and thus could imply type I fibers are surrounded by more collagen. This would make these fibers less than ideal to isolate due to the amount of enzymatic activity by collagenase required to allow for adequate dissociation, while also assuring that the integrity of the muscle fiber remains intact and nonpermeabilized. Thus, as a future direction, utilizing different collagenases (type I/crude, type 3, or type 4) and/or dissociation agents (trypsin and elastase) could be investigated to ultimately allow for isolation of type I fibers.

Proposal for Future Research

The results of Studies 1-3 in this dissertation have raised important questions and also have opened the door for future experiments. By combining the single fiber analysis in the Zucker rat models (Obese and Lean; Study 1), along with genetic manipulation of the rat skeletal muscle (Study 3), the results of this dissertation were used to develop a brief proposal for future research described below.

A. SPECIFIC AIMS

The long-range goal is to elucidate mechanisms underlying skeletal muscle insulin resistance, a central component of the metabolic syndrome. Insulin resistance in humans with type 2 diabetes (T2D) is not because of reduced skeletal muscle GLUT4 protein levels; rather it is secondary to a reduced ability of insulin to induce GLUT4's redistribution to the cell surface. Therefore, it is valuable to identify processes that regulate GLUT4 traffic and which are impaired in insulin resistant humans. Akt substrate of 160 kDa (AS160) phosphorylation is the most distal insulin signaling step that is

known to regulate GLUT4 trafficking, and phosphorylation of AS160 is reduced in muscle of humans with T2D (38). The overall hypothesis is that reduced AS160 phosphorylation (which regulates the GAP domain) is a major mechanism for muscle insulin resistance in obese rats, and that we can correct some or all of the insulin resistance by genetically modifying AS160's GAP domain

Aim 1: Determine if key Akt-phosphomotifs (Thr^{318}, Ser^{588}, Thr^{642}, Ser^{751}) of AS160 are essential for AS160's regulation of glucose uptake in rat skeletal muscle and muscle single fibers from Lean or Obese Zucker rats.

Hypothesis 1*: Mutation of 4 key Akt-phosphomotifs within AS160 (with Ala substitution for Thr^{318}, Ser^{588}, Thr^{642}, Ser^{751}; 4P mutant) will cause reduced insulin-stimulated glucose uptake by whole skeletal muscle and muscle single fibers of each fiber type from Lean and Obese Zucker rats, with a relatively greater reduction in insulin-stimulated glucose uptake found in Lean vs. Obese rats.*

Aim 2: Determine if eliminating the functional GTPase activating protein (GAP) domain within AS160 will alter insulin-stimulated glucose uptake in rat skeletal muscle and muscle single fibers from Obese or Lean Zucker rats.

Hypothesis 2: *Mutation of the key arginine within AS160 (Arg^{973}; R/K mutant), rendering the GAP domain non-functional, will elevate the insulin-stimulated glucose uptake in skeletal muscle and muscle single fibers of each fiber type from Obese, but not Lean Zucker rats compared to controls lacking the R/K mutant.*

Aim 3: Determine if eliminating the functional GTPase activating protein (GAP) domain simultaneously with mutation of the Akt-phosphomotifs within AS160 will prevent the effect of the 4P mutation alone on glucose uptake in rat skeletal muscle and muscle single fibers from Lean or Obese Zucker rats.

Hypothesis 3: *The decrement in insulin-stimulated glucose uptake by skeletal muscle and muscle single fibers of each fiber type from Obese and Lean Zucker rats induced by the mutation of 4 key Akt-phosphomotifs within AS160 will be eliminated by the simultaneous mutation of both* Arg^{973} *and the 4 key Akt-phosphomotifs of AS160 (4P-R/K double mutant).*

B. BACKGROUND

This study will couple the novel method to measure glucose uptake in single fibers with mutations of AS160, a key insulin signaling protein. Insulin-mediated glucose uptake relies on cooperation between 2 functional elements of AS160 (Akt phosphomotifs and a GTPase activating protein, GAP, domain). Gus Lienhard's group made a breakthrough discovery when they convincingly demonstrated that Akt substrate of 160 kDa (AS160, also called TBC1D4) (39, 40), is an Akt substrate that regulates GLUT4 translocation in 3T3L1 cells. Subsequent research by Bruss et al. revealed that insulin also regulates AS160 phosphorylation in skeletal muscle (41). Lienhard's group performed a clever series of experiments using several mutations of AS160 expressed in 3T3L1 cells to reveal that key functional domains of AS160 are important for insulin-stimulated glucose uptake. Expression of mutated AS160 in which Ala was substituted for Ser or Thr in Akt consensus sequences blocked insulin's stimulation of phosphorylation of these sites and

reduced insulin's stimulation of GLUT4 translocation (40). Insulin resistance was greatest in cells expressing AS160 mutated on 4 Akt-phosphomotifs (4P mutant). Because Rab proteins regulate GLUT4 vesicles, Lienhard's group also evaluated the role of AS160's Rab-GTPase activating protein (GAP) domain. A mutation substituting lysine for a key arginine in the GAP domain (R/K mutant) abolished AS160's GAP activity. Simultaneous expression of 4P and R/K mutations (4P-R/K) relieved the inhibition of insulin-stimulated glucose uptake found in 4P mutants indicating that insulin-stimulated AS160 phosphorylation was needed for increased GLUT4 translocation only if AS160 had a functional GAP domain. Apparently GDP-bound Rab restrains intracellular GLUT4 vesicles, and GTP-bound Rab favors GLUT4 exocytosis. AS160 has been likened to a "brake" on glucose uptake, and insulin's ability to induce AS160 phosphorylation is the mechanism to "release the brake" (42, 43).

The obese Zucker (OZ) rat, a widely used model for metabolic syndrome, is characterized by insulin resistance, dyslipidemia, mild glucose intolerance, hyperinsulinemia, and hypertension (44-47). As in obese humans, the cause for insulin resistance in OZ rats is a reduced ability of insulin to stimulate GLUT4 translocation rather than reduced GLUT4 expression by muscle (48). Moreover, as in humans with T2D, AS160 phosphorylation is decreased in muscle from OZ rats (49, 50).

In vivo transfection of rodent muscle with plasmid-delivered DNA is an established method, but the process does not have 100% transfect efficiency which can complicate the data interpretation. Glucose uptake by whole muscles from normal mice transfected

with 4P-AS160 had an ~50% decrease in insulin-stimulated glucose uptake (51). It is possible that only ~50% of the fibers were transfected, and glucose uptake was nearly completely blocked in each transfected fiber. Another possibility is that almost all fibers were transfected, but glucose uptake was only reduced ~50% in each transfected fiber. The proposed strategy will turn this "complication" into a major advantage. Muscles will be transfected with a pIRES2-DsRed2-Flag-AS160 plasmid allowing for co-expression of AS160 and DsRed2, enabling the identification of transfected fibers. Thus glucose uptake results will not be "diluted" by including the glucose uptake of non-transfected fibers.

B. RESEARCH DESIGN AND METHODS

All experiments will use male Lean (LZ) and Obese Zucker (OZ) rats, aged 12 wk, when their paired epitrochlearis muscles will be dissected out for *in vitro* incubation and glucose uptake measurement. Some rats will be used to evaluate whole muscle glucose uptake by an established method (52) while other rats will be used to measure single fiber glucose uptake. Fiber type will be determined based on myosin heavy chain (MHC) isoform expression in whole muscles and single fibers. Protein abundance (AS160 and GLUT4) will be measured in whole muscles and individual single fibers. Insulin signaling (insulin receptor, Akt and AS160 phosphorylation and IRS1-PI3K activity) will be assayed in whole muscles.

Experiments for Aims 1, 2 and 3 will use *in vivo* electroporation of skeletal muscle for delivery of DNA as follows: 2 wk prior to isolated muscle incubations, LZ and OZ rats will be anesthetized and both of their epitrochlearis muscles will be surgically exposed.

Plasmid DNA will be delivered through a non-viral electroporation approach that has been shown to achieve ~30-40% transfection efficiency (49, 53-58). The contralateral muscle from each rat will undergo appropriate control treatments. The plasmid will include an internal ribosome entry sequence (IRES) allowing for co-expression of our proteins of interest (59); a DsRed2 fluorescent gene (60) will be included in the plasmid providing a visible reporter for fibers that are transfected, making it possible for both transfected and non-transfected control (NTC) fibers from each muscle to be identified and separately analyzed. Two weeks after electroporation, the rats will be anesthetized and both epitrochlearis muscles will be dissected out and undergo identical *in vitro* treatment ±insulin.

C. RATIONALE & INTERPRETATION OF EXPECTED RESULTS.

Aim 1: Determine if key Akt-phosphomotifs (Thr^{318}, Ser^{588}, Thr^{642}, Ser^{751}) of AS160 are essential for AS160's regulation of glucose uptake in rat skeletal muscle and muscle single fibers from Lean or Obese Zucker rats.

Rationale for Experiment 1: Whole muscles from OZ vs. LZ rats have reduced insulin-stimulated AS160 phosphorylation concomitant with reduced insulin-stimulated glucose uptake (49, 50), reminiscent of the reduced AS160 phosphorylation found in insulin-resistant muscle from humans with Type 2 Diabetes (38). The results beg the question: Does the reduced AS160 phosphorylation account for some or all of the insulin resistance for glucose uptake? To answer this question, we will modify the approach that Lienhard and colleagues used in their seminal experiments which elucidated how AS160 regulates

insulin-stimulated glucose uptake (40). Studying 3T3L1 adipocytes, they found that although overexpression of WT-AS160 did not alter basal or insulin-stimulated glucose uptake (we will measure glucose uptake in fibers overexpressing a range of WT-AS160 levels to confirm), expression of the AS160 4P mutant (with Ala replacing Ser or Thr on each Akt-phosphomotif, preventing their phosphorylation) led to a marked decrease in insulin-stimulated GLUT4 translocation. For this project the 4P mutant will be tested to determine if preventing AS160 phosphorylation on key phosphomotifs can induce insulin resistance in single fibers from LZ rats comparable to the level of insulin resistance found in non-transfected fibers of the same fiber type from OZ rats (i.e., is prevention of AS160 phosphorylation in LZ fibers sufficient to recapitulate the insulin resistance found in OZ fibers?). This project will also determine if blocking AS160 phosphorylation with the 4P mutant further worsens the insulin resistance in OZ fibers.

Hypothesis 1: Mutation of 4 key Akt-phosphomotifs within AS160 (Thr^{318}, Ser^{588}, Thr^{642}, Ser^{751}; 4P mutant) will cause reduced insulin-stimulated glucose uptake by whole skeletal muscle and muscle single fibers of each fiber type from Lean and Obese Zucker rats, with a relatively greater reduction in insulin-stimulated glucose uptake found in Lean vs. Obese rats.

Interpretation of Predicted Results for Experiment 1:

- Predict no rat group (LZ vs. OZ) differences for basal glucose uptake.
- Predict non-transfected control (NTC) will not differ from WT-transfected fibers for basal or insulin-stimulated glucose uptake because studies with cells or whole muscles

have found that up to 12-fold increase in WT expression has no effect on glucose uptake. In the unexpected event that there is a WT-effect, it will be an important result. Further studies would be performed with injection of differing amounts of WT-DNA to identify the dose-effect of WT-AS160 on glucose uptake.

- Figure 6.3 illustrates the prediction for glucose uptake of NTC vs. 4P-transfected fibers of LZ and OZ rats (for clarity, possible fiber type effects are not depicted).
- It is very likely that insulin-stimulated glucose uptake of NTC-LZ > NTC-OZ, consistent with the expected insulin resistance in OZ muscle.
- It is also very likely that NTC-LZ > 4P-LZ, consistent with a role for insulin-stimulated AS160 phosphorylation in insulin-stimulated glucose uptake.
- A <u>crucial comparison</u> will be if 4P-LZ > NTC-OZ, this result would suggest that the mechanism for insulin resistance in NTC-OZ rats is not entirely attributable to reduced AS160 phosphorylation (*i.e.*, there may also be AS160-independent mechanisms).
- Another <u>key comparison</u> will be if NTC-OZ > 4P-OZ, this result would suggest that residual AS160 phosphorylation accounts for a portion of the residual insulin-stimulated glucose uptake above basal glucose uptake values in the NTC-OZ group.

<u>Alternative Experimental Approaches:</u>

- *Why not aim for the highest possible transfection efficiency?* By using electroporation voltages lower than needed for maximal transfection efficiency, we can avoid muscle damage (55). Moderate transfection efficiency also offers an opportunity to study non-transfected and transfected fibers from each muscle, providing an ideal internal control.

- *Why not make a muscle-specific AS160 knockout mouse?* By modifying key regions of AS160 (phosphorylation sites and GAP domain), we will learn more than by eliminating the protein. In addition, knocking out (or "knocking in" modified AS160) of all muscles would likely induce systemic modifications (hormones, substrates, etc.) that could indirectly induce changes and confound interpretation. Two recent studies have phenotyped distinct AS160 knockout mouse models with rather ambiguous results lending to the inherent issues (compensatory mechanisms) of mouse knockout models (61, 62). By focusing on one muscle and analyzing on those fibers which are genetically manipulated, whole body alterations due to genome manipulation are avoided.

Aim 2: Determine if eliminating the functional GTPase activating protein (GAP) domain within AS160 will alter insulin-stimulated glucose uptake in rat skeletal muscle and muscle single fibers from Obese or Lean Zucker rats.

Rationale for Experiment 2: Research by Lienhard's group and by others provides strong evidence that the ability of AS160 to participate in insulin's regulation of GLUT4 translocation requires AS160's functional GAP domain (39, 63). By mutating a key arginine in this domain to lysine, AS160's GAP activity is eliminated. Thus, the R/K-mutant is unable to restrain insulin's ability to increase GLUT4 translocation and glucose uptake. This experiment will exploit the R/K mutant to learn if AS160's GAP function is essential for the insulin resistance in fibers from OZ rats. In other words: Does blocking

AS160's GAP domain-dependent restraint of glucose uptake partly or completely "cure" the insulin resistance in muscle fibers from OZ rats?

Hypothesis 2: Mutation of the key arginine within AS160 (Arg^{973}; R/K mutant), rendering the GAP domain non-functional, will elevate the insulin-stimulated glucose uptake in skeletal muscle and muscle single fibers of each fiber type from Obese, but not Lean Zucker rats compared to controls lacking the R/K mutant.

Interpretation of Predicted Results for Experiment 2:

- Predict unaltered basal glucose uptake for R/K-LZ vs. NTC-LZ or R/K-OZ vs. NTC-OZ based on previous work showing the R/K mutant does not alter basal glucose uptake or GLUT4 translocation in cells or whole mouse muscles (40, 51, 64). The lack of an R/K effect on basal glucose uptake suggests that although AS160 with a functional GAP domain restrains GLUT4 vesicle recruitment, other insulin-controlled steps are required for the GLUT4 vesicle's fusion with surface membranes and subsequently increased glucose uptake (*i.e.*, GTP-bound Rab is apparently necessary, but not sufficient for increased glucose uptake).
- Figure 6.3 illustrates the prediction for glucose uptake values of NTC vs. R/K-transfected fibers from LZ and OZ rats (for clarity, possible fiber type differences are not depicted).
- Expect that insulin-stimulated glucose uptake of NTC-LZ = R/K-LZ, as previously reported for cultured cells and whole muscles and consistent with the notion that in "normal" cells that are not insulin resistant, insulin can effectively inhibit AS160's

GAP activity. Thus, in fibers from LZ rats, the R/K mutation is not expected to boost glucose uptake to "supranormal" values.

- It will be important to learn if glucose uptake for R/K-OZ > NTC-OZ. This result would strongly suggest that in NTC-OZ fibers, the attenuated ability of insulin to stimulate glucose uptake is attributable, at least in part, to insulin's inability to inhibit AS160's GAP-domain-linked restraint of glucose uptake.
- Another very informative comparison will be if NTC-LZ > R/K-OZ. This result would suggest that the mechanism for insulin resistance in NTC-OZ fibers is not entirely attributable to a defective ability to remove AS160's restraint of GLUT4 (pointing toward AS160-independent mechanisms for this residual portion of the OZ insulin resistance, e.g., defects in proximal signaling steps).

Aim 3: Determine if eliminating the functional GTPase activating protein (GAP) domain simultaneously with mutation of the Akt-phosphomotifs within AS160 will prevent the effect of the 4P mutation alone on glucose uptake in rat skeletal muscle and muscle single fibers from Lean or Obese Zucker rats.

Rationale for Experiment 3:

Experiment 4 is important to verify, in skeletal muscle and single fibers from both normal and insulin resistant rats, that a functional GAP domain links insulin's ability to phosphorylate AS160 on key phosphomotifs to insulin's ability to elicit a normal increase in glucose uptake (i.e., insulin-mediated glucose uptake relies on cooperation between these 2 functional domains).

Hypothesis 3: The decrement in insulin-stimulated glucose uptake by skeletal muscle and muscle single fibers of each fiber type from Obese and Lean Zucker rats induced by the mutation of 4 key Akt-phosphomotifs within AS160 will be eliminated by the simultaneous mutation of both Arg^{973} and the 4 key Akt-phosphomotifs of AS160 (4P-R/K double mutant).

Interpretation of Predicted Results for Experiment 3:

- Predict no differences for basal glucose uptake between the 4P-R/K-LZ vs. NTC-LZ or 4P-R/K vs. NTC-OZ fibers, consistent with the data from cells and whole mouse muscles.
- Figure 6.3 illustrates the prediction for glucose uptake values for NTC, 4P and 4P-R/K fibers from LZ and OZ rats (for clarity, possible differences among fiber types are not depicted).
- If NTC-LZ = 4P-R/K-LZ > 4P-LZ, these results would verify that AS160's phosphorylation sites and GAP-domain cooperatively control glucose uptake.
- If NTC-LZ > 4P-R/K-OZ > NTC-OZ, these results would suggest that the insulin resistance in the NTC-OZ group is not entirely attributable to dysfunctional AS160 (e.g., may involve defects in proximal insulin signaling steps).

Summary and Conclusions

In both rodents and humans, there are many different skeletal muscles ranging in size, function, and metabolic demands. Every skeletal muscle is made up of hundreds to

thousands of individual fibers, each of which can display substantial heterogeneity depending on many factors, including their fiber type. Because of the important role that skeletal muscle plays in whole body glucose homeostasis, investigating the glucose uptake capacity of a muscle single fiber was an overarching aim of the studies throughout this dissertation. Through the development and validation of a novel method to isolate single fibers from rat skeletal muscle, this dissertation has provided novel insights regarding MHC isoform expression, glucose uptake, fiber size, and protein abundance in rat epitrochlearis muscle single fibers.

Studying single fibers avoids limitations often encountered in traditional tissue analysis. Results from Study's 1-3 in this dissertation demonstrated that glucose uptake varied among the fibers (of different fiber types) and was distinct with regards to the type of stimulation (e.g., insulin or AICAR). Greater fiber type characterization was achieved with the ability to measure protein abundance in single fibers. GLUT4 abundance measurements supported the hypothesis that insulin-stimulated glucose uptake capacity is in part, a function of the GLUT4 transporter expression. The ability to study single fibers from rat models of disease and aging provided an additional component to better understand the physiological variations occurring in muscles at the cellular level. Furthermore, genetic manipulation of skeletal muscle has served as a valuable tool to help understand the role of specific proteins. Thus, application of single fiber analysis to investigate ectopic gene expression to study proteins of interest (both wild type and mutant version as described in the future research proposal) will be valuable for future research. Ultimately, this dissertation provided unique methods and results to better

understand glucose uptake and protein expression in skeletal muscle at the single fiber level.

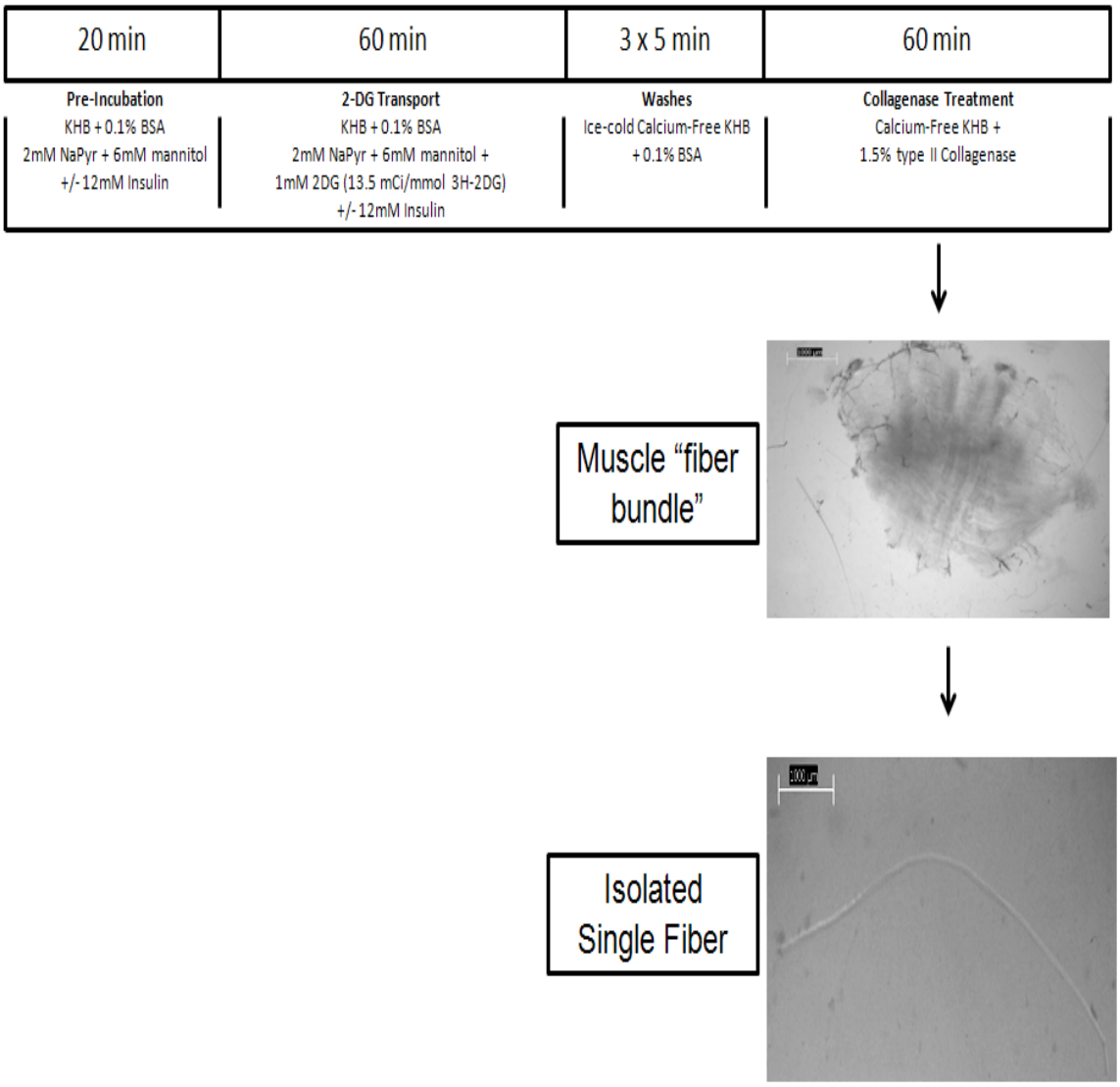

Figure 6.1 Incubation Protocol for Glucose Uptake Measurements by Single Fibers. KHB, Krebs Henseleit buffer

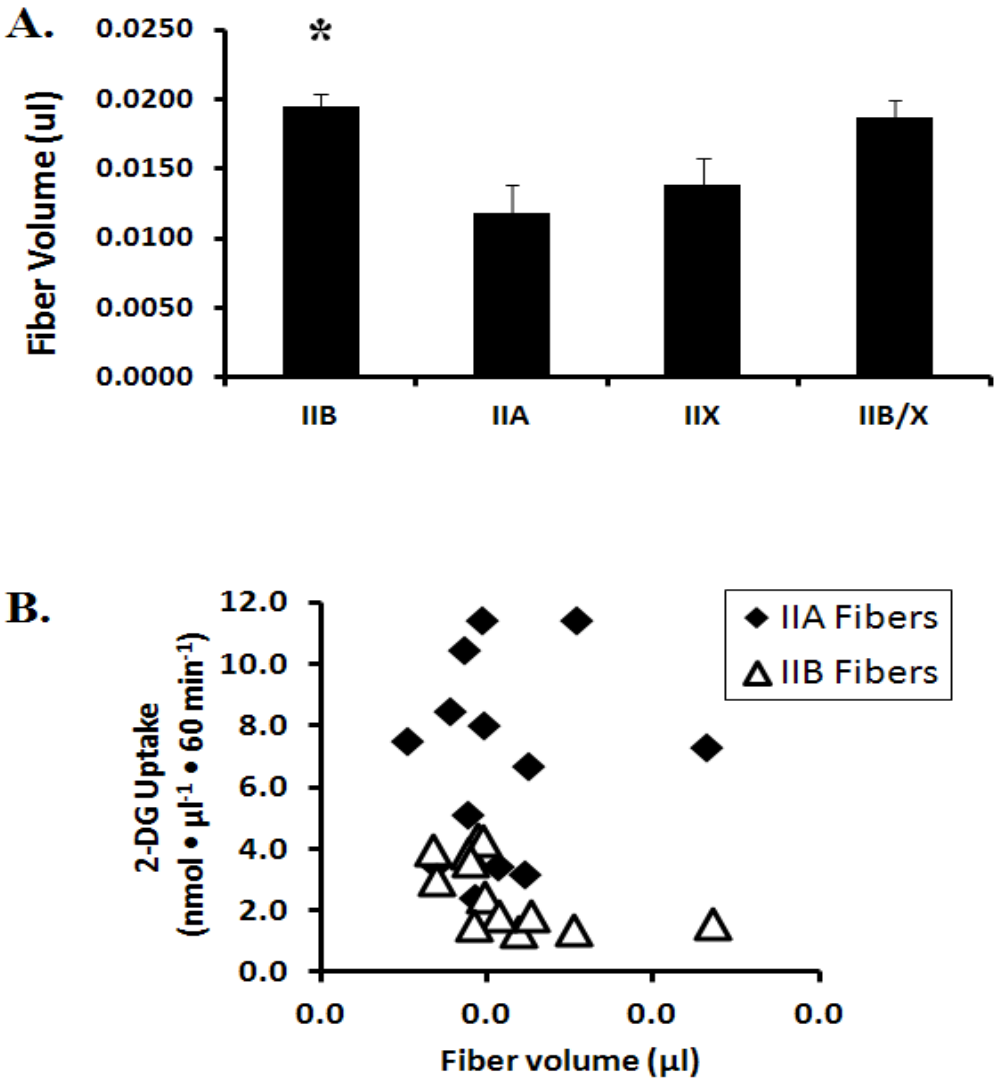

Figure 6.2 Volume of Single Fiber from 2-3 Month old Male Wistar Rats & Correlation of 2-DG Uptake versus Fiber Volume for Volume-matched IIA and IIB Fibers. **A.** Unpublished data for size (volume, µl) of muscle single fibers expressing the same MHC isoform from 2-3 month old male Wistar epitrochlearis muscles. The number of fibers for each MHC isoform is in parentheses: IIB (222), IIA (31), IIX (20), IIB/X (71). There was a main effect of fiber type ($p<0.05$). Data are means ± SEM and were analyzed by one-way ANOVA. Post hoc analysis revealed the IIB MHC isoform to be significantly different from IIA isoform (*$p<0.05$ for IIB vs. IIA) **B.** Correlation of 2-DG uptake versus fiber volume for volume-matched IIA and IIB fibers. Each symbol represents one fiber. Fibers were matched for volume (close as possible) and 2-DG Uptake was compared.

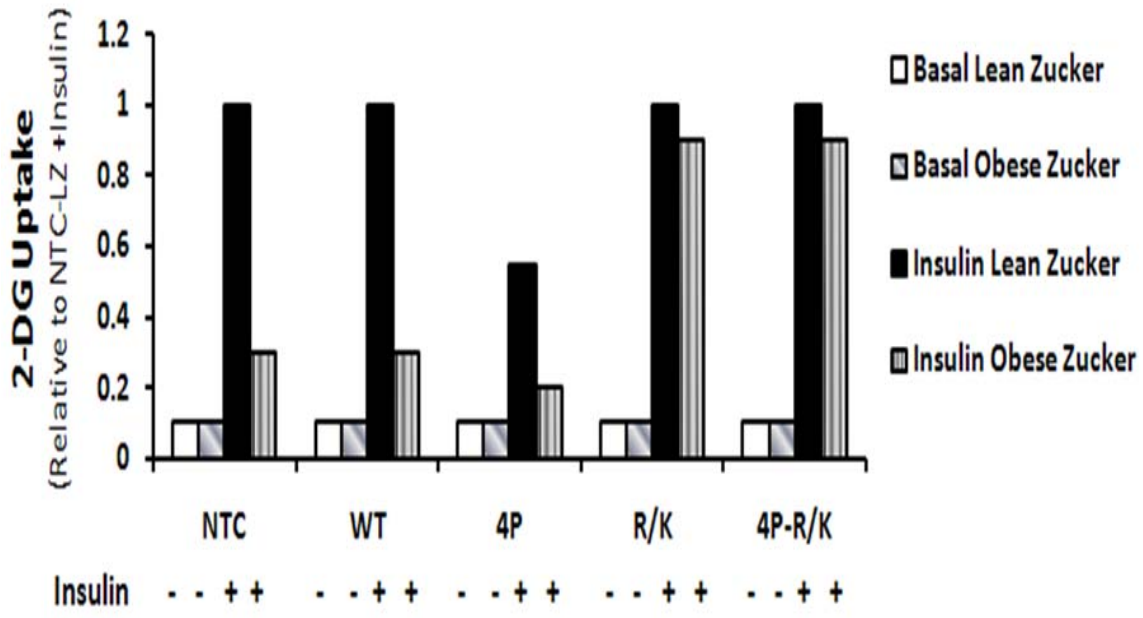

Figure 6.3 Predicted Results for Glucose Uptake in Proposal for Proposal for Future Research. Each bar represents the estimated 2-DG Uptake by the epitrochlearis muscle and is relative to the non-transfected lean Zucker (NTC-LZ) with insulin stimulation. Abbreviation: Non-transfected control (NTC); wildtype (WT); AS160-4P mutation (4P); AS160-R/K mutation (R/K); AS160-4P-R/K double mutation (4P-R/K).

References

1. Henriksen EJ, Bourey RE, Rodnick KJ, Koranyi L, Permutt MA, Holloszy JO. Glucose transporter protein content and glucose transport capacity in rat skeletal muscles. The American journal of physiology. 1990;259(4 Pt 1):E593-8.
2. Birnbaum MJ. The insulin-sensitive glucose transporter. Int Rev Cytol. 1992;137:239-97.
3. Lavan BE, Lienhard GE. Insulin signalling and the stimulation of glucose transport. Biochem Soc Trans. 1994;22(3):676-80.
4. Constable SH, Favier RJ, Cartee GD, Young DA, Holloszy JO. Muscle glucose transport: interactions of in vitro contractions, insulin, and exercise. J Appl Physiol. 1988;64(6):2329-32.
5. Cartee GD, Young DA, Sleeper MD, Zierath J, Wallberg-Henriksson H, Holloszy JO. Prolonged increase in insulin-stimulated glucose transport in muscle after exercise. The American journal of physiology. 1989;256(4 Pt 1):E494-9.
6. Cartee GD, Holloszy JO. Exercise increases susceptibility of muscle glucose transport to activation by various stimuli. The American journal of physiology. 1990;258(2 Pt 1):E390-3.
7. Holloszy JO. A forty-year memoir of research on the regulation of glucose transport into muscle. Am J Physiol Endocrinol Metab. 2003;284(3):E453-67.
8. Merrill GF, Kurth EJ, Hardie DG, Winder WW. AICA riboside increases AMP-activated protein kinase, fatty acid oxidation, and glucose uptake in rat muscle. The American journal of physiology. 1997;273(6 Pt 1):E1107-12.
9. Ai H, Ihlemann J, Hellsten Y, Lauritzen HP, Hardie DG, Galbo H, et al. Effect of fiber type and nutritional state on AICAR- and contraction-stimulated glucose transport in rat muscle. Am J Physiol Endocrinol Metab. 2002;282(6):E1291-300.
10. Bergeron R, Russell RR, 3rd, Young LH, Ren JM, Marcucci M, Lee A, et al. Effect of AMPK activation on muscle glucose metabolism in conscious rats. The American journal of physiology. 1999;276(5 Pt 1):E938-44.
11. Hayashi T, Hirshman MF, Kurth EJ, Winder WW, Goodyear LJ. Evidence for 5' AMP-activated protein kinase mediation of the effect of muscle contraction on glucose transport. Diabetes. 1998;47(8):1369-73.
12. Jorgensen SB, Viollet B, Andreelli F, Frosig C, Birk JB, Schjerling P, et al. Knockout of the alpha2 but not alpha1 5'-AMP-activated protein kinase isoform abolishes 5-aminoimidazole-4-carboxamide-1-beta-4-ribofuranosidebut not contraction-induced glucose uptake in skeletal muscle. J Biol Chem. 2004;279(2):1070-9.
13. McGee SL, Howlett KF, Starkie RL, Cameron-Smith D, Kemp BE, Hargreaves M. Exercise increases nuclear AMPK alpha2 in human skeletal muscle. Diabetes. 2003;52(4):926-8.
14. Gong H, Xie J, Zhang N, Yao L, Zhang Y. MEF2A binding to the Glut4 promoter occurs via an AMPKalpha2-dependent mechanism. Med Sci Sports Exerc. 2011;43(8):1441-50.
15. Murphy RM. Enhanced technique to measure proteins in single segments of human skeletal muscle fibers: fiber-type dependence of AMPK-alpha1 and -beta1. J Appl Physiol. 2011;110(3):820-5.

16. DeNardi C, Ausoni S, Moretti P, Gorza L, Velleca M, Buckingham M, et al. Type 2X-myosin heavy chain is coded by a muscle fiber type-specific and developmentally regulated gene. J Cell Biol. 1993;123(4):823-35. PMCID: 2200149.
17. Stephenson GM. Hybrid skeletal muscle fibres: a rare or common phenomenon? Clin Exp Pharmacol Physiol. 2001;28(8):692-702.
18. Goodman CA, Mabrey DM, Frey JW, Miu MH, Schmidt EK, Pierre P, et al. Novel insights into the regulation of skeletal muscle protein synthesis as revealed by a new nonradioactive in vivo technique. FASEB J. 2011;25(3):1028-39. PMCID: 3042844.
19. Torrella JR, Whitmore JM, Casas M, Fouces V, Viscor G. Capillarity, fibre types and fibre morphometry in different sampling sites across and along the tibialis anterior muscle of the rat. Cells Tissues Organs. 2000;167(2-3):153-62.
20. Panisello P, Torrella JR, Esteva S, Pages T, Viscor G. Capillary supply, fibre types and fibre morphometry in rat tibialis anterior and diaphragm muscles after intermittent exposure to hypobaric hypoxia. Eur J Appl Physiol. 2008;103(2):203-13.
21. Rogers MA, Evans WJ. Changes in skeletal muscle with aging: effects of exercise training. Exerc Sport Sci Rev. 1993;21:65-102.
22. Frontera WR, Hughes VA, Fielding RA, Fiatarone MA, Evans WJ, Roubenoff R. Aging of skeletal muscle: a 12-yr longitudinal study. J Appl Physiol. 2000;88(4):1321-6.
23. Lexell J, Taylor CC, Sjostrom M. What is the cause of the ageing atrophy? Total number, size and proportion of different fiber types studied in whole vastus lateralis muscle from 15- to 83-year-old men. J Neurol Sci. 1988;84(2-3):275-94.
24. Connelly DM, Rice CL, Roos MR, Vandervoort AA. Motor unit firing rates and contractile properties in tibialis anterior of young and old men. J Appl Physiol. 1999;87(2):843-52.
25. Cartee GD. What insights into age-related changes in skeletal muscle are provided by animal models? J Gerontol A Biol Sci Med Sci. 1995;50 Spec No:137-41.
26. Eddinger TJ, Moss RL, Cassens RG. Fiber number and type composition in extensor digitorum longus, soleus, and diaphragm muscles with aging in Fisher 344 rats. J Histochem Cytochem. 1985;33(10):1033-41.
27. Daw CK, Starnes JW, White TP. Muscle atrophy and hypoplasia with aging: impact of training and food restriction. J Appl Physiol. 1988;64(6):2428-32.
28. Coggan AR, Spina RJ, King DS, Rogers MA, Brown M, Nemeth PM, et al. Histochemical and enzymatic comparison of the gastrocnemius muscle of young and elderly men and women. J Gerontol. 1992;47(3):B71-6.
29. Alnaqeeb MA, Goldspink G. Changes in fibre type, number and diameter in developing and ageing skeletal muscle. J Anat. 1987;153:31-45. PMCID: 1261780.
30. Holloszy JO, Chen M, Cartee GD, Young JC. Skeletal muscle atrophy in old rats: differential changes in the three fiber types. Mech Ageing Dev. 1991;60(2):199-213.
31. Cartee GD, Kietzke EW, Briggs-Tung C. Adaptation of muscle glucose transport with caloric restriction in adult, middle-aged, and old rats. The American journal of physiology. 1994;266(5 Pt 2):R1443-7.
32. Cartee GD. Influence of age on skeletal muscle glucose transport and glycogen metabolism. Med Sci Sports Exerc. 1994;26(5):577-85.
33. Bekoff A, Betz W. Properties of isolated adult rat muscle fibres maintained in tissue culture. J Physiol. 1977;271(2):537-47. PMCID: 1353585.

34. Rosenblatt JD, Lunt AI, Parry DJ, Partridge TA. Culturing satellite cells from living single muscle fiber explants. In Vitro Cell Dev Biol Anim. 1995;31(10):773-9.
35. Ravenscroft G, Nowak KJ, Jackaman C, Clement S, Lyons MA, Gallagher S, et al. Dissociated flexor digitorum brevis myofiber culture system--a more mature muscle culture system. Cell Motil Cytoskeleton. 2007;64(10):727-38.
36. Wallberg-Henriksson H. Glucose transport into skeletal muscle. Influence of contractile activity, insulin, catecholamines and diabetes mellitus. Acta Physiol Scand Suppl. 1987;564:1-80.
37. Kovanen V, Suominen H, Heikkinen E. Collagen of slow twitch and fast twitch muscle fibres in different types of rat skeletal muscle. Eur J Appl Physiol Occup Physiol. 1984;52(2):235-42.
38. Karlsson HK, Zierath JR, Kane S, Krook A, Lienhard GE, Wallberg-Henriksson H. Insulin-Stimulated Phosphorylation of the Akt Substrate AS160 Is Impaired in Skeletal Muscle of Type 2 Diabetic Subjects. Diabetes. 2005;54(6):1692-7.
39. Kane S, Sano H, Liu SC, Asara JM, Lane WS, Garner CC, et al. A method to identify serine kinase substrates. Akt phosphorylates a novel adipocyte protein with a Rab GTPase-activating protein (GAP) domain. J Biol Chem. 2002;277(25):22115-8.
40. Sano H, Kane S, Sano E, Miinea CP, Asara JM, Lane WS, et al. Insulin-stimulated phosphorylation of a Rab GTPase-activating protein regulates GLUT4 translocation. J Biol Chem. 2003;278(17):14599-602.
41. Bruss MD, Arias EB, Lienhard GE, Cartee GD. Increased phosphorylation of Akt substrate of 160 kDa (AS160) in rat skeletal muscle in response to insulin or contractile activity. Diabetes. 2005;54(1):41-50.
42. Cartee GD, Wojtaszewski JF. Role of Akt substrate of 160 kDa in insulin-stimulated and contraction-stimulated glucose transport. Appl Physiol Nutr Metab. 2007;32(3):557-66.
43. Sakamoto K, Holman GD. Emerging role for AS160/TBC1D4 and TBC1D1 in the regulation of GLUT4 traffic. Am J Physiol Endocrinol Metab. 2008;295(1):E29-37.
44. Zucker TF, Zucker LM. Fat accretion and growth in the rat. J Nutr. 1963;80:6-19.
45. Zucker LM, Antoniades HN. Insulin and obesity in the Zucker genetically obese rat "fatty". Endocrinology. 1972;90(5):1320-30.
46. Ionescu E, Sauter JF, Jeanrenaud B. Abnormal oral glucose tolerance in genetically obese (fa/fa) rats. The American journal of physiology. 1985;248(5 Pt 1):E500-6.
47. Muller S, Cleary MP. Glucose metabolism in isolated adipocytes from ad Libitum- and restricted-fed lean and obese Zucker rats at two different ages. Proc Soc Exp Biol Med. 1988;187(4):398-407.
48. Etgen GJ, Jr., Wilson CM, Jensen J, Cushman SW, Ivy JL. Glucose transport and cell surface GLUT-4 protein in skeletal muscle of the obese Zucker rat. The American journal of physiology. 1996;271(2 Pt 1):E294-301.
49. Benton CR, Holloway GP, Han XX, Yoshida Y, Snook LA, Lally J, et al. Increased levels of peroxisome proliferator-activated receptor gamma, coactivator 1 alpha (PGC-1alpha) improve lipid utilisation, insulin signalling and glucose transport in skeletal muscle of lean and insulin-resistant obese Zucker rats. Diabetologia. 2010.
50. Thyfault JP, Cree MG, Zheng D, Zwetsloot JJ, Tapscott EB, Koves TR, et al. Contraction of insulin-resistant muscle normalizes insulin action in association with

increased mitochondrial activity and fatty acid catabolism. Am J Physiol Cell Physiol. 2007;292(2):C729-39.
51. Kramer HF, Witczak CA, Taylor EB, Fujii N, Hirshman MF, Goodyear LJ. AS160 regulates insulin- and contraction-stimulated glucose uptake in mouse skeletal muscle. J Biol Chem. 2006;281(42):31478-85.
52. Hansen PA, Gulve EA, Holloszy JO. Suitability of 2-deoxyglucose for in vitro measurement of glucose transport activity in skeletal muscle. J Appl Physiol. 1994;76(2):979-85.
53. Clarke DC, Miskovic D, Han XX, Calles-Escandon J, Glatz JF, Luiken JJ, et al. Overexpression of membrane-associated fatty acid binding protein (FABPpm) in vivo increases fatty acid sarcolemmal transport and metabolism. Physiol Genomics. 2004;17(1):31-7.
54. Holloway GP, Lally J, Nickerson JG, Alkhateeb H, Snook LA, Heigenhauser GJ, et al. Fatty acid binding protein facilitates sarcolemmal fatty acid transport but not mitochondrial oxidation in rat and human skeletal muscle. J Physiol. 2007;582(Pt 1):393-405. PMCID: 2075306.
55. Benton CR, Nickerson JG, Lally J, Han XX, Holloway GP, Glatz JF, et al. Modest PGC-1alpha overexpression in muscle in vivo is sufficient to increase insulin sensitivity and palmitate oxidation in subsarcolemmal, not intermyofibrillar, mitochondria. J Biol Chem. 2008;283(7):4228-40.
56. Benton CR, Yoshida Y, Lally J, Han XX, Hatta H, Bonen A. PGC-1alpha increases skeletal muscle lactate uptake by increasing the expression of MCT1 but not MCT2 or MCT4. Physiol Genomics. 2008;35(1):45-54.
57. Holloway GP, Gurd BJ, Snook LA, Lally J, Bonen A. Compensatory increases in nuclear PGC1alpha protein are primarily associated with subsarcolemmal mitochondrial adaptations in ZDF rats. Diabetes. 2010;59(4):819-28. PMCID: 2844829.
58. Lira VA, Benton CR, Yan Z, Bonen A. PGC-1alpha regulation by exercise training and its influences on muscle function and insulin sensitivity. Am J Physiol Endocrinol Metab. 2010;299(2):E145-61.
59. Allera-Moreau C, Delluc-Clavieres A, Castano C, Van den Berghe L, Golzio M, Moreau M, et al. Long term expression of bicistronic vector driven by the FGF-1 IRES in mouse muscle. BMC Biotechnol. 2007;7:74. PMCID: 2180170.
60. Bevis BJ, Glick BS. Rapidly maturing variants of the Discosoma red fluorescent protein (DsRed). Nat Biotechnol. 2002;20(1):83-7.
61. Lansey MN, Walker NN, Hargett SR, Stevens JR, Keller SR. Deletion of Rab GAP AS160 modifies glucose uptake and GLUT4 translocation in primary skeletal muscles and adipocytes and impairs glucose homeostasis. Am J Physiol Endocrinol Metab. 2012;303(10):E1273-86.
62. Wang HY, Ducommun S, Quan C, Xie B, Li M, Wasserman DH, et al. AS160 deficiency causes whole-body insulin resistance via composite effects in multiple tissues. The Biochemical journal. 2012.
63. Roach WG, Chavez JA, MÃ®inea CP, Lienhard GE. Substrate specificity and effect on GLUT4 translocation of the Rab GTPase-activating protein Tbc1d1. The Biochemical journal. 2007;403(2):353-8.

64. Thong FSL, Bilan PJ, Klip A. The Rab GTPase-Activating Protein AS160 Integrates Akt, Protein Kinase C, and AMP-Activated Protein Kinase Signals Regulating GLUT4 Traffic
10.2337/db06-0900. Diabetes. 2007;56(2):414-23.

APPENDIX

Appendix A includes the detailed novel single fiber isolation protocol for rat epitrochlearis muscle. This protocol includes details not found within Methods sections of the thesis as well as specific supplies necessary.

Appendix A. Single Fiber Isolation Protocol for Rat Epitrochlearis Muscle

The protocol below provides detailed information on the procedures used for isolating single fiber in the experiments included in this thesis.

~Solutions (modify volume as required) & Incubation Procedure~

Make Ca^{2+} Free Krebs Henseleit Buffer (KHB) solution (made fresh daily)

____ 40 ml "ultrapure" H_2O
____ 5ml KHB Stock 1
____ gas with 95% O_2/5%CO_2 on ice for ~15 minutes
____ 5ml KHB Stock 2 – CALCIUM FREE

Make KHB(Ca^{2+} Free) + 0.1% Bovine Serum Albumin (KHB/BSA) solution (made fresh daily)
____ 20ml KHB (Ca^{2+} Free)
____ 20mg BSA (RIA grade), 0.1%

Make 1.5% Collagenase (Type 2 from Worthington Biochem Corp) solution (made fresh daily)
1.5% collagenase (w/v)
1.5% = x grams / 1 ml
x grams = 0.015 * 1 ml
=15mg of type 2 collagenase added to 1ml of KHB/BSA (Ca^{2+} Free)

___Make up appropriate volume of solution: X ml of KHB/BSA (Ca^{2+} Free) + 15mg/ml type 2 collagenase
___Aliquot 2ml of collagenase solution into vials in which muscles will be incubated

___**Incubate muscles** in vials containing collagenase solution for ~1 hour @ 35°C, shaking gently (~45 rpm) while being gassed (95% O_2/5%CO_2)

* Incubate until connective tissue appears adequately digested for pulling fibers, resulting in a **"fiber bundle"**
** This is a subjective decision – with experience you will recognize when a muscle has been suitably digested. In brief, the entire muscle should be "mucus like" in its appearance and texture since a majority of the connective tissue has been digested.

~Isolating Fibers from Fiber Bundle~
___Pour collagenase & fiber bundle in small petri dish (35x10mm, see Supplies)
___Trim ends of tissue so only muscle of interest is present
___Transfer trimmed fiber bundle to petri dish containing 3-4ml KHB(Ca^{2+}Free) to wash remaining collagenase
* Must be gentle with fiber bundle at this point – suggest transferring using spoon/spatula (see Supplies)

___ Transfer trimmed fiber bundle to petri dish containing 3-4ml KHB(Ca^{2+}Free) & 2-3 drops trypan blue (TB)
___Isolate/Tease fiber from bundle using forceps (see Supplies)
* Isolation method comes with practice – in brief, two forceps will need to be used at all times. Grip end of fiber and slowly pull from fiber bundle. The fiber bundle may need to be restrained with the other forcep while fiber is pulled from bundle. Only fibers nonpermeable to TB should be isolated (with experience, fibers permeable to TB should be very rare).
___Image fiber using microscope camera (used for length and width, see Fiber Size Measurements)
___Pipette individual fiber up in 10ul of solution and aliquot into individual eppendorf tubes (see Supplies)
*It is helpful to have a separate microscope allowing for visualization of the fiber being pipetted into the eppendorf tube because fibers will sometimes stick to side of the pipette tip.
___If measuring GU, remove 5ul (of 10ul, making sure to not pipette up the fiber) and aliquot into separate small eppendorf tube for 2-DG blank of solution

~Processing of Fibers for MHC, Glucose Uptake, and Immunoblotting~
Boiling Homogenization Technique (employ heating block as heat source)
____Add 45ul Homogenization buffer and 50ul 2X Laemmli buffer to 5ul+fiber solution Homogenization
____Briefly vortex tube and spin if necessary
____Put tube into heating block once temperature has reached ~100°C
____Boil for ~10 minutes
____Spin briefly
____Aliquots to be used for MHC isoform characterization gels, Glucose Uptake Measurements, & Immunoblotting (see MacKrell & Cartee *Diabetes* 61(5):995-1003, 2012 for specifics)

~Fiber Size Measurements~
Using ImageJ software, fiber dimensions are measured. The width (mean value for width measured at three locations per fiber: near the fiber midpoint and approximately halfway between the midpoint and each end of the fiber) and length of each fiber are used to estimate volume ($V = \pi r^2 l$, where r refers to radius as determined by half of the width measurement and l refers to length).

Reagents & Supplies:
- KHB Stock 1 Solution (118.5mM NaCl, 4.7mM KCl, 1.2mM KH_2PO_4, 25.0mM $NaHCO_3$)
- KHB Stock 2 Solution (1.2mM $MgSO_4$, *do <u>not</u> add 2.5mM $CaCl_2$)*
- Bovine serum albumin: Sigma Aldrich (Cat. # A7888)
- Type 2 Collagenase: Worthington Biochemical Corp (CLS-2)
- Petri Dish: Fisherbrand Media-Miser Disposable Petri Dishes, 35mmx10mm (Cat. #08-757-11YZ)
- Stainless-Steel Spoon and Spatula: Fisher Scientific (Cat. # 14-356-10)

- Forceps: Fine Science Tools, Dumont #5 Forceps (Cat. # 11251 -20)
- Small Eppendorf Tubes: Fisherbrand 0.2ml Flat- and Domed-Cap PCR Tubes (Cat. # 14230225)
- Homogenization Buffer: T-PER (Pierce Biotech, Cat. # 78510), 1 mmol/L EDTA, 1 mmol/L EGTA, 2.5 mmol/L sodium pyrophosphate,1 mmol/L Na_3VO_4, 1 mmol/L b-glycerophosphate, 1 mg/mL leupeptin, and 1 mmol/L phenylmethylsulfonyl fluoride
- Laemmli Sample Buffer: BioRad (cat. # 161-0737)

Abbreviations

KHB: Krebs Henseleit buffer
BSA: Bovine Serum Albumin
TB: Trypan Blue
GU: Glucose Uptake
MHC: Myosin heavy chain